IDC

►Carcinoma, Ductal, Invasive

Idiopathic Interstitial Lung Diseases

►Interstitial Lung Diseases, Unknown Etiology

Idiopathic Respiratory Distress Syndrome

►Chest, Neonatal

Ileus

Dilated small bowel.
►Occlusion and Subocclusion, Small bowel in adults

Iliac Artery Obstruction

►Stenosis, Artery, Iliac

Iliac Artery Occlusion

►Occlusion, Artery, Iliac

Iliac Artery Stenosis Artery

►Occlusion, Artery, Iliac

Iliac Vein Obstruction

►Thrombosis, Vein, Ilia

Iliac Vein Occlusion

►Thrombosis, Vein, Ilia

Immature Teratomas

Immature teratomas are malignant germ cell tumors that occur in children. They are solid tumors with fast growth that may contain small foci of fat and scattered calcification.
►Teratoma, Ovaries, Mature, Ovalar

Immune Thyroiditis Type Basedow

►Thyroid Autoimmune Disease

Immunoproliferative Small Intestinal Disease

Also known as alpha-chain disease or Mediterranean lymphoma, IPSID is associated with microbial or parasitic colonization of the small bowel.
►Neoplasms, Small Bowel

Imperforate Anus

▶Anorectal Malformation

Imperforated Hymen

Caused by the persistence of the central epithelial cells of the urogenital diaphragm; it is not associated with other abnormalities. It may cause hydro- or hematometrocolpos.

▶Genital Tract

Impotence

Räto T. Strebel[1], Hubert John[2]
[1]Department of Urology, University Hospital Zurich, Zurich, Switzerland
[2]Klinik Hirslanden, Leiter Zentrum für Urologie, Zurich, Switzerland
raeto.strebel@usz.ch

Synonym

Erectile dysfunction (ED); Impotentia coeundi

Definition

Impotence is defined as "male erectile dysfunction, that is, the inability to achieve or maintain an erection sufficient for satisfactory sexual performance" (1).

Imaging

Prescription of a PDE-5-inhibitor is the recommended primary treatment in most men, irrespective of the etiology. Therefore, imaging studies in the field of erectile dysfunction will rarely influence the treatment of these patients. Imaging in the field of erectile dysfunction is warranted in men with a presumed vasculogenic erectile disorder that may be amenable to surgical or interventional treatment. A Doppler ultrasound examination of the penile arteries after pharmacologically inducing an erection (intracavernosal injection of prostaglandin E1, e.g., 10 µg Alprostadil) is the preferred technique to assess an arteriogenic ED (depending on peak systolic arterial flow rates). Moreover, a veno-occlusive ED can be suspected when high end-diastolic arterial flow rates are recorded. The index of vascular resistance (RI) can be calculated and adds further information when considering a veno-occlusive ED. Several investigator and patient dependent factors make this examination subject to artifacts. Patient's anxiety and a cold and busy examination room are not helpful to facilitate relaxation of smooth muscle cells within the corpus cavernosum after pharmacostimulation.

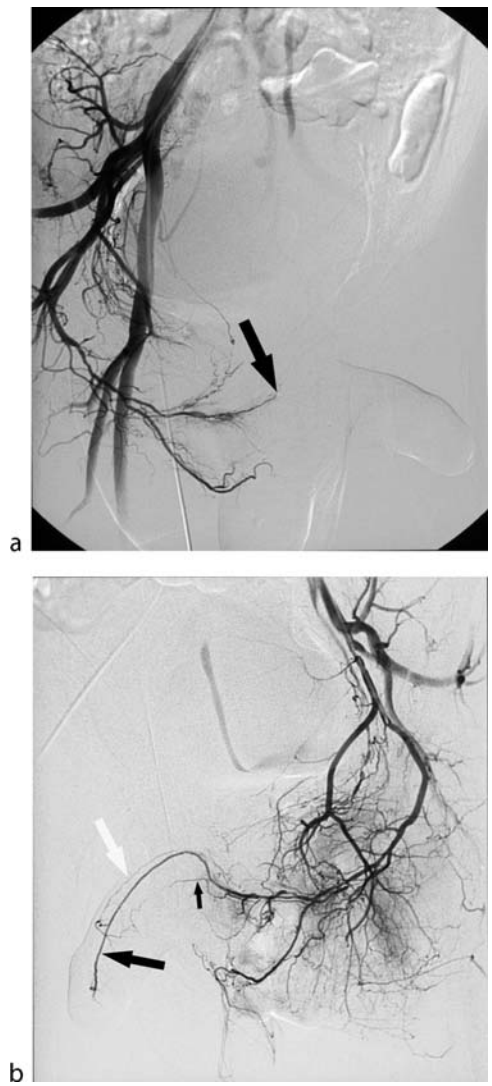

Impotence. Figure 1 **(a) Selective arteriography of the anterior trunk of the right internal hypogastric artery depicting an occlusion of the right common penile artery (black arrow). (b) Selective arteriography of the left internal pudendal artery depicting normal dorsal penile (fat black arrow) and cavernosal artery (small black arrow). The right dorsal penile artery is filled through collaterals from the left side (white arrow) (With courtesy of the department of radiology, University Hospital Zurich, Switzerland.).**

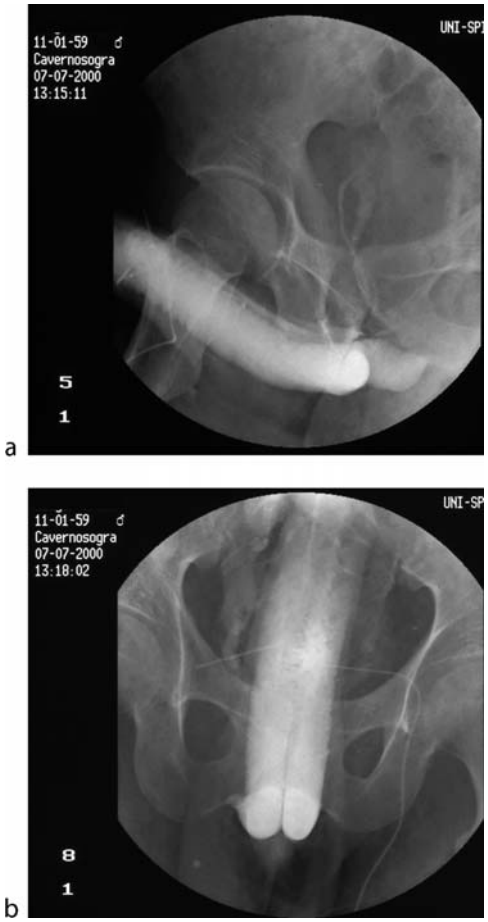

Impotence. Figure 2 (a and b) Cavernosography depicting early venous outflow in superficial dorsal and pelvic veins.

Selective penile arteriography is advisable before planning surgery when Doppler ultrasound examination results are abnormal (Fig. 1a, b). Arteriography offers the best anatomical information concerning the pelvic arterial inflow. Additionally, a dynamic infusion cavernosometry and cavernosography can help to confirm the diagnosis of a veno-occlusive ED (Fig. 2a, b). However, the clinical consequences and diagnostic yield of this study, in the light of color Doppler flow studies, remain limited.

Bibliography

1. Montague DK, Jarow JP, Broderick GA et al (2005) Chapter 1: The management of erectile dysfunction: an AUA update. J Urol 174(1):230–239

Impotentia Coeundi

▶Impotence

In vivo Receptor Imaging

Visualization of receptors mainly by means of nuclear medicine. Radiolabeled vectors are administered to patients. After a distribution phase, the radiopharmaceutical binds stably to the receptors and can be visualized with gamma cameras, including positron emission tomography (PET) scanners.

▶Receptor Studies, Neoplasms

Inborn Errors of Metabolism

Refers to a number of rare genetic defects that result in (a) abnormalities in the synthesis of enzymes and transportation proteins that result in the normal metabolic pathways and (b) accumulation of abnormal metabolites.

▶Congenital Malformations, Adrenals
▶Neurometabolic Disorders

Inborn Splenic Abnormalities

▶Congenital Anomalies, Splenic

Incidental Findings

Incidental findings are defined as observations of potential clinical significance made unexpectedly in healthy subjects or in patients recruited to research and that are unrelated to the purpose or variables of a study.

▶Incidental Neuroradiological Findings

Incidental Neuroradiological Findings

Judy Illes[1,2], Matthew P. Kirschen[1,2,3]
[1]Stanford Center for Biomedical Ethics, Stanford University, Stanford, USA
[2]Department of Radiology, Stanford University, Stanford, USA
[3]Program in Neurosciences, Stanford University, Stanford, USA
illes@stanford.edu

Synonyms

Accidental clinical findings; Incidentalomas; Lesions of unknown etiology; Unexpected clinical findings

Definitions

►Incidental findings are defined as observations of potential clinical significance made unexpectedly in healthy subjects or in patients recruited to research that are unrelated to the purpose or variables of a study. Clinically significant incidental findings in research, such as that of a tumor or arteriovenous malformation (Fig. 1), are distinguished from discovery of significant findings in clinical situations because they are not prompted by a complaint or an individual's medical history. This entry will focus on the complex issues surrounding the discovery of incidental findings primarily in the domain of neuroimaging research in which tens of thousands of human subjects are scanned each year as healthy volunteers.

A decade of empirical work on incidental findings in brain imaging, genomics, and other areas of research has yielded new knowledge about the frequency, investigator responsibility, and risks and benefits of disclosure. Early guidance on how such unexpected findings might be handled, especially given the variation in clinical significance with which they occur, is offered by the genetics literature. The 1999 National Bioethics Advisory Commission (NBAC) and the 2004 *Working Group on Reporting Genetic Results of NIH's National Heart Lung and Blood Institute*, for example, recommended that research results should be given to subjects if (a) the findings are scientifically valid and confirmed, (b) the findings have significant implications for the subject's health, and (c) a course of action to ameliorate or treat the concerns is readily available. However, the genetics guidelines and discussion address, as intended, data that might predict a health condition rather than reveal the presence of a potentially clinically significant medical condition.

Characteristics

Although case reports and retrospective studies of incidental findings in clinical medicine have been published in the past with some frequency, there were only a few reports of incidental neuroradiological findings in healthy control subjects recruited to brain imaging for research purposes until recently. Early data suggest anomalies in as many as 18–20% of research subjects (1). In 2–8% of the subjects, findings were clinically significant and required clinical evaluation with various degrees of urgency, from routine to immediate, depending on the nature of the finding. In another retrospective study, three of four findings in adults aged 18–59 years were found to require urgent referral (e.g., arteriovenous malformations, extra-axial lesions) (2). In the same study, incidental findings were discovered in 47% of older adults (≥60 years), although most required only routine follow-up such as for nonspecific white matter lesions. In

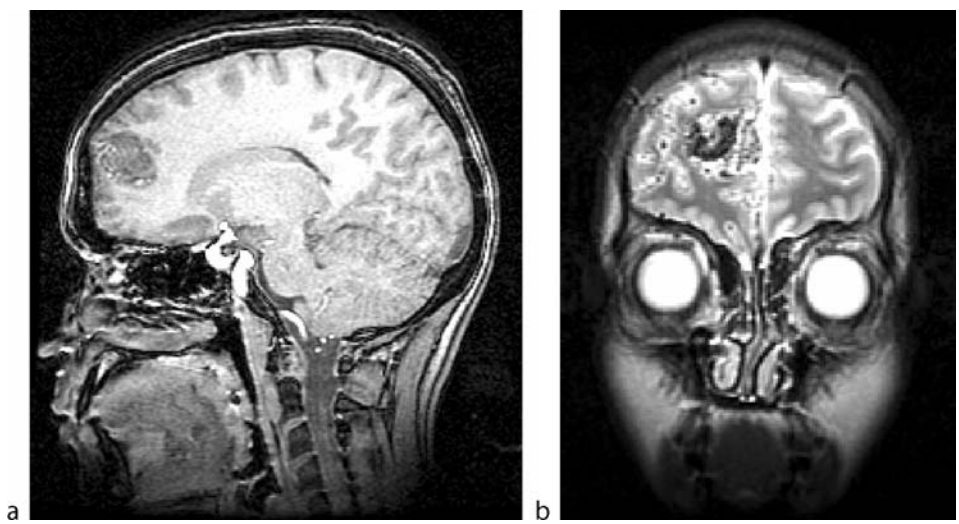

Incidental Neuroradiological Findings. Figure 1 Sagittal T1-weighted (a) and coronal T2-weighted (b) research MRI scans collected at 3T showing an arteriovenous malformation in the right frontal cortex of a 25-year-old woman. The image is displayed in radiological convention. (Courtesy of the Richard M. Lucas MRI Center, Stanford University.)

another study based on a sample of ultra healthy air force pilots, incidence was only a fraction of a percent (3). In a study of 225 pediatric subjects, incidental findings were found in 21%. In 5% of the cohort, the findings were clinically significant (4).

Management

Protocols

Wide variability exists in the way that incidental findings are handled. One group worked for more than a year to develop practical guidelines for managing incidental findings. This group of leaders in neuroscience, bioethics, policy, and law reached consensus that investigators engaged in brain imaging research must anticipate incidental findings in their experimental protocols and establish a pathway for handling them (5). A majority of this group felt that an individual with medical training should review any suspicious brain finding. If there is sufficient reason to think that the finding may be significant, the principal investigator or designate should inform the subject or the subject's surrogate in the case of children or subjects with limited decisional capacity. A minority of the group felt that given continuing uncertainty about true incidence and risks of ▶false positive findings, subjects should be given the option to decline to be told (i.e., right to not know). In addition, they maintained that investigators should have the option not to pursue findings beyond clearly articulating a management plan both to the Institutional Review Board (IRB) and to participants when obtaining informed consent (see also "Disclosure" below). Principal investigators bear primary responsibility for handling all findings in their research and for managing them appropriately.

A variable element in research protocols is the extent and immediacy of the involvement of medically trained staff. Physicians may be involved as principal investigators of a study, as collaborators, or as ad hoc consultants. One obvious impact of physician involvement in a research protocol is in the cost of conducting the research. Another is in the accessibility of medically trained personnel. Beyond the issues of cost and availability is the level of responsibility of a clinician in a research setting. A limited clinical relationship is established that may confer responsibility beyond the researcher–subject relationship when a clinician provides a clinical read of a research scan even for the sole purpose of assessing whether a clinical work-up is mandated, and even with the inherent limitations of the scan given research acquisition parameters.

Disclosure

One of the greatest risks to participants, just as to patients in the clinical setting, is the communication of a suspicious finding that ultimately has no clinical significance. The major consequences involve personal and psychological cost, financial cost, and cost to privacy.

1. Psychological cost: Awaiting clinical work-up for a finding detected in the context of research participation may cause significant anxiety for an individual who, by all measures, is asymptomatic and has contributed altruistically to the research enterprise.

   While mortality of follow-up tests such as routine MRI or CT scans is certainly slight, morbidity may be greater with the administration of contrast or the use of radiation. For certain types of findings (e.g., vascular malformation or tumors) further more risky diagnostic tests such as angiography or biopsy might be indicated. Anxiety may be exacerbated for patients for whom MRI is contraindicated because of claustrophobia.
2. Financial cost: The financial cost of clinical follow-up of an incidental finding is borne by the participant or a third party insurance carrier since such coverage is not a usual part of the funding for research. This is different at a small number of imaging centers in the United States, such as at the National Institutes of Health, where every research subject is required to be a patient and undergoes a complete clinical examination before being entered into a protocol.
3. Cost to privacy: Discovery and follow-up of an incidental finding may have implications for a participant's future medical insurability, even if the result is negative, and possibly to employability in cases where fitness is partly assessed by medical history.

Subject Selection

Challenges to subject selection arise in designing research protocols when incidental findings are a possibility. These include proper inclusion/exclusion criteria based on the risk of incidental findings occurring, subjects' ability to obtain follow-up health care, researchers' ability to track or contact subjects for follow up, and the inclusion of populations that may be vulnerable. Ethical considerations play an important role when thinking about special populations such as pediatric subjects, pregnant subjects, and subjects with limited access to health care and health insurance.

Good neuroimaging studies providing baseline images of "normal" pediatric brains in various developmental stages are lacking and make predictions about the possible clinical significance of a pediatric incidental finding particularly difficult.

Involvement of subjects such as university students and employees of imaging laboratories must be carefully considered given risks to privacy, such as the discovery of an incidental finding and other broader ethics risks such as the possibility of coercion in recruitment. The sense of

subjects' rights in research, such as that of the right to withdraw, maybe also be compromised in a setting in which a power relationship exists.

In the case of adults with diminished decision-making capacity, it is important to clarify who is empowered to make research decisions for the participant. Inclusion of disadvantaged or disenfranchised subjects who do not have ready access to health care, either through a lack of insurance or the availability of medical facilities, is essential to much research involving mental illness and addiction disorders. Protocols should have a safety net for these subjects and for the real costs that may directly stem from the discovery of a finding requiring work up. Requiring contact information is justifiable because of potential for the discovery of life-saving information.

Overall, ensuring the protection of human subjects in neuroimaging, and trust in and integrity of the scientific process are of paramount importance.

References

1. Katzman GL, Dagher Azar P, Patronas Nicholas J (1999) Incidental findings on brain magnetic resonance imaging from 1000 asymptomatic volunteers. JAMA 281:36–39
2. Illes J Rosen AC, Huang L et al (2004) Ethical consideration of incidental findings on adult brain MRI in research. Neurology 62:888–890
3. Weber F, Knopf H (2006) Incidental findings in magnetic resonance imaging of the brain of healthy young men. J Neurol Sci 240:81–84
4. Kim BS, Illes J, Kaplan RT, et al (2002) Incidental findings on pediatric MR images of the brain. Am J Neuroradiol 23:1674–1677
5. Illes J, Kirschen MP, Edwards E et al (2006) Incidental findings in brain imaging research. Science 311:783–784. For further information please visit http://www.ninds.nih.gov/news_and_events/proceedings/ifexecsummary.htm

Incidentalomas

►Incidental Neuroradiological Findings

Incomplete Border Sign

A radiographic finding commonly seen with a pleurally based mass. The inferior border of the mass is well defined as it is imaged tangential to the X-ray beam, whereas the superior border is imaged en-face and therefore appears ill defined.

►Pleural Mesothelioma, Malignant

Incontinence, Urinary

Catherine Roy
Department of Radiology B, University Hospital of Strasbourg, Hôpital Civil 1, Strasbourg, France
catherine.roy@chru-strasbourg.fr

Definition

Dysfunction of the bladder, caused by various abnormalities, is a rather common clinical symptom, especially in women. ►Incontinence, Urinary is defined as any involuntary urine loss that is a social or a hygienic problem. Stress urinary incontinence is defined as urine loss during daily or physical activities that increase abdominal pressure (in the absence of detrusor contraction or overdistended bladder). Perineal descent, cystoceles, and prolapses are often associated with urinary incontinence. Cystoptosis corresponds to the descent of any part of the bladder below the horizontal line drawn at the inferior edge of the pubic bone symphysis. When the neck and the bladder base fall, the result is cervicocystoptosis. When, rarely, the isolated neck falls, it is called cervicoptosis.

Pathology

Urinary incontinence requires integrity of both the nervous system and overall pelvic anatomical support structures, including muscular and fascial components. If the intravesical pressure exceeds the intraurethral pressure, incontinence results. Alternatively, it has been suggested that urethral compression against the endopelvic fascia and vagina is responsible for closure, as stated in the "hammock theory" (1). The most important risk factor for urinary incontinence is obstetric injury first with vaginal delivery, second with prolonged labor, and then forceps delivery. The mechanism of urinary incontinence in pregnancy remains unclear, but it may be due to a combination of endocrine and mechanical factors. Less common causes of urinary incontinence include urethral diverticula, overflow incontinence secondary to pharmacologic or neurologic causes, and very rarely in women bladder outlet obstruction.

Urinary incontinence is divided into two main etiologic groups (1).

Urge Urinary Incontinence (or Vesical Incontinence)

Urge incontinence is the involuntary loss of urine associated with an abrupt and strong desire to void. It is the occurrence

of involuntary contractions during filling or provoked by coughing or postural changes which the patient is unable to inhibit. The diagnosis is made by urodynamic testing. The role of imaging techniques is limited to searching for a rare cause such as a morphologic abnormality, an adjacent pathology, or a neurological disease.

Stress Urinary Incontinence (or Urethral Incontinence)

Stress Urinary incontinence is defined as urine loss during current daily or physical activities that increase abdominal pressure (in the absence of detrusor contraction or overdistended bladder). It may result from two distinct mechanisms: hypermobility of the bladder neck in 75% of cases (HBN) or intrinsic sphincter deficiency (ISD) in the others 25% of cases.

- With HBN, the basic anatomy and function of the bladder neck and urethra are intact. It is primarily caused by weakened pelvic floor support caused by denervation, musculofascial defects, or both secondary to aging, obesity, pregnancy, and vaginal delivery. The bladder neck and proximal urethra descend below their normal pelvic positions during straining, owing to weak musculofascial bladder and urethra attachments to the pelvic wall. When this normal anatomic position is altered, the urethra is no longer able to respond to the increase in abdominal pressure.
- In the case of ISD, the urethral sphincter is defective. It is unable to generate adequate urethral pressure to collapse the urethral lumen, and the bladder neck remains open even at rest. The bladder neck and urethra are well supported in their pelvic position. ISD can be caused by sympathetic nerve injury (surgery, trauma) or by degenerative processes (myelodysplasia, spinal cord lesions at the conus medullaris). Indeed, in most cases, it remains idiopathic.

Clinical presentation

It occurs in 38% of women over the age of 60 years and 59% of women after 75 years. The problem is seen even in the young, occurring episodically in as many as 45% of women over 18 years of age. The initial and essential step for the diagnosis of Urinary incontinence is a clinical examination and urodynamic testing with voiding speed evaluation. Voiding speed, the simplest urodynamic study, is performed particularly on patients with no obvious neurological lesion or those who may have an obstructed bladder outlet.

Imaging

Over the past decade, the most widely used imaging studies were voiding bead chain cystourethrograms and dynamic retrograde urethrograms, in addition to the minimally invasive colpocystodefecography, developed by Bethoux in France (2), and transabdominal ultrasound. These studies are designed to analyze and quantify the mechanisms of incontinence, whereas transabdominal ultrasound is used to assess overall urinary status and postvoiding bladder volume. Alternative advanced ultrasound techniques and ►magnetic resonance imaging (MRI) are now emerging as new tools for imaging pelviperineal defects.

Ultrasound: Ultrasound offers major advantages over X-rays for imaging the bladder and urethra. It provides good soft-tissue morphologic analysis of the urethrovesical junction and dynamic bladder neck imaging with quantified movements. Examinations are easy, relatively quick (10–15 min), and inexpensive. Evaluation is limited, however, to the anterior pelvic compartment, and requires operators to have experience and knowledge of urodynamics (3).

Three different approaches to ultrasound are available today: external ultrasound (transabdominal, perineal, and introital); endosonography (transvaginal and transrectal); and endoluminal (intraurethral) sonography. Transabdominal ultrasound gives an overall evaluation of the urinary tract, but misses the perineal floor.

In perineal scanning, a narrow curved array linear probe (3–5 MHz) or a common sectorial vaginal or transrectal probe (5–7.5 MHz) is applied to the perineum, whereas for introital sonography only the second one can be used, placed under the distal part of the urethra at the introïtus. Image quality depends partly on the probe's proximity to the target area, meaning that endosonography produces the clearest images. However, route choice requires a compromise between image quality and degree of interference in normal lower urinary tract function. Probe placement in endosonography displaces the bladder neck and compresses the urethra. Dynamic studies can consequently be limited, inhibiting normal voiding. Thus, perineal or introïtal US seems to be the pertinent technique using a common endoluminal probe. The sagittal plane is used to obtain a cross-sectional view through the bladder and urethra. The best image quality is obtained with a bladder filled with approximately 300 mL of urine (Fig. 1). Evaluation is first performed at rest in lateral decubitus with knee flexion and in standing position. Dynamic studies are then carried out during pelvic floor contraction and maximum straining in each position.

The normal aspect is a closed bladder neck in all positions or situations (Fig. 2). Correct identification of

I

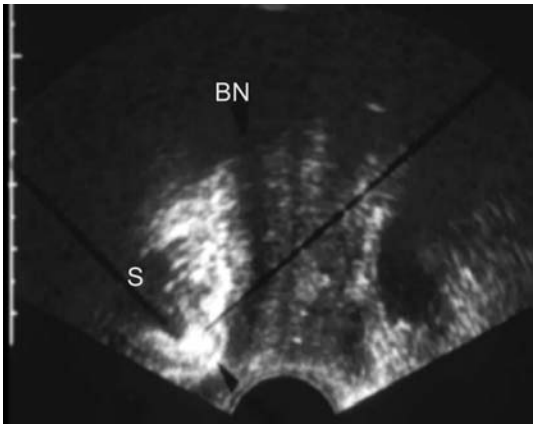

Incontinence, Urinary. Figure 1 ***Ultrasound*** **perineal technique. Sagittal view. Lateral decubitus. Rest. Normal aspect. The probe is located just behind the urethral meatus. The bladder neck (BN) is clearly above the reference line. It is closed. The urethra has a hypoechoic pattern. (S): symphysis pubic bone.**

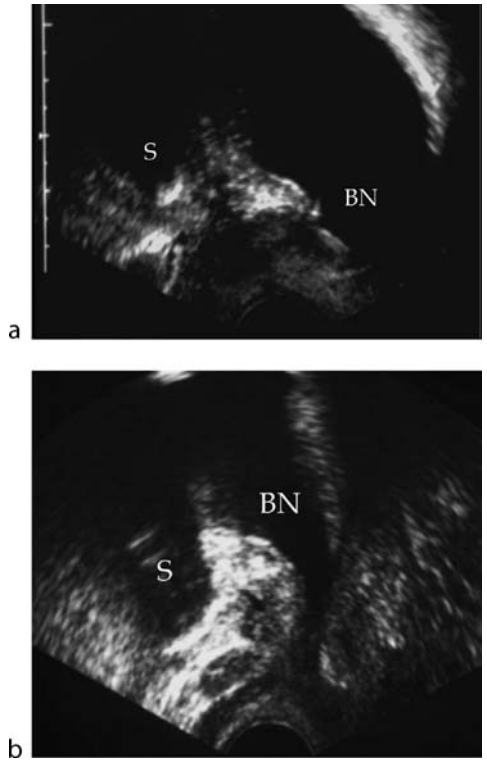

Incontinence, Urinary. Figure 2 ***Perineal ultrasound technique*****. Sagittal view. Lateral decubitus. (a) Hypermobility of bladder neck (HBN). Maximum straining. The bladder neck is under the reference line. It appears slightly funneled. The urethra has moved down and horizontally. Cystocele is associated with enlargment of the angle between the urethra and bladder base. (b) Rest. Intrinsic sphincter insufficiency (ISD). The bladder neck (BN) is opened at rest with a clear funneled aspect. It is located at the level of the inferior border of the symphysis pubic bone (S). There was no abnormal displacement during straining.**

the bladder neck, which should remain closed, can be problematic with external techniques. In certain orientations, notably a strict sagittal view, an anechoic posterior shadow artifact caused by the urethra's fibrous normal component hides the bladder neck. This is easily avoided by tilting the probe slightly.

The long axis of the symphysis and the lower border of the symphysis pubic bone are used as fixed landmarks. The position of the bladder neck and displacements are calculated using a horizontal line as reference perpendicular to the axis of the symphysis (Fig. 1). At rest, the normal position of the bladder neck is above or at the level of the reference line and the angle is around 50°.

The diagnosis of HBN (Fig. 2) can be made with a displacement up to 1 cm associated or not with a low position of the bladder neck at rest under the reference line.

Isolated ISD is suggested by bladder neck funneling or a clearly opened urethra at rest and vesicalization of the urethra or opened urethra with voiding during maximum straining (Fig. 2). However, the position of the bladder inside the pelvic cavity remains within normal limits.In the recommendations of the First International Consultation on Incontinence held in Monaco in 1998 (4), bladder neck and pelvic floor ultrasound were considered only as a complementary investigational imaging technique in the evaluation of female incontinence and pelvic floor disorders and not as diagnostic for stress Urinary incontinence. They also recommended that only residual urine measurement by transabdominal ultrasound should be included in the routine initial evaluation of incontinent patients. However, ultrasound evaluation of the bladder neck can help to document the pelvic floor anatomy and discover mixed abnormalities, which is a rather common finding. Ultrasound can also be used to evaluate postsurgical slings or other medical devices and complications.

Magnetic Resonance Imaging

Pelvic floor weakness is a global abnormality, affecting all three compartments. Noninvasive dynamic imaging of the whole pelvic cavity may also be possible.

Morphologic analysis of muscles is made by T1-weighted spin-echo imaging, whereas T2-weighted fast spin-echo imaging is used for pelvic organs. Highly detailed morphologic evaluation of soft tissues, especially the urethra and bladder neck, is provided by addition of an endoluminal coil, located endovaginally or endorectally. This may be used in combination with a phased array multicoil to assess the

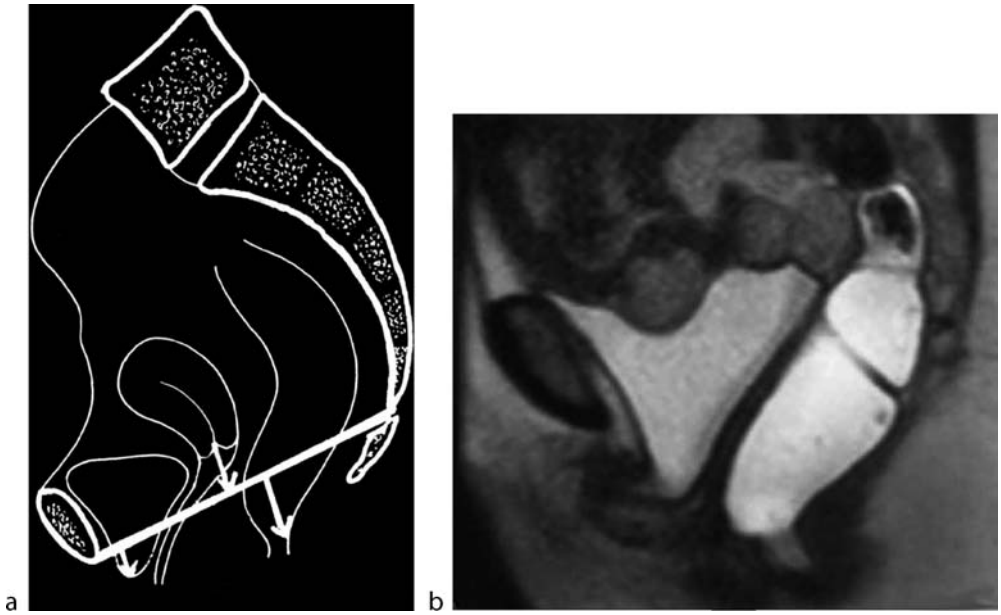

Incontinence, urinary. Figure 3 ***MRI. Sagittal view*****. (a) Drawing of reference line. The pubococcygeal line is commonly used. At normal aspect during rest, the bladder neck is slightly above or at the level of this line. Displacements are easily calculated as shown. This figure demonstrates hypermobility of the bladder neck with normal middle and posterior compartments. (b) Maximum straining. Hysterectomy. Hypermobility with opened bladder neck. Note the associated posterior descent.**

entire pelvic cavity. Fast T2-weighted imaging allows dynamic imaging of the mobility of pelvic floor structures during straining, without any kind of opacification except for the rectum filled with 120 cc of sonographic gel to obtain homogeneous hypersignal inside. Imaging is performed sagittally, to assess displacement, and coronally, to assess levator ani muscles curves. Pelvic prolapse can be imaged in all three compartments simultaneously. Dynamic MRI is used to determine the frequency of associated urinary, genital, and anorectal abnormalities in women with pelvic floor dysfunction.

Pelvic organ descent is measured in relation to a reference line drawn from the inferior border of the symphysis pubic bone to the last coccygeal joint (pubococcygeal or pubosacral lines) on a sagittal plane (Fig. 3). At rest, the normal bladder neck is located between 1 and 2 cm above the reference line or at its level. During straining, the bladder neck goes back and down but remains at the level or slightly below the line. While not as accurate as ultrasound in finding tiny details on the bladder neck or urethra during movement, dynamic MRI can demonstrate an open or funneled bladder neck (Fig. 3). Endoluminal MRI demonstrates the characteristic "target" appearance of the urethra. It is useful in identifying urethral abnormalities (including diverticula) and periurethral tissues (congenital abnormalities, fistulae, tumors).

References

1. De Lancey JO (1994) Structural support of the urethra as it relates to stress urinary incontinence:the hammock hypothesis. Am J Obstet Gynecol 170:1713–1723
2. Béthoux A, Bory S, Huguier M et al (1965) Le colpocystogrramme. Son application à l'étude des prolapsus vaginaux et des incontinences d'urine. J Chir 90:51–62
3. Khullar V, Abbott D, Cardozo LD et al (1994) Perineal ultrasound measurement of the urethral sphincter in women with urinary incontinence:an aid to diagnosis. Br J Radiol 67:713–718
4. Artibani W, Andersen JT, Ostergard DR et al (1998) Imaging and other investigations. In Incontinence. Report of the Ist International Consultation on Incontinence, Monaco
5. Kirschner-Hermanns R, Wein B, Niehaus S et al (1993) The contribution of MRI of the pelvic floor to the understanding of urinary incontinence. Br J Urol 72:715–718

Indirect Imaging

Carmel T. Chan, Sanjiv Sam Gambhir
Department of Radiology, Molecular Imaging Program at Stanford (MIPS) and Bio-X Program, Stanford University School of Medicine, Stanford, USA
carmelc@stanford.edu
sgambhir@stanford.edu

Definition

Indirect imaging refers to imaging a process or molecular target indirectly. For example, if one is imaging a protein target and using that information to infer location(s), activity, or numbers of a different molecular target, which would be considered indirect imaging. The target is often considered a surrogate for the true target of interest. The indirect imaging approach is in distinction to direct imaging in which the target of interest is directly imaged.

Imaging

Indirect imaging is useful when production of an imaging probe specific for a target of interest is difficult/impossible, or when the target of interest is present in relatively low amount and cannot be imaged directly using standard techniques such as labeled antibodies and ligands. For the latter, higher levels of imaging signal per unit level of target and probe interaction can be achieved with indirect imaging through different signal amplification strategies that will be described below (1). Indirect imaging can be accomplished by both radiolabeled probes and optical probes in conjugation with micropositron emission tomography (microPET), bioluminescence/fluorescence imaging respectively, as well as magnetic resonance imaging (MRI). As in the case for direct imaging, a time delay between injection of the probe and imaging is required for clearance of untrapped/unbound probes and enhancement of signal to background ratios, since the scanner cannot distinguish the parent tracer from the bound or metabolized tracer.

Applications Indirect Imaging

Indirect Imaging of Endogenous Gene Expression

In order to monitor endogenous gene expression noninvasively, one would need to develop specific probes that will recognize the gene product(s). For example, labeled antibodies or ligands are needed to detect cell surface proteins and those secreted into the extracellular space whereas another set of probes that can penetrate the cells will be needed to image intracellular targets. Ideally, specific probes can be made to allow direct imaging of targets of interest (See Applications of Direct Imaging in "Direct Imaging".). However, when such probes are not readily available, the expression of an endogenous gene can still be imaged indirectly by fusing the promoter of that gene to drive the expression an imaging reporter gene (Fig. 1). In order to study the regulation of vascular endothelial growth factor (VEGF) noninvasively during wound healing in skin, the express of VEGF protein was indirectly imaged using the Firefly Luciferase (FL) (2, 3)

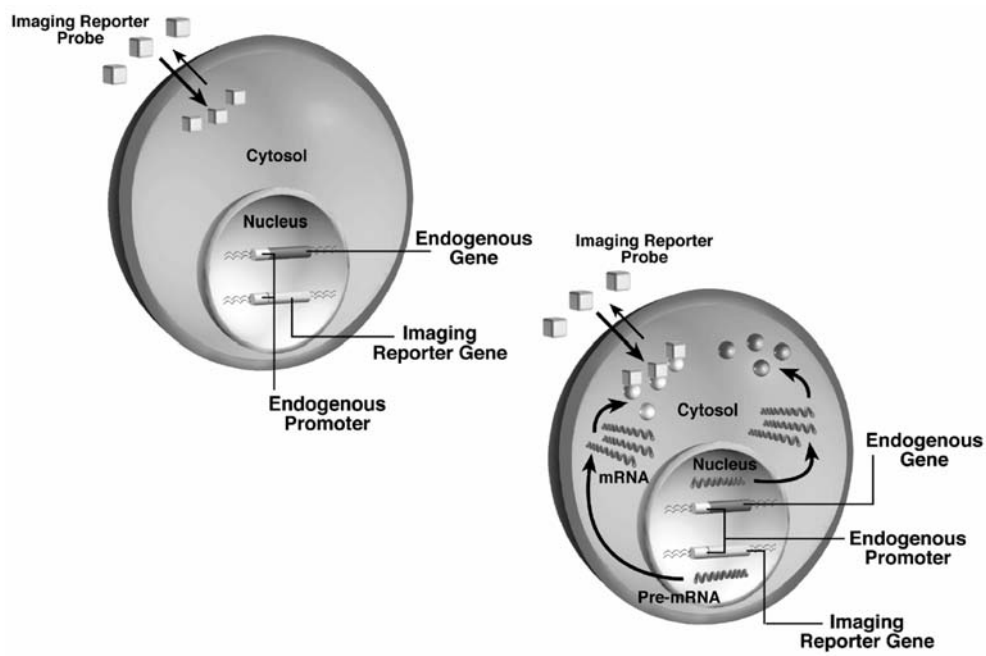

Indirect Imaging. Figure 1 Concept of indirect imaging to monitor endogenous gene expression. An endogenous promoter is fused to an imaging reporter gene of interest. Transcription of the endogenous gene and imaging reporter genes are regulated by the same endogenous promoter. Expression of the endogenous gene can then be indirectly inferred from that of the imaging reporter gene.

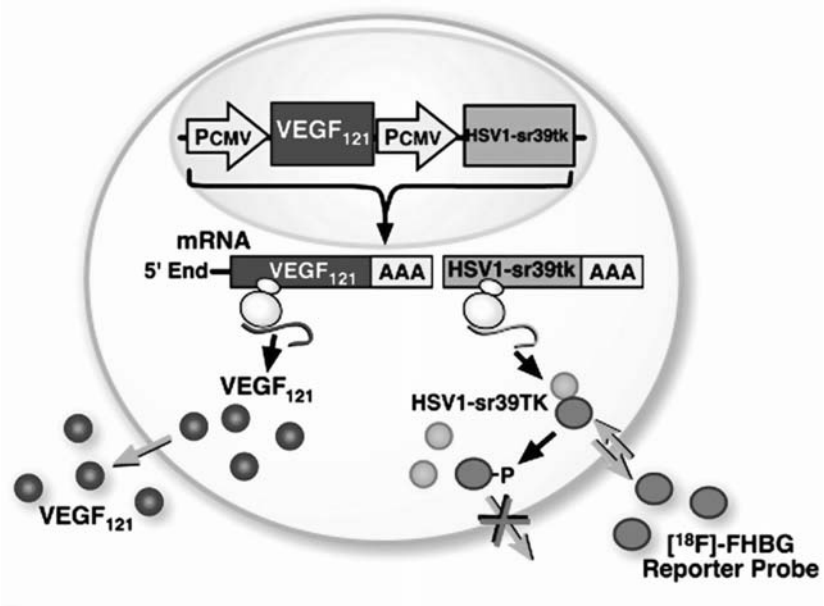

Indirect Imaging. Figure 2 Schematic diagram for indirect imaging of vascular endothelial growth factor (VEGF) expression in a rat myocardium infarction model. An adenovirus carry the gene cassettes expressing the therapeutic $VEGF_{121}$ and HSV1-sr39tk reporter gene was used to infect the rat myocardium. The production of VEGF protein was indirectly imaged by microPET using HSV1-sr39tk as the reporter gene and [^{18}F]-FHBG as the substrate. Reproduced with permission from Wu JC et al (2004) Circulation 110:685–691.

as the optical reporter gene for bioluminescence imaging. The kinetics of VEGF production in the ischemic rat myocardium infected with an adenovirus carrying both VEGF and the Herpes Simplex Virus Type 1 thymidine kinase (HSV-tk) was indirectly imaged by microPET using the HSV-Tk as the reporter gene (1) (Fig. 2). The promoter activity of the prostate-specific antigen (PSA) in a prostate cancer xenograft models was also indirectly imaged using the same approach, in which FL and the mutant HSV-TK (HSV1-sr39tk) were used the reporter gene for optical bioluminescence and microPET imaging respectively. To noninvasively determine the influence of protein diets on endogenous albumin gene expression, a transgenic mouse model in which the endogenous albumin promoter was used to drive the expression of the Mutant HSV-TK reporter gene was utilized. The expression of the albumin gene was indirectly monitored from HSV-tk activity, using microPET in conjunction with 9-[4-[^{18}F]fluoro-3-(hydroxymethyl) butyl]guanine (FHBG) as the HSV-TK substrate. Even though endogenous promoters are highly specific for the genes of interest, they are relatively weak compared to other constitutively active viral promoters such as the cytomegalovirus (CMV) promoter. As a result, direct fusion of an endogenous promoter to the reporter gene(s) often leads to very low levels of reporter mRNA/protein and hence low sensitivity for imaging in living subjects. To circumvent this issue of high specificity but poor sensitivity, the two-step transcriptional amplification (TSTA) system was developed to monitor transcription of a weak/endogenous promoter noninvasively in living animals. The TSTA system is based on the use of a weak/tissue-specific promoter to drive the expression of a strong transcriptional activator (effector), which in turns binds to a strong promoter (e.g. CMV) that drives the expression of the reporter gene (Fig. 3). A bidirectional TSTA system has also been developed that allows simultaneous amplification of two different reporter genes driven by the same promoter, as well as possible replacement of one of the reporter gene with a therapeutic gene of interest. Most recently, transgenic mice models utilizing TSTA system have also been developed to image the tissue-specific and temporal regulation of the PSA promoter and VEGF promoter activity using FL as the reporter gene.

Indirect Imaging of Protein–Protein Interactions

Protein–protein interactions play an important role in all aspects of cell function, including biosynthesis and degradation of macromolecules (DNA, RNA, and proteins), as well as cellular responses to proliferation, differentiation, survival and apoptosis signals. Despite of the rapid increase in number of molecularly targeted agents, the technologies available for studying protein–protein have been limited to *in vitro* analyses such as co-

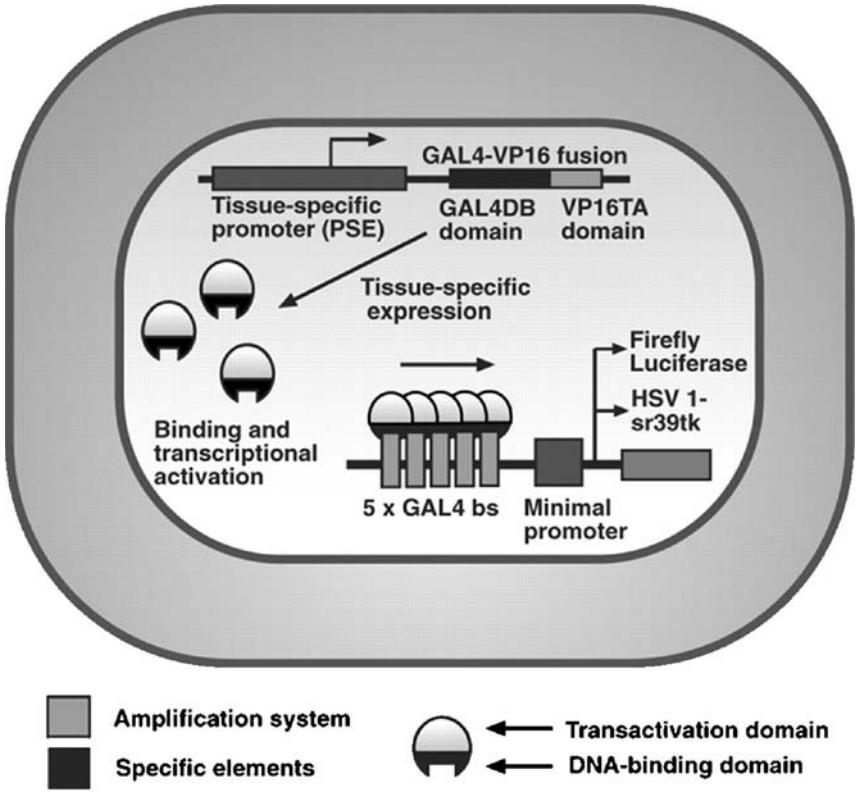

Indirect Imaging. Figure 3 Schematic diagram for indirect imaging of endogenous promoter activity using the two-step transcriptional amplification (TSTA) system. In the first step, the expression of the GAL4-VP16 transactivator is driven by a tissue-specific promoter (e.g., PSE). In the second step, GAL4-VP16 transactivator binds to the GAL4 response elements in a minimal promoter to drive the expression of reporter genes (either *fl* or HSV1-sr39tk), leads to reporter protein, which in turn leads to a detectable signal in the presence of the appropriate reporter probe (D-Luciferin for FL and FHBG for HSV-sr39tk). The TSTA system thus allows amplification of the imaging signals without sacrificing tissue specificity. Reproduced with permission from Iyer M et al (2001) PNAS 25:14595–14600).

immunoprecipitation (co-I.P.)/western blotting and cell binding and cytotoxicity assays, which are labor intensive and invasive in nature. To overcome limitations in studying protein–protein interactions intact cells in their native environment, the split Renilla Luciferase (RL)–Protein-Fragment-Assisted-Complementation (SRL–PFAC) technology and other split reporter protein strategies were developed and validated for noninvasive, indirect imaging of protein–protein interactions, both in cell culture and in living animals (4). The SRL–PFAC is based on the complementation of N-terminal (amino acids (aa) 1–229) and C-terminal fragments (aa 230–311) of full length RL mediated by two interacting proteins. As proof-of-principle, interaction between the transcription factors MyoD and Id was imaged noninvasively in tumor cells, both in cell culture and in living animals. The SRL–PFAC has also been adapted to monitor homodimerization of HSV1-TK (5) as well as rapamycin-mediated interaction between mTOR kinase and immunophilin FKBP12. In addition to the split RL, split firefly luciferase, split β-galactosidase and split β-lactamase PFAC have also been developed to monitor protein–protein interactions and protein translocation in intact cells. Advantages of using split enzyme fragment-assisted-complementation technologies for indirect imaging of protein–protein interactions include signal amplification through the enzymatic reaction in the presence of the substrates, the ability to study protein–protein interactions in intact cells in their native environment and repetitively image the same animal for dynamic monitoring of protein–protein interaction in response to therapies. See "Protein–Protein Interactions, Applications." for a more detailed description of molecular imaging of protein–protein interactions.

Indirect Imaging of Pharmacokinetics and Pharmacodynamics of Drug Treatment

Indirect imaging has also been utilized to monitor the pharmacokinetics and pharmacodynamics of drug treatment. For example, contrast enhanced ^{1}H MRI and

functional magnetic resonance spectroscopy (fMRS) have been used to indirectly monitor the release of the antimetabolite fludarabine monophosphate and gadolinium (Gd)-DTPA from an interstitial liposome depot in rats, respectively (6). The effect of tamoxifen in a murine breast cancer xenograft model in rats was indirectly imaged by dynamic contrast-enhanced MRI to monitor vascular permeability (7). Most recently, the stomach acidity (pH) in rats treated with different nitroxide compounds were monitored using low-field electron paramagnetic resonance techniques that can be extended for monitoring of drug pharmacology and different biological processes such as wound healing and tumor acidosis (8). Indirect imaging has also been used for evaluation of the pharmacodynamics of response to therapy. Heat shock protein 90 (HSP90) is involved in protein folding and is overexpressed in cancer cells. 17-allylamino-demethoxy geldanamycin (17-AAG) is a HSP90 inhibitor known to degrade HSP90 client proteins such as HER2. The efficacy of 17-AAG in a mouse tumor xenograft models was determined using cell-surface HER2 receptor as a surrogate marker (9). The expression of cell-surface HER2 before and after treatment with 17-AAG was determined by microPET imaging. 17-AAG was found to decrease the level of cell-surface HER2. However, since 17-AAG inhibits the chaperone activity of HSP90 and subsequently lead to degradation of multiple client proteins, down-regulation of cell-surface HER2 alone may not be the sole determinant for response to 17-AAG treatment.

Indirect Imaging Tumor Grades and Responses to Treatment Using Radiolabeled Metabolic Tracers and MRI Contrast Agents

Chemotherapy and radiation treatment can lead to decrease in tumor size, proliferation as well as metabolism and these events can be imaged indirectly using metabolic tracers (10). For example, ^{18}F-2-fluoro-2-deoxyglucose [^{18}F-FDG] is a biochemical mimic of glucose that can be transported into the cells by the glucose transporter and phosphorylated by hexokinase and retained inside the metabolically (glycolytic) active cells. FDG can be considered a direct imaging technique if one is interested in determining glucose transporter levels and/or hexokinase activity, but if instead FDG uptake/accumulation is being used to infer levels of other proteins or a cellular process than this should be considered indirect imaging. FDG has been used for diagnosis, staging and evaluation of response to chemotherapy in different cancers in human. Another metabolic tracer that has been used for cancer imaging is 3′-deoxy-3′-[^{18}F] fluorothymidine (FLT). FLT is transported into cells by the nucleoside transporter and subsequently phosphorylated by human thymidine kinase, which is upregulated before and after DNA proliferation. FLT has also been used as a marker for cell proliferation in staging as well as evaluation of response to chemotherapy in tumor xenograft models as well as in human clinical trials. In addition to being indirect imaging agents for evaluation of a drug/treatment that is targeted to an upstream or downstream effects of proliferation, FLT and FDG can also be used for direct imaging for mammalian thymidine kinase activity and hexokinase activity respectively. In addition to PET, MRI has also been used for screening, staging of tumor grades and responses to treatment in conjunction with different contrast agents such as gadolinium and superparamagnetic iron oxide particles.

Nuclear Medicine

- PET

Diagnosis

- Oncology-tumor staging and diagnosis
- Cardiology-indirect imaging of promoter activity and gene expression
- Pharmacokinetics and pharmacodynamic of chemotherapy agents and tracers

References

1. Massoud TF et al (2003) Molecular imaging in living subjects: seeing fundamental biological processes in a new light. Genes Dev 17 (5):545–580
2. Zhang N et al (2004) Tracking angiogenesis induced by skin wounding and contact hypersensitivity using a Vegfr2-luciferase transgenic mouse. Blood 103(2):617–626
3. Ryan PL et al (2005) Photonic monitoring in real time of vascular endothelial growth factor receptor 2 gene expression under relaxin-induced conditions in a novel murine wound model. Ann NY Acad Sci 1041(1):398–414
4. Paulmurugan R et al (2005) Imaging protein-protein interactions in living subjects. TrAC Trend Anal Chem 24(5):446–458
5. Massoud TF et al (2004) Molecular imaging of homodimeric protein-protein interactions in living subjects. FASEB J 18(10): 1105–1107
6. Port R et al (2006) Simultaneous sustained release of fludarabine monophosphate and Gd-DTPA from an interstitial liposome depot in rats: potential for indirect monitoring of drug release by magnetic resonance imaging. Cancer Chemother Pharmacol 1–11
7. Marzola PP et al (2005) Effect of tamoxifen in an experimental model of breast tumor studied by dynamic contrast-enhanced magnetic resonance imaging and different contrast agents. Invest Radiol 40(7):421–429
8. Potapenko DI et al (2006) Real-time monitoring of drug-induced changes in the stomach acidity of living rats using improved pH-sensitive nitroxides and low-field EPR techniques. J Magnetic Resonance, 182(1):1–11
9. Smith-Jones PM et al (2004) Imaging the pharmacodynamics of HER2 degradation in response to Hsp90 inhibitors 22(6):701–706
10. Barentsz J et al (2006) Commonly used imaging techniques for diagnosis and staging. J Clin Oncol 24:3234–3244

Induratio Penis Plastica (IPP)

▶Peyronie's Disease

Indurative Mastopathy

▶Radial Scar, Breast

Infantile Choriocarcinoma

Rare tumor developing from the mother's placenta and spreading to the child. Hypervascularized lesion with infant anemia. Usually rapid tumor progression with deathly outcome. High levels of beta-HCG are diagnostic.
▶Hepatic Pediatric Tumors, Malignant

Infantile Cortical Hyperostosis

▶Caffey Disease

Infantile Hemangioendothelioma, Hepatic

Variant of cavernous hemangioma. Lesion presents often in the first 6 months of life and the majority of the patients are less than 1 month of age. Infantile hemangioendothelioma is most commonly a diffuse alteration with typical histological findings. The vascular channels in hemangioendothelioma are thinner compared to the vascular channels in hemangioma.
▶Hepatic Pediatric Tumors, Benign

Infarction, Renal

O Hélénon, E Dekeiser, JM Correas
Necker Hôpital, Service de Radiologie
Paris, France
olivier.helenon@nck.aphp.fr

Synonyms

Infarct; Ischemic necrosis; Necrotic area

Definition

Renal infarction is defined as a coagulated necrotic area of renal parenchyma that results from renal arterial occlusion.

Pathology/Histopathology

The loss of blood supply results in a wedge-shaped area of coagulative necrosis that affects mostly the renal cortex but can extend into the medulla. It produces a pale area of ischemic renal tissue. Some blood supply from capsular vessels is responsible for the presence of a viable subcapsular band of cortex. The size of parenchymal loss depends on both the distribution of the occluded artery and the development of collateral arterial supply arising from the pelvicalyceal arterial network and transcapsular perforating arteries. After several weeks the infarcted parenchyma starts to shrink and will leave a cortical scar.

Renal infarction can result from various causes including embolism mechanism in patients with cardiovascular diseases, renal artery spontaneous dissection, vasculitis, shock, and trauma. In renal transplant, it is mostly due to renal arterial branch injuries occurring during surgery including kidney removal in donor and transplantation.

Clinical Presentation

Acute renal infarction produces acute symptoms including sudden onset of flank pain and tenderness or upper abdominal pain, fever, hypertension, hematuria, proteinuria and leukocytosis. Patient also can be asymptomatic.

Imaging

Color-Doppler Ultrasound

At color-Doppler ultrasound (CDUS), segmental infarct appears as hypoechoic area with complete loss of Doppler signals showing color flow defects with sharp edges (1) (Fig. 1). Appropriate settings (low pulse repetition frequency, PRF and optimal gain) are mandatory to obtain optimal sensitivity of the technique. Although CDUS is a valuable method in the detection of renal allograft necrosis, it is less accurate for the diagnosis of perfusion defects in native kidneys because of their deeper location. Perfusion assessment at the level of the upper and lower poles is limited by the direction of the vessels perpendicular

to the US beam. The diagnosis of small perfusion defects in native and transplanted kidneys also remains difficult despite the improvement of the Doppler technique, particularly in small hypoperfused kidneys.

Ultrasound contrast agents are helpful to improve the performance of CDUS in case of technical problems and/or the small infarct size. When the renal function is compromised, they provide critical information without any renal toxicity even at the bedside of the patients. Postcontrast studies using nonlinear gray-scale imaging provide the highest resolution and sensitivity in the detection of cortical defects at an early arterial phase following contrast injection (2, 3) (Fig. 2). In renal transplants, contrast-enhanced US plays a critical role to differentiate ischemia due to medical complications, such as acute tubular necrosis and acute rejection, from true infarction.

CT and MRI

►Contrast-enhanced CT remains the gold standard in the diagnosis of renal infarction. It easily demonstrates the presence of a perfusion defect, as a wedge-shaped nonenhancing area triangular in shape and cortically based, typically associated with a subcapsular enhanced rim of cortex supplied by capsular arteries (called "rim sign") (4) (Fig. 3). Such a cortical rim helps differentiate defects of ischemic origin from hypoattenuating infiltrative lesions such as acute pyelonephritis. Focal renal swelling can also be seen at an acute phase. Follow-up CT examinations show progressive reduction of the size of the cortical defect that lead to a cortical scare after several months (Fig. 4).

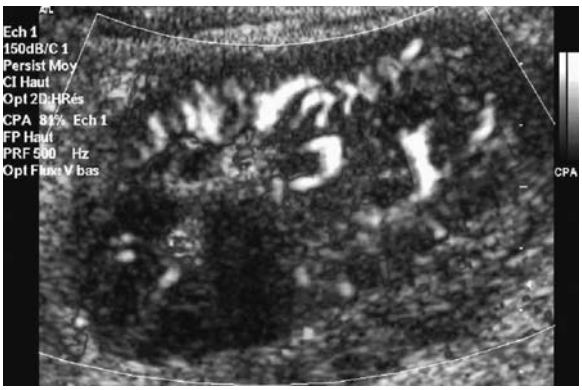

Infarction, Renal. Figure 1 Power Doppler US of a renal infarction. Longitudinal scan of the left kidney shows hypoechoic area of the upper pole with loss of color Doppler signal.

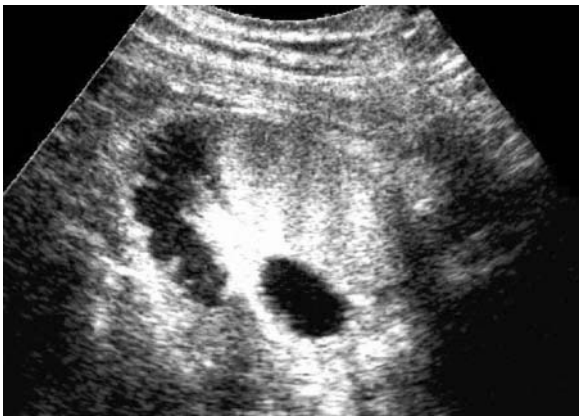

Infarction, Renal. Figure 2 Contrast-enhanced gray-scale US of a renal infarction. Transverse scan following contrast injection shows a wedge-shaped nonenhancing area related to arterial perfusion defect.

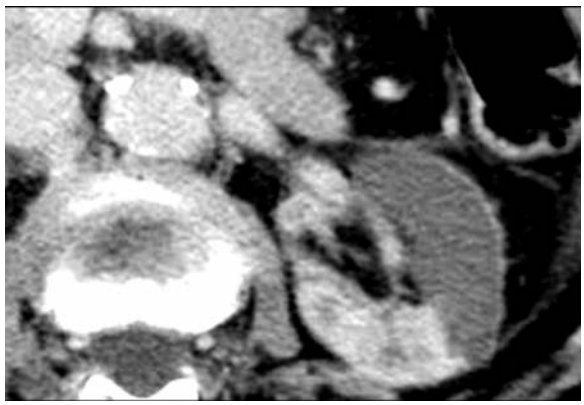

Infarction, Renal. Figure 3 Acute segmental infarction of the left kidney. Contrast-enhanced CT scan shows the presence of a large wedge-shaped nonenhancing perfusion defect associated with a subcapsular enhanced rim of cortex.

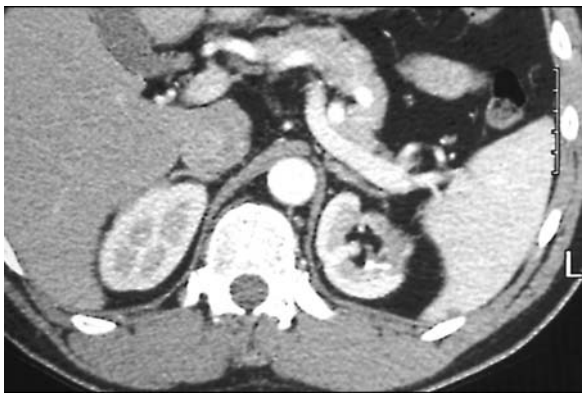

Infarction, Renal. Figure 4 Follow-up CT scan 6 months after infarction of the left kidney. Segmental infarction has lead to a cortical scare.

I

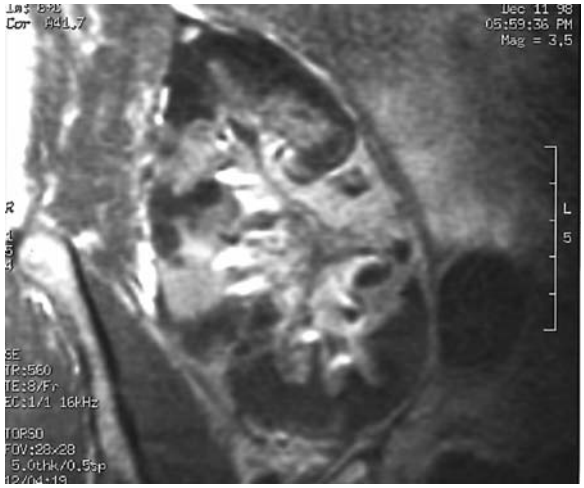

Infarction, Renal. Figure 5 Multifocal cortical infarction after renal transplantation. Contrast-enhanced MR imaging shows multiple perfusion defects. Note the presence of a typical rim sign at lower pole.

Gadolinium-enhanced MR imaging, especially in patients with critical renal failure, is also a modality of choice particularly when early accurate diagnosis is clinically required. The infarcted area exhibits a slight increase in signal intensity on T2-weighted images and is hypointense on T1-weighted images (5). Postcontrast features are similar to that of CT findings (Fig. 5).

Nuclear Medicine

Scintigraphy is of limited value in the diagnosis of renal of renal infarction. It can however demonstrate a focal loss of tracer uptake corresponding to the region of parenchymal infarction.

Diagnosis

Clinical history and findings are often confusing since it can mimic acute pyelonephritis or renal colic. While CDUS can strongly suggest the diagnosis at initial screening, accurate diagnosis relies on contrast-enhanced cross-sectional techniques (CT or MRI) or even contrast-enhanced US in skill hands.

Bibliography

1. Hélénon O, El Rody F, Correas JM, et al (1995). Color Doppler US of renovascular disease in native kidneys. Radiographics 15: 833–854
2. Taylor GA, Barnewolt CE, Claudon M, et al (1999). Depiction of renal perfusion defects with contrast-enhanced harmonic sonography in a porcine model. Am J Roentgenol 173:757–760
3. Correas JM, Hélénon O, Moreau JF (1999). Contrast-enhanced ultrasonography of native and transplanted kidney diseases. Eur Radiol S3:394–400
4. Wong WS, Moss AA, Federle MP, et al (1984). Renal infarction: CT diagnosis and correlation between CT findings and etiologies. Radiology 150:201–205
5. Hélénon O, Attlan E, Legendre C, et al (1992). Gd-Dota-enhanced MR imaging and color Doppler US of renal allograft necrosis. Radiographics 12:21–33

Infarction, Spleen

Splenic infarction is a relatively rare disease. It is the result of arterial or venous compromise and is associated with a heterogeneous group of diseases, including embolic and autologic disorders, splenic vascular diseases, and anatomic abnormalities. Splenic infarction may be segmental or global, involving the entire organ.

▶Spleen, Infectious Diseases

Infected Necrosis, Pancreatic

Pancreatic necrosis is a diffuse or focal area of nonviable pancreatic parenchyma, which is typically associated to acute pancreatitis with peripancreatic fat necrosis. Secondary infection of the pancreatic necrosis is a possible complications and leads to clinical findings of infection. Distinction between sterile and infected necrosis is critical, since development of infection increases the mortality risk. Often cultures obtained by needle aspiration are necessary and surgical drainage is needed.

▶Pancreatitis, Acute

Infection

An inflammation resulting from the invasion of the body by pathogenic microorganisms.

▶Oral Cavity, Inflammatory Diseases
▶Infection Imaging

Infection of Skeletal Muscle

▶Infection, Soft Tissue

Infection of the Breast

►Breast, Infection

Infection, Opportunistic, Brain

Majda M. Thurnher
Universitätsklinik für Radiodiagnostik, Medizinische Universität Wien, Vienna, Austria
majda.thurnher@meduniwien.ac.at

Synonyms

Cerebral infections; Immunsuppression

Definition

►Opportunistic infections are infections caused by organisms that usually do not affect persons with a healthy immune system, but can affect people with a poorly functioning immune system.

Pathology/Histopathology

Viral Infections

Cytomegalovirus

Cytomegalovirus (CMV) is the member of the herpesvirus family, the infection in adults is a result of the reativation of a latent infection. Small microglial nodules and inclusion-bearing cytomegalic cells are widely distributed in the cortex, basal ganglia, brain stem, and cerebellum in CMV diffuse micronodular encephalitis (1).

Progressive Multifocal Leukoencephalopathy

►Progressive multifocal leukoencephalopathy (PML) is a subacute opportunistic infection caused by JC *Polyomavirus* (JCV) with increased incidence due to the acquired immunodeficiency syndrome (AIDS) epidemic (0.7–11% of HIV patients will develop PML during the course of their illness) (2). The histopathological hallmark of PML is demyelination with enlarged oligodendroglial nuclei and bizzare astrocytes. The disease is usually multifocal, and the lesions may occur in any location in the white matter.

Fungal Infections

Cryptococcosis

Approximately 5–10% of patients with AIDS develop CNS ►cryptococcosis caused by *Cryptococcus neoformans*. The infection is a result of a newly acquired infection with hematogenous dissemination of the infection from the lung to the CNS. Cryptococcal meningitis is the most common manifestation, where the subarachnoid spaces are thickened and filled with multiple organisms and their material. From the subarachnoid space, cryptococcus extends along the Virchow-Robin perivascular spaces into the basal ganglia, thalami, midbrain, and cerebellum. The Virchow-Robin spaces become dilated. With disease progression, dilated perivascular spaces become confluent and cystic lesions develop called "gelatinous pseudocysts." Cryptococcoma is the only parenchymal form of the cryptococcal CNS infection. The lesions result from the direct invasion of the brain by the fungus with the development of a granulomatous reaction.

Aspergillosis

Aspergillusis accounts for 18–28% of all fungal brain abscesses, and it is the most common CNS complication following bone marrow transplantation. Meningitis, abscess or granuloma, vascular invasion with thrombosis and infarction, and hemorrhage and aneurysm formation are manifestations of cerebral ►aspergillosis. Pathologically, hyphal elements invade cerebral vessels, resulting in thrombosis and infarctions. Sterile infarctions become septic when the fungus erodes the wall of the vessel with extension into the brain parenchyma with inflammatory reactions and necrosis.

Parasitic Infections

Toxoplasmosis

Cerebral ►toxoplasmosis results from infection by an intracellular protozoan, *Toxoplasma gondii*.

After the acute infection, the latent form, called encysted bradyzoites, remains in the tissues until a decline in immunity. Rupture of the cysts releases the free tachyzoite, which causes acute illness. In AIDS patients, toxoplasma causes necrotizing encephalitis.

Clinical Presentation

Viral Infections

Cytomegalovirus

In immunocompromised patients, CMV can produce a variety of clinical syndromes. Five distinct neurological

syndromes due to the CMV infection have been described: retinitis, myelitis/polyradiculopathy, diffuse micronodular encephalitis, ventriculoencephalitis, and mononeuritis multiplex.

Progressive Multifocal Leukoencephalopathy

Pyramidal signs, gait disturbances, hemiparesis, extrapyramidal and cerebellar signs, sensory deficits, cognitive dysfunctions are parts of the "multifocal" clinical picture of PML. Without treatment, the prognosis for PML is usually poor, with death occurring after 2.5 to 4 months. Only a small number of cases will have a more benign clinical course (only 7 to 9% of patients demonstrate prolonged survival without therapy). Recent studies have shown clinical and radiological improvements in patients with PML who underwent highly active antiretroviral therapy (HAART).

Fungal Infections

Aspergillosis

Clinical presentation of cerebral aspergillosis includes fever, alterations of mental status, seizures, depression. In some cases stroke-like symptoms will develop.

Parasitic Infections

Toxoplasmosis

The clinical symptoms in cerebral toxoplasmosis are nonspecific; usually patients have fever, seizures, headaches, or altered mental status.

Imaging

Viral Infections

Cytomegalovirus

The most common imaging findings in patients with CMV encephalitis are: cortical atrophy, periventricular enhancement, and diffuse white matter abnormalities. Generalized atrophy is the most commonly reported CT abnomality, but it is a nonspecific finding. Periventricular enhancement is also not diagnostic; it has been described in cases of lymphoma, toxoplasmosis, and other infections. Rarely, cerebral mass lesions due to CMV or choroids plexitis were observed.

Progressive Multifocal Leukoencephalopathy

The findings on MR imaging correlate very well with macroscopic changes. PML lesions are patchy, scalloped, high signal intensity lesions on T2-WI MR images located in the white matter with extension along the white fibers (2). Subcortical arcuate fibers are involved, mass effect is mild or absent, and peripheral, faint enhancement is a rare feature. On T1-WI images, the PML lesions are marked hypointense (Fig. 1).

Fungal Infections

Cryptococcosis

In cases of cryptococcal meningitis CT scans rarely show meningeal enhancement, whereas enhanced T1-WI MR

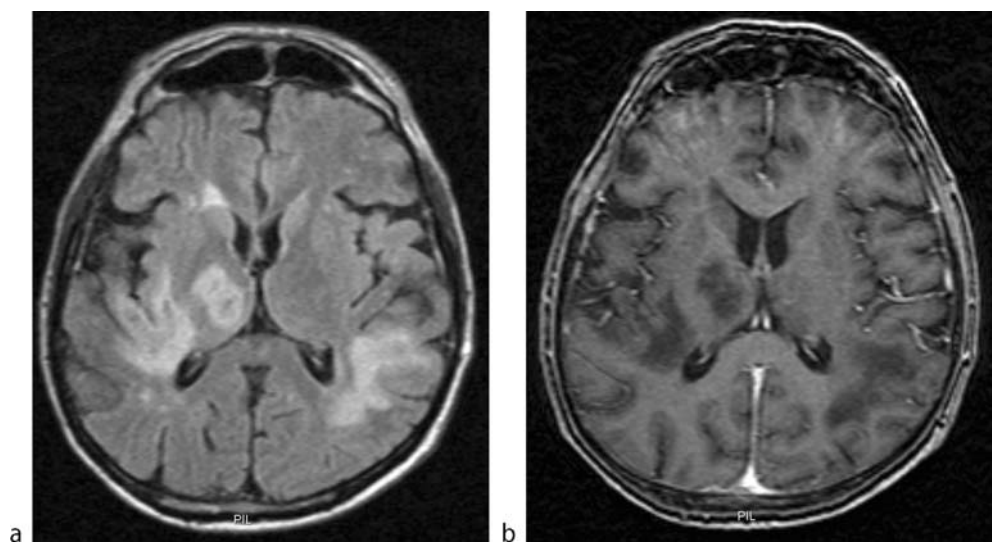

Infection, Opportunistic, Brain. Figure 1 PML in an 35-year-old male HIV positive patient. On axial fluid-attenuated inversion-recovery (FLAIR) MR image (a) high signal intensity lesions located bilateral in the white matter, without involvement of the subcortical fibers are observed. The lesions are hypointense on T2-WI MR image (not shown) and do not show enhancement on postcontrast images (b). Mass effect is also not present.

images may demonstrate meningeal disease. Dilated perivascular spaces will be recognized on MR images as multiple, bilateral, small round- or oval-shaped lesions, located usually in the basal ganglia, which show high signal on T2-WI images, and have signal slightly higher than the CSF on T1-WI MR images. Enhancement is not present. Gelatinous cysts do not differ from the dilated Virchow-Robin spaces on MR images. Enhancement and mass effect are also absent. On CT, cryptococcomas are hypodense with high signal on T2-WI images, and low signal on T1-WI MR images. On enhanced images, the lesions usually demonstrate a ring-like or nodular enhancement, and cannot be distinguished from granulomas of other origin.

Aspergillosis

On MR imaging, brain lesions in aspergillosis usually have low signal centrally or peripherally on T2-WI images, probably due to accumulation of fungi containing iron, magnesium, and manganese, as well as blood breakdown products (Fig. 2). Contrast enhancement is rarely present, depending on the severity of the immunocompetence (3).

Parasitic Infections

Toxoplasmosis

On nonenhanced CT scans, toxoplasma lesions are hypodense with edema and mass effect. Solid, nodular- or ring-enhancing lesions are typically observed on postcontrast scans. On T1-WI MR images, toxoplasma lesions have iso-to-low signal centrally. Signal intensity on T2-WI images depends on the stage of the lesion, which could be iso, hypo, or hyperintense (4). Enhanced T1-WI images reveal ring or nodular enhancement. Approximately 10 days after the initiation of therapy, a decrease in the number and size of the lesions with reduction in edema and mass effect should be observed on follow-up MR examinations (Fig. 3). Calcifications are often seen in healed foci. The MR spectroscopic pattern of toxoplasma lesions is nonspecific, consistent with anaerobic inflammation within the abscess.

Nuclear Medicine

Viral Infections

Progressive Multifocal Leukoencephalopathy

Patients with PML had two different patterns on thalium and gallium scans: patients with positive gallium and negative thallium scans, and a second group with negative thallium and gallium scans. Demyelination and destruction explain negative thallium and gallium scans. Positive gallium and negative thallium scans may be a result of coexisting pathology.

Parasitic Infections

Toxoplasmosis

Based on conventional MR imaging, cerebral toxoplasmosis cannot be distinguished from primary cerebral lymphoma.

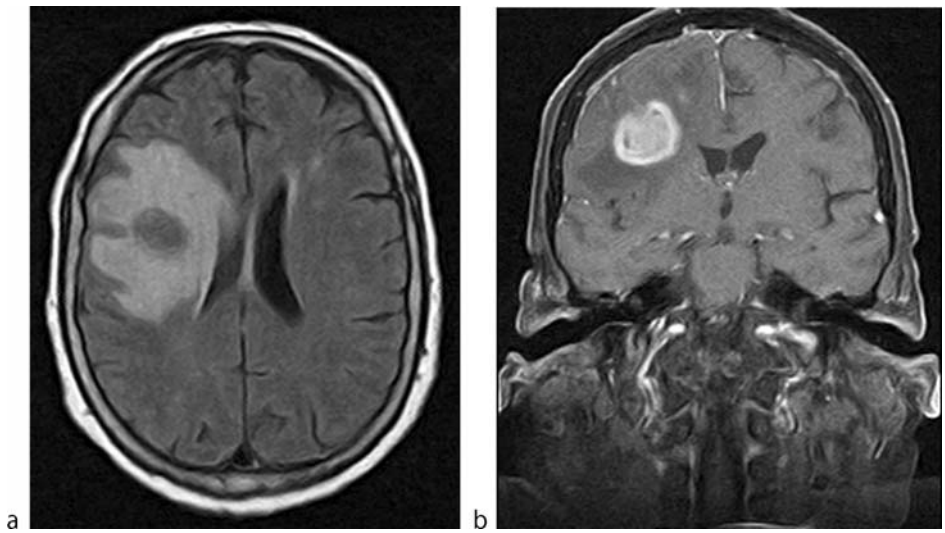

Infection, Opportunistic, Brain. Figure 2 Cerebral aspergillosis in a female patient 2 months after bone marrow transplantation. Low signal intensity lesion with extensive perifocal edema located in the white matter of the right frontal lobe is shown on axial FLAIR MR image. (a) Marked enhancement of the lesion is demonstrated on coronal postcontrast T1-weighted MR image with fat suppression (b).

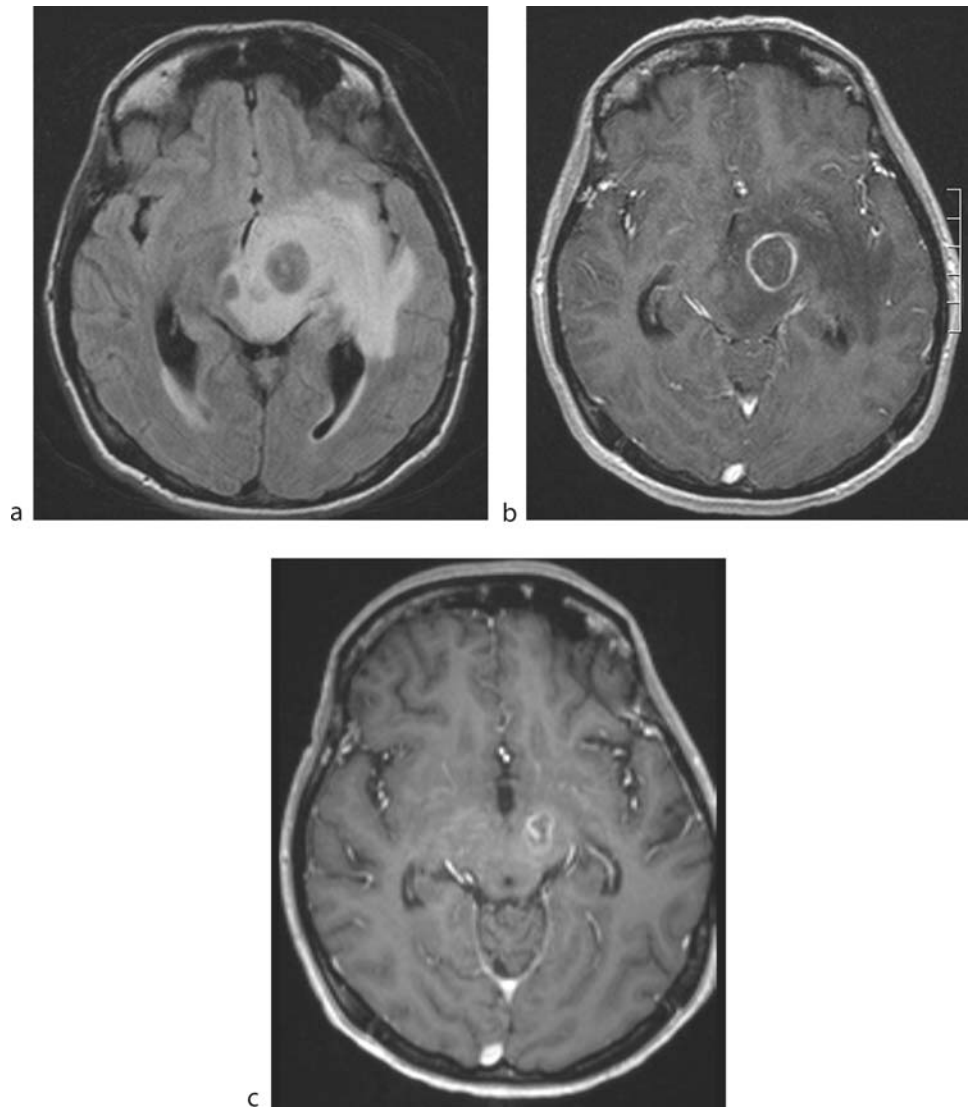

Infection, Opportunistic, Brain. Figure 3 Cerebral toxoplasmosis in an AIDS patient. On axial FLAIR MR image (a) hypointense lesion with perifocal edema located in the left basal ganglia region is hown. On axial postcontrast T1-weighted MR image (b) ring-like enhancement of the lesion is demonstrated. Decrease in size and enhancement is shown on follow-up MR examination (c) 1 month after the initiation of antitoxoplasmosis treatment.

The use of Thallium-201 (^{201}TI) brain SPECT in AIDS patients has been proven to be very helpful in distingushing toxoplasmosis from lymphoma (Ruiz). Positive ^{201}TI brain SPECT is suggesstive of CNS lymphoma, and negative uptake suggests infection in AIDS patients.

The potential use of F-18 fluorodeoxyglucose (FDG)-positron emission tomography (PET) in differentiating lymphoma from toxoplasmosis in AIDS patients has been also examined (5). The standardized uptake values (SUVs) over cerebral lesions were much higher in lymphomas than in toxoplasma lesions.

Diagnosis

Viral Infections

Cytomegalovirus

The infection of the CNS due to CMV is difficult to diagnose while the patient is alive because the virus is difficult to culture from cerebrospinal fluid (CSF). The recent development of the polymerase chain reaction (PCR) technique has allowed isolation of CMV based on the presence of DNA within the CSF.

Progressive Multifocal Leukoencephalopathy

A rapid onset of symptoms in an HIV positive patient with multifocal clinical picture, typical MR imaging findings, and positive JCV PCR in CSF are sufficient evidence for clinical diagnosis of PML. However, a negative result of JCV DNA PCR of the CSF does not rule out PML.

Fungal Infections

Aspergillosis

Because of the high mortality rate of 85–100% early suspicion of aspergillosis is essential. The diagnosis is usually based on a combination of clinical findings in a patient with risk factors and isolation of the microorganism, radiological data, serological detection of antibodies or antigens, or histopathological evidence of invasion.

Parasitic Infections

Toxoplasmosis

Differentiation between lymphoma and toxoplasmosis in AIDS patients remains a diagnostic dilemma. The combination of a neuroradiological examination, a compatible radionuclide study (^{201}TI SPECT, PET), and CSF analysis (Epstein–Barr virus DNA) is a current approach in those patients.

Bibliography

1. Morgello S, Cho E, Nielsen S et al (1987) Cytomegalovirus encephalitis in patients with acquired immunodeficiency syndrome: an autopsy study of 30 cases and a review of the literature. Hum Pathol 18:289–297
2. Thurnher MM, Thurnher SA, Mühlbauer B et al (1997) Progressive multifocal leukoencephalopathy in AIDS: initial and follow-up CT and MRI. Neuroradiology 39:611–618
3. Dietrich U, Hettmann M, Maschke M et al (2001) Cerebral aspergillosis: comparison of radiological and neuropathologic findings in patients with bone marrow transplantation. Eur Radiol 11:1242–1249
4. Brightbill TC, Ihmeidan ICH, Donovan Post MJ et al (1995) Neurosyphilis in HIV-positive and HIV-negative patients: neuroimaging findings. Am J Nuroradiol 16:703–711
5. Villringer K, Jager H, Dichgans M et al (1995) Differential diagnosis of CNS lesions in AIDS patients by FDG-PET. J Comput Assist Tomogr 19:532–536

Infection, Soft Tissue

Catherine M Phan, Thomas M Link
Hôpital de Bicêtre, Service de Radiologie BROCA, Le Kremlin-Bicêtre, France
catherine.phan@bct.aphp.fr

Synonyms

Infectious myositis; Infection of skeletal muscle; Primary muscle abscess; Pyomyositis

Definition

Soft tissue infections can develop separately, but frequently they are associated with musculoskeletal infections involving joints and bones. Infection is often considered as a therapeutic emergency requiring the radiologist's assessment of the presence or absence of infectious disease and its extent. Soft tissue infections can be focal (►abscess) or diffuse (►cellulitis) and are subdivided according to the compartment involved. The specific entities discussed are cellulitis, pyomyositis, abscess, ►necrotizing fasciitis, tenosynovitis, and septic bursitis. They could be the primary event (cellulitis, muscle abscess) possibly leading to infective periostitis, osteitis, and osteomyelitis, or the consequence of spread of infection from adjacent structures (spondylodiskitis, osteomyelitis, and arthritis).

Pathophysiology

Soft tissue infections cause considerable morbidity with variable degrees of severity. Predisposing factors are open fracture, foreign bodies, and prosthetic material, as well as impaired immunity affecting drug abusers, diabetics, patients with immunodeficiency virus or leukemia, and patients taking immunosuppressive medication. Patients with human immunodeficiency virus infection are susceptible to bacterial and fungal infections (1). They are predisposed to osteomyelitis, septic arthritis, and pyomyositis.

Isolated soft tissue infections are less common than those involving bone and joint at the same time. The principal routes by which soft tissue can be contaminated are hematogenous spread of infection, spread from a contiguous source of infection, direct implantation, and postoperative infection (2). Isolated soft tissue infections arise from direct implantation (skin breaches, penetrating wounds, foreign bodies, decubitus ulcers, open fracture, and surgery) and less frequently from hematogenous spread from distant sites of infection. Human bites (*Staphylococcus aureus, Bacillus fusiformis*) and animal bites (*Pasteurella multocida, S. aureus*, and *Staphylococcus epidermidis*) are also common causes of infection from direct implantation. Infection could extend to adjacent soft tissue by progressing from osteomyelitis to osteitis to periostitis or from the vertebral body endplate to the disk to the closest adjacent vertebral body to soft tissue

I

(subligamentous, paraspinous phlegmon, or abscess) in the case of spondylodiskitis.

Pyomyositis consists of a primary muscle abscess, and is prevalent in tropical countries, in immunocompromised patients, and in drug abusers. Bacteria, mycobacteria, fungi, viruses, and parasitic agents may be responsible.

Clinical Presentation

Clinical features of soft tissue infection are not specific to the compartment involved and initially include pain, rigor, fever, and soft tissue enlargement.

Clinical diagnosis is based on the appearance of lesions, degree of pain, and systemic toxicity. Knowledge of the organisms involved does not always help define the tissue depth of disease, but aids in choosing antimicrobial therapy.

Cellulitis represents acute, febrile, and diffuse inflammation of subcutaneous fat and skin. Stiffness may precede visible signs of skin involvement or lymphangitis by 24 h. Tender regional lymphadenitis often develops. The involved area may show blistering and local necrosis. Desquamation may occur on recovery.

Myositis—Muscular Abscess

Nonspecific clinical features of myositis are fever, localized myalgia and stiffness, swelling, and tenderness. In certain instances, it is the anatomic location rather than the morphologic characteristics of the lesion or the etiologic infecting agent that distinguishes the particular type of infection. Clinical manifestations of psoas abscess include fever, lower abdominal or back pain, or pain referred to the hip or knee.

Necrotizing fasciitis **(NF)** usually afflicts patients with impaired immunity. It is characterized by rapidly extensive infection of superficial and deep soft tissue. The overlying skin is classically warm, indurated with a mottled appearance and purple patches. Crepitus due to superficial fascial emphysema is rarely palpable. Extreme pain followed by anesthesia suggests the diagnosis. At the late stages, there is local coagulopathy and thrombosis of the blood vessels with necrosis of the deep soft tissues. NF is differentiated from the other soft tissue infections by a rapid progression to multisystem failure and death without early recognition and treatment.

Imaging

Conventional Radiographs

In the case of a suspected musculoskeletal infection, plain radiographs (XR) are normal until soft tissue infections are advanced; however, they allow assessment of associated bony destruction or joint erosion. They are of little value, showing a nonspecific thickening of soft tissue. They can reveal the presence of gas in subcutaneous fascial planes (necrotizing fasciitis) or in muscle (a minority of muscle abscess). The presence of subcutaneous gas on a radiograph does not necessarily indicate a clostridial infection, because *Escherichia coli, Peptostreptococcus* species, and *Bacteroides* species may produce gas under appropriate conditions.

Ultrasonography

Ultrasonography (US) is an important modality for evaluation of musculoskeletal infections especially in children because it is nonionizing and very sensitive for fluid collection and joint effusions (3). It allows detection of clinically occult collections providing guidance for diagnostic aspiration and could change the management of patients with initially diagnosed cellulitis. It should be performed in conjunction with radiography and could help to differentiate abscess from necrotic or cystic tumors, hematoma, and joint fluid. With the development of high-frequency and color Doppler sonography, US remains an accessible and inexpensive technique for studying infectious tenosynovitis and bursitis.

Computed Tomography

Computed tomography (CT) provides high spatial resolution and allows a precise visualization of the anatomic structures involved by infection. After contrast medium administration, enhancement of abscess walls, internal septa, and inflammation of deep fascia are well visualized. CT may also be used to guide interventional procedures to drain abscesses.

MRI

Magnetic resonance (MR) imaging is the ideal technique for assessing the soft tissue abnormalities produced by infectious processes. On MR images, soft tissue alterations consist of signal intensity changes that reflect the increased water content of the inflammatory soft tissues. These changes are nonspecific; however, they are helpful in detecting the presence and extent of the infection, which is suspected clinically on the basis of physical and laboratory findings and predefined by other imaging studies.

Intravenously administered gadolinium allows differentiation of an abscess from cellulitis or phlegmon in the soft tissues, or an abscess from bone marrow edema in the marrow space; Gadolinium also increases the visualization of sinus tracts and sequestra, and plays an important role in the diagnosis of fascia abnormalities in necrotizing fasciitis, if readily available at an early stage.

Diagnosis

Cellulitis

The diagnosis is usually clinical, but imaging excludes underlying abscess formation or other complication. *Plain radiographs* depict nonspecific findings: soft tissue swelling, displacement of fat planes, and the presence or absence of radiolucent gas foci (streaks, bubbles by gas-forming organisms) and radiopaque foreign bodies (needle, tips).

US typically shows edema as diffuse thickening of skin and subcutaneous fat, dissected by a reticular pattern of anechoic strands (Fig. 1a) with progressive transition to normal tissue. CT provides similar information with a precise depiction of the infectious focus and the presence of gas (Fig. 1b). MR findings show diffuse areas of low signal intensity on T1-weighted and high signal intensity on T2-weighted images, with a reticulated pattern in the subcutaneous fat and skin thickening without abnormality of deep fascial planes. The signal intensity in the same pathological areas is increased by gadolinium contrast.

Abscess

Abscesses, even sizeable ones, are difficult to discern on plain radiographs, but their visualization is facilitated by signs such as periosteal reaction or joint effusions. US detects abscesses as a fluid collection, totally or partially anechoic with well-marginated hyperechoic rim in the acute and subacute phases (Fig. 2). Echogenicity can vary by the presence of internal debris, hemorrhage, or septum. The abscess content could be hyperechoic, isoechoic, or appears as diffuse homogeneous low-level echoes, mimicking a solid mass. Color Doppler imaging, dynamic compression of the fluid collection, and motion of the purulent material within the collection may help differentiate echogenic fluid from a solid tumor or hematoma.

CT and MRI are the best imaging modalities for the extent of abscess formation. On CT scans, abscess walls and internal septa typically enhance after contrast administration (Fig. 3).

On MR scans, muscle abscesses are fluid-filled cavities that are bright on T2-weighted images, with a rim that shows postcontrast enhancement (Fig. 4). Such a pattern is typical for an abscess, but it may be seen in other entities including ischemic foci in muscle and necrotic soft tissue tumors.

Infectious Myositis—Pyomyositis

MR findings are not specific in pyomyositis. There is diffuse muscle enlargement with intermediate signal intensity on T1-weighted images, and diffuse high signal intensity on T2-weighted images sometimes with abscesses (4). The precise diagnosis is made after aspiration or biopsy and the culture of the abnormal muscle.

Necrotizing Fasciitis

CT and MRI are used to distinguish cellulitis from necrotizing fasciitis (Fig. 5) (1). With necrotizing fasciitis, the abnormalities are seen in the subcutaneous fat, as for cellulitis, with an extension in the deep fasciae between muscles and into muscles. The abnormalities are best demonstrated with MRI on short T1 inversion recovery (STIR) images. Muscle involvement is not required for making the diagnosis of necrotizing fasciitis but fascial involvement is. Linear high signal intensity is seen in both superficial and deep fasciae representing the fascial necrosis. The associated muscle involvement, when present, is seen as areas of high signal intensity within the muscles on T2-weighted or STIR images with or without hyperintense fluid collections from abscesses. Postcontrast T1-weighted images show linear enhancement of the fascia, focal enhancement of the affected muscles, and peripheral enhancement of the abscesses. Contrast administration is not necessary for making the diagnosis of necrotizing fasciitis. During the surgical debridement,

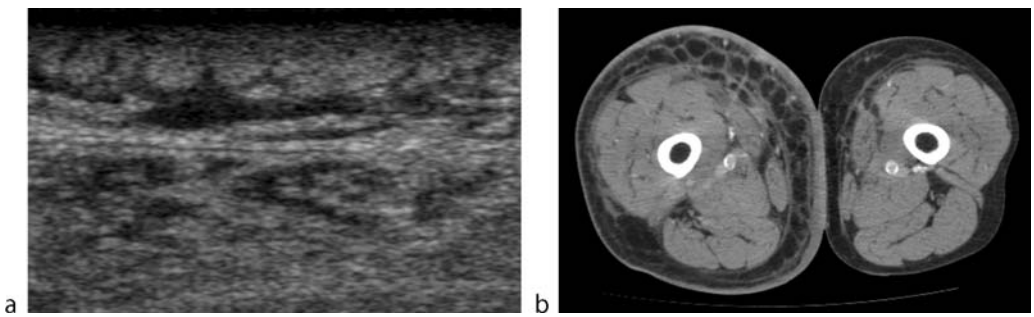

Infection, Soft Tissue. Figure 1 Infectious cellulitis of the right thigh. Ultrasonography (a) shows diffuse thickening of the skin and subcutaneous tissues characterized by a reticular pattern of anechoic strands. The CT image (b) also demonstrates findings of cellulitis (e.g., skin thickening, stranding of the subcutaneous fat, and blurring of the fat).

tissue biopsies are performed to obtain proper cultures for microorganisms.

Septic Tenosynovitis/Septic Bursitis

Septic or aseptic causes of tenosynovitis and bursitis cannot be distinguished by imaging features. They are often described with adjacent cellulitis. Septic cases result from tuberculosis or usually from penetrating trauma. The most common pathogen is *S. aureus* or *Staphylococcus pyogenes* (2). US findings for septic tenosynovitis are accumulation of fluid within the tendon sheath, tendon enlargement compared with the contralateral size, and hyperemia seen with Doppler. US may help to exclude other diagnoses such as septic arthritis, cellulitis, or foreign bodies. Septic bursitis most frequently involves the olecranon or prepatellar bursa. US demonstrates a fluid collection within the bursa with possible thickened wall, hyperemia in the walls, and debris or septae within the collection. Fluid surrounding a tendon or within a bursa is well depicted with US and will be seen as low signal intensity on T1-weighted and high signal intensity on T2-weighted images, with enhancement of the synovial lining after intravenous injection of gadolinium contrast.

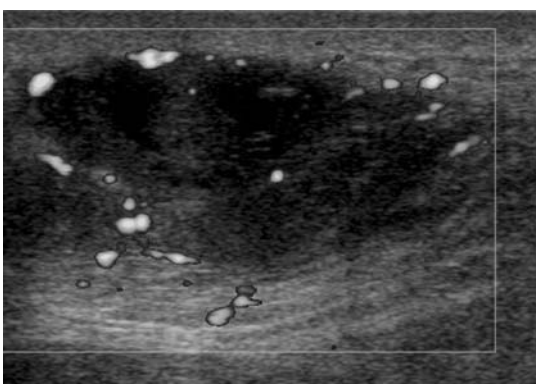

Infection, Soft Tissue. Figure 2 Fifty-year-old diabetic woman with erythema, edema, and firm mass on the thigh. Transverse sonogram with 7.5-MHz linear-array transducer shows well-defined, subcutaneous, anechoic mass with few internal echoes. Thick, hyperemic rim of the soft tissue abscess is seen at the periphery with color Doppler sonogram. *Staphylococcus* was cultured from abscess fluid after aspiration.

Diabetic Foot Infection

Foot disease in diabetics is a common problem and results frequently in one or more of the following: vascular disease, infection, and neuroarthropathy. Infection in diabetics is usually related to a soft tissue injury, followed by cellulitis; the infection may remain limited to the soft tissues or extend to the bones and the joints. CT scans and XR offer useful bony anatomic information, in particular for sequestrum. However, soft tissue details are limited and sensitivity and specificity for determining infection are low, especially in the early stages of infection. MRI remains the optimal imaging modality for soft tissue infection. Combined indium-111-labeled leukocyte technetium phosphate bone scintigraphy is the radionuclide procedure of choice for determining infection in neuropathic joints. Soft tissue ulcerations account for more than 90% of diabetic pedal osteomyelitis cases. They usually occur under pressure areas of the foot, such as the plantar soft tissues beneath or adjacent to the first and fifth metatarsal heads, the calcaneal tuberosity, the distal phalanges, and the malleoli. Ulcers can be identified on MRI as soft tissue defects of low signal intensity on both T1-weighted and T2-weighted images. Findings that suggest infection instead of diabetic neuropathy include osteomyelitis with bone marrow areas of low signal on T1-weighted and high signal on T2-weighted or STIR images associated with soft tissue ulcer or sinus tract overlying the abnormal bone and located as

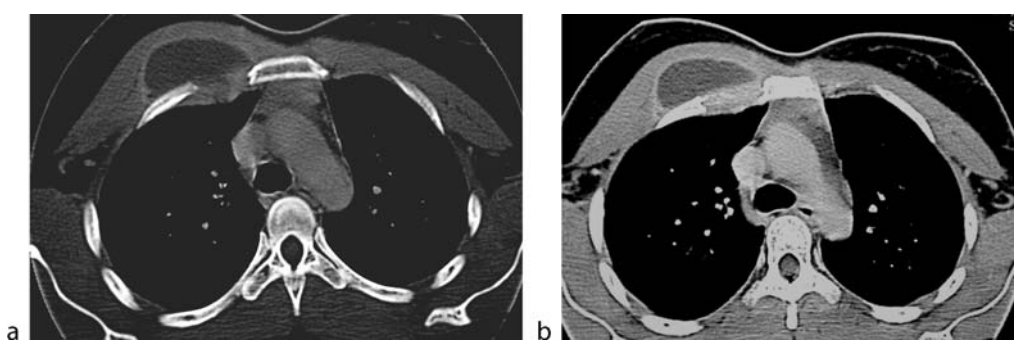

Infection, Soft Tissue. Figure 3 Chest wall tuberculosis arising from costochondral infection in a 65-year-old woman with active pulmonary tuberculosis. Thoracic axial CT images (a, b) show a soft tissue lesion of homogeneous low density in the right chest wall with a rim enhancement by iodine contrast. Aspirated fluid revealed *Mycobacterium tuberculosis*.

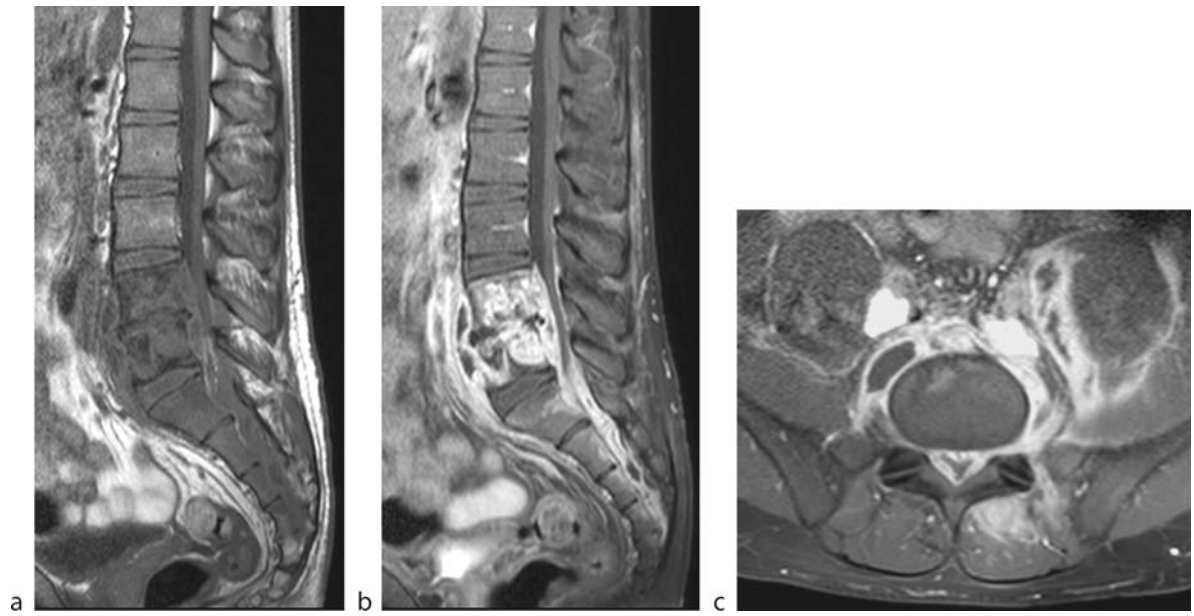

Infection, Soft Tissue. Figure 4 MRI depicts well a paraspinal and subligamentous abscess associated with lumbar spondylodiskitis in a 29-year-old North African man. T1 sagittal image (a) shows abnormal, low signal in two adjacent vertebral bodies with endplate destruction. There are soft tissue masses extending anteriorly and posteriorly to the vertebral bodies. Fat-saturated T1 sagittal (b) and axial (c) contrast-enhanced axial images show the anterior subligamentous, epidural, and paraspinal abscesses.

previously described. Abnormalities suggesting diabetic neuroarthropathy are joint misalignment and destruction and fragmentation of bone at the intertarsal and tarsometatarsal joints.

Foreign Bodies

Foreign bodies are most often wood, thorns, or glass. Their sites of predilection are the feet and hands. Foreign bodies in the soft tissue create an inflammatory reaction and may lead to the occurrence of an abscess, a sinus tract, or osteomyelitis. The identification of particles of glass or wood is difficult and can be done using XR combined with US or CT. On MR images, foreign bodies usually have a linear form with low signal intensity on all sequences surrounded by high signal intensity on T2-weighted images corresponding to granulation tissue, cellulitis, or abscess.

Nuclear Medicine

Nuclear medicine plays an important role in the assessment of periprosthetic infection and osteomyelitis in children, including early detection of infectious disease, differentiation of osteomyelitis from cellulitis, and identification of renewed activity in cases of chronic osteomyelitis. However, radionuclide studies are currently less widely used in the evaluation of infectious diseases due to the development of CT and MRI. Three main radionuclide studies including technetium phosphate bone scintigraphy, indium-111-labeled leukocyte scintigraphy, and fluorodeoxyglucose-PET (FDG-PET) can be performed for diagnosing soft tissue or bony infection (5).

Technetium phosphate bone scintigraphy with three phases is commonly used if bone infection is suspected: serial images are obtained at the angiographic phase (first minute just after intravenous technetium compound bolus), a postinjection image is obtained at the blood pool phase (end of the first minute), and further images are obtained at a delayed phase (2 or 3 h later). Osteomyelitis shows increased accumulation of the radionuclide within the bone during all three phases. In the case of cellulitis, early scans show increased uptake of soft tissue corresponding to hyperemia and later scans are normal.

Indium-111-labeled leukocyte scintigraphy based on leukocyte accumulation within the abscess is more sensitive in detecting peripheral than axial disease, and soft tissue infections than bone infections and chronic ones.

FDG-PET with CT has the advantage of high-resolution anatomical depiction of infectious sites, higher sensitivity in the uptake, and reliable diagnosis of axial infection compared to other radiotracers tested (gallium, radio-labeled serum albumin, thymidine) (5) (6). FDG-PET may be limited in differentiating between malignant and infectious processes as well as in postoperative patients.

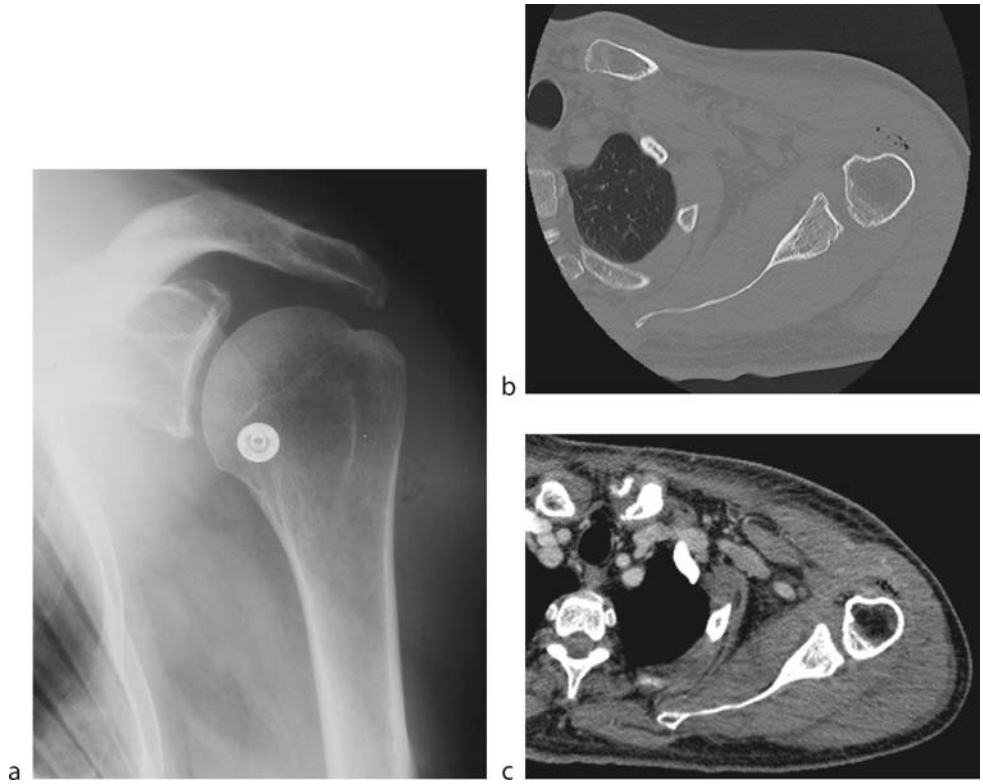

Infectious Diseases. Figure 5 **Anterioposterior radiograph (a) of the left shoulder demonstrates gas bubbles in the deep soft tissue in a splenectomized, diabetic, 80-year-old man. CT scan (b) obtained after ultrasonography confirms gas bubbles under the deep fascia of the deltoid, and shows an abscess within the deltoid associated with fluid collection and thickening of subcutaneous fat. After iodine injection (c), typical enhancement of the fascia associated with abscess in the deltoid muscle are well depicted suggesting the diagnosis of an early necrotizing fasciitis, which was surgically confirmed.**

Bibliography

1. Restrepo CS, Lemos D, Gordillo H et al (2004) Imaging findings in musculoskeletal complications of AIDS. Radiographics 24:1029–1049
2. Resnick D (1989) Osteomyelitis, septic arthritis, and soft tissue infection: mechanisms and situation. In Bone and Joint Imaging. 3rd edn. Philadelphia, PA 19106, Saunders pp 729–755
3. Loyer EM, DuBrow RA, David CL et al (1996) Imaging of superficial soft-tissue infections: sonographic findings in cases of cellulites and abscess. Am J Roentgenol 166:149–152
4. Soler R, Rodriguez E, Aguilera C et al (2000) Magnetic resonance imaging of pyomyositis in 43 cases. Eur J Radiol 35:59–64
5. Love C, Tomas MB, Tronco GG et al (2005) FDG PET of infection and inflammation. Radiographics 25:1357–1368
6. Zhuang H, Yu J, Alavi A (2005) Application of fluorodeoxyglucose-PET imaging in the detection of infection and inflammation and other benign disorders. Radiol Clin North Am 45:121–134

Infections of the Spleen

▶Spleen, Infectious Diseases

Infectious Diseases

Heinrich K. Geiss
Qualitätsmanagement-Hygiene-Konzern,
Bad Neustadt/Saale, Germany
h.geiss.qm@rhoen-klinikum-ag.com

In 1969 the US federal government's principal spokesperson on matters of public health, Surgeon General William H. Stewart, testified to the US Congress: "The time has come to close the book on infectious diseases." In fact, infections are still the most frequent diseases, and prospects of improving the situation in the near future are dismal. According to the World Health Organization, infections account for about one-third of all deaths worldwide, second only to cardiovascular diseases (Table 1).

Additionally, within the last 30 years a plethora of new and reemerging infections were recognized and face

Infectious Diseases. Table 1 Deaths by cause worldwide, estimates for 2002 (Source: The World Health Report 2003)

Cause	Number of deaths	%
Total deaths	57,027,000	
Cardiovascular diseases	16,655,000	29.2
Infectious diseases	14,967,000	26.3
Neoplasms	7,254,000	12.8
Injuries	5,188,000	9.1
Respiratory diseases	3,696,000	6.5
Perinatal diseases	2,464,000	4.3
Digestive diseases	1,963,000	3.4
All other causes	4,840,000	9.2

mankind with almost insurmountable problems. Not only are new epidemics like AIDS and SARS of significant concern, but the resurgence of diseases like malaria and tuberculosis are also ominous developments. At the same time, the underdeveloped world has to bear the brunt; in these areas of the world—with poor sanitation, overcrowding, uncontrolled urbanization, poverty, and little or no access to medical care—infectious diseases continue to cause significant morbidity and mortality. So as long as this part of the world cannot provide its inhabitants with the basic needs of clean water, sufficient and healthy food, shelter, and adequate medical care, the fight against infections can never be won.

In contrast, in developed countries, mortality from infectious diseases has been reduced significantly by improvements in sanitation, widespread vaccination, and access to medical care. However, new problems have evolved. So-called infections of leisure or diseases that complicate exposure to vacation climates, pets, recreational activities, and exotic cuisine pose problems of diagnosing and adequately treating these infections. Also, we have to pay a high price for medical progress: organ transplantation, invasive surgery, implantation of prosthetic devices, and immunosuppressive therapies have prolonged survival for some diseases but also resulted in compromised immunity and render previously normal individuals susceptible to microbes formerly considered to be pure saprophytes.

Even more intriguing is the steadily increasing resistance of bacteria, fungi, and viruses against anti-infective agents. The stunning success of the pharmaceutical industry in the western world in creating new antibiotics over the past four decades has caused the society and the scientific community to become complacent about the potential of bacterial resistance. Despite the warning in renowned textbooks that "it requires but a moment's reflection to realize that the substitution of a prescription for a broad-spectrum antibiotic or a quick injection of penicillin for the systematic collection of facts and thoughtful consideration of diagnostic possibilities is a fallacious, unwise, and dangerous practice….They should never be prescribed as placebos, antipyretics, or substitutes for diagnosis" (1), the misuse and overuse of these originally termed "miracle drugs" became more or less general practice and finally led to the situation that is described as the postantimicrobial era. The increasing frequency of drug resistance has been attributed to combinations of microbial characteristics, selective pressures of antimicrobial use, and societal and technologic changes that enhance the transmission of drug-resistant microorganisms. Antimicrobial resistance is resulting in increased morbidity, mortality, and health-care costs. In fact, this problem is dramatic not only because microorganisms "invent" new mechanisms of drug resistance but also because most pharmaceutical companies withdraw from research on new antiinfectives because their profit margin is too small in the long run.

The relationship between the human host and the microbial world represents the interaction of two very complex systems. Microbial forms are ubiquitous on the Earth's surface, on plants, and in water and constitute more than half of our planet's biomass. Bacteria and archaea, the two domains of the prokaryotic world, were the first forms of life to appear on Earth about 3.8 billion years ago. They were the absolute sovereigns of the world for about 1 billion years and created the global geochemical cycles that allowed other forms of life to develop. It is obvious that in the course of their long records, bacteria developed an abundant variety of metabolic capabilities that allowed them to survive even under unfavorable conditions. Bacteria acquired knowledge of how to maximize the plasticity of their genomes, constantly acquiring new genetic information and mutating or rearranging existing genes. These ever-changing capabilities enable bacteria to colonize all the niches the Earth provides. When warm-blooded animals and humans appeared on the evolutionary scene, of course bacteria immediately took advantage of these new niches for colonization. Taking into consideration that the human body is an almost infinite source of nutrients and offers shelter under constant temperature and humidity conditions, humans are an optimal habitat for continuous colonization, creating a biosphere of their own. Colonization begins when the primarily germ-free fetus leaves the protective amniotic sac. Within a very short period, the normal flora is constituted, forming a dense bacterial covering mainly of the skin, the oropharynx, and the intestinal and vaginal tracts. In fact, reduced to pure numbers, the human body consists of 10% mammalian cells and at least 90% prokaryotic cells, which form our normal flora. The human host is also surrounded by an abundant number of environmental microorganisms, some of which

may interact transiently with the human body. Therefore, it is clear that the ability of bacteria to grow and damage human tissue has an effect on human evolution.

Under normal conditions, this microbe–human interaction is in equilibrium based on the microbes' capability to harm and the host's defense system. This equilibrium is just one aspect of the human–microbe interaction. At the other end of the scale is the ultimate damage by microorganisms: death. However, infection and disease, like everything else in life, are continuous processes. Nevertheless, as with other complex continuous processes, it is convenient and, perhaps because of the limitations of our imagination, necessary to describe and define the dynamics of an infection as a sequence of more or less discrete steps.

In scientific terms, "infection" is defined as the process of microorganisms that are capable of causing disease to occupy and multiply in a particular area of the human body. An infection that produces symptoms is called an infectious disease. Thus, infection does not inevitably result in disease. Because common speech usually associates the term "infection" with disease, it seems rational to replace the scientific meaning by the term "colonization" because its understanding is more neutral. This proposal seems justified with regard to the fact that microorganisms forming the body's normal flora, which are usually regarded as noninfecting or benign, nevertheless may cause infectious disease depending on the immune status of the host involved. Healthy people colonized with obvious pathogens, such as *Salmonella typhi*, are called asymptomatic carriers, but they may serve as sources of infectious diseases when they transmit their "bug" to other people. Another example is the asymptomatic carriage of highly antibiotic-resistant bacteria, like methicillin-resistant *Staphylococcus aureus* (MRSA), which is a much feared and epidemically spreading hospital pathogen.

Although a specific infectious disease will not occur in the absence of the causative organism, the mere presence of the organism in the body does not invariably lead to clinical illness. Indeed, the production of symptoms in humans by many microorganisms is the exception rather than the rule. The occurrence of disease depends on the contributions of both host and pathogen to this process that is based on a microbe's ability to cause damage as a function of the host's immune response. In fact, the host may experience damage during the state of colonization by a given microorganism, the damage being part of a continuum spanning from "none" to "significant." Progressive damage that results from the host's inability to contain or eliminate the inflicting microorganism may lead to disease or death. However, damage may be mediated not only by the pathogen but also by the host's immune response (e.g., aberrant immune responses such as those associated with rheumatic fever or poststreptococcal glomerulonephritis). In this respect, damage is an inclusive term that encompasses cell, tissue, and organ damage. Damage at the cellular level includes necrosis, apoptosis, and malignant transformation. Damage at the organ and tissue levels includes granulomatous inflammation, fibrosis resulting from chronic inflammation, and tumor.

The transition from colonization to an infectious disease is defined by characteristic symptoms that have been well known since antiquity: fever (calor), pain (dolor), inflammation (rubor), swelling (tumor), and impaired function (functio laesa), of which fever has been recognized as a cardinal manifestation of disease. However, in clinical practice the variability of the disorders attributable to infection of humans by microorganisms is so variable that generalizations about them are difficult. The clinical manifestations of infection can duplicate those of diseases of any other etiology. It is obvious that the presence of one, several, or all of the so-called characteristic features of infection does not constitute proof of the microbial origin of illness in a given patient. Conversely, serious, even fatal, infectious disease may exist in the absence of fever or other signs and symptoms.

Nevertheless, the majority of acute infectious diseases are accompanied by fever, and its occurrence accounts for a large proportion of visits to physicians worldwide. In evaluating patients with elevated body temperature it is important to distinguish between disorders that lead to hyperthermia—an imbalance between heat-generating and heat-dissipating mechanisms—and fever, defined as a controlled elevation of body temperature in response to a control setpoint change in the hypothalamus mediated by endogenous pyrogens. But even when hyperthermia is excluded, a wide variety of diseases causing fever have to be considered: Besides infection, other causes include inflammatory, immune, granulomatous, neoplastic, vascular, and metabolic disorders; trauma; and tissue infarction.

This diagnostic dilemma is best exemplified with the case of sepsis, the most severe and life-threatening form of a febrile state. The clinical situation of a physician confronted with a patient in whom sepsis is suspected is best described using the statement of the US Supreme Court Justice P. Stewart: "I can't define obscenity, but I know it when I see it." However, in contrast to this theoretical problem, modern medicine needs clear definitions to provide a sound basis for diagnostic and therapeutic approaches in critically ill patients.

In the late 1980s and early 1990s it was recognized that the original definition of sepsis by Schottmüller (continuous or intermittent release of pathogenic microorganisms into the bloodstream from a focus within the body, leading to subjective and objective signs of disease) focusing on bacteria recovered from blood cultures was

far too narrow because a variety of overlapping clinical conditions may mimic an acute infectious process and be equally catastrophic. Progress in medical knowledge and expanding therapeutic modalities made clear that the clinical picture of sepsis falls within a more general inflammatory response of the organism, which is triggered not only by localized or generalized infection but also by trauma, thermal injury, or sterile inflammatory processes such as acute pancreatitis.

This was the background for a consensus conference of the American College of Chest Physicians and the Society of Critical Medicine, leading to the concept of systemic inflammatory response syndrome, or SIRS (2), which was updated in 2001 (3). The term "sepsis" is now divided into four different disease entities:

- SIRS
- Sepsis
- Severe sepsis
- Septic shock

The common denominator is the occurrence of a systemic inflammation, and differentiation is based on the fact that signs of systemic inflammation can and do occur in the absence of infection among patients with a variety of disease states in which clinical manifestations are protean and even distinct biochemical features (such as interleukin 6, procalcitonin, or C-reactive protein) are not consistently present.

The distinction of infectious from noninfectious SIRS is based on the definition of infection as "a pathological process caused by invasion of normally sterile tissue or fluid or body cavity by pathogenic or potentially pathogenic micro-organisms" (3). However, as mentioned earlier, this definition does not encompass the so-called toxi-infections that may be induced by members of the normal body flora (enterocolitis by *Clostridium difficile* enterotoxin). Because of these limitations, the systemic response to infection is designated "sepsis," which includes a wide set of diagnostic criteria. Besides general parameters such as fever, tachycardia, tachypnea, and altered mental status, the criteria include a set of inflammatory, hemodynamic, and tissue perfusion parameters. Again, it is emphasized that in clinical reality, none of these findings is specific for sepsis.

This example illustrates how the definition of a certain infection may change over time depending on our ever-increasing knowledge in pathophysiology and the ongoing improvement and progress in diagnostic methods or single diagnostic parameters. Similar to the complexity in the diagnosis of sepsis, an increasing number of patients present with nonspecific signs of infection, especially immunocompromised patients or patients in intensive care units. In these patients a single diagnostic step almost never suffices to unequivocally confirm the diagnosis of an infection. It is always the combination of different tests, the interpretation of which with respect to the clinical picture should enable the clinician to establish a diagnosis.

Diagnostic procedures are usually divided into laboratory and imaging studies. Laboratory tests obtained in patients with suspected infectious diseases fall into three categories: (i) those that assess the degree and severity of the inflammatory response to infection, (ii) those that help determine the site and complication of organ involvement by the process, and (iii) those that are employed to determine the etiology of the infectious agent, either by culture or histology or by a specific immune response. In addition, imaging technologies are categorized into traditional and conventional techniques (such as X-ray and ultrasound), more advanced techniques (such as computed tomography and magnetic resonance imaging), and finally, specific nuclear imaging techniques. In contrast to the first two methodologies, the latter techniques allow, for the first time, detection of infection-related abnormalities based on physiological or biochemical tissue changes. A dazzling array of changes within the different body compartments can be visualized by diagnostic imaging, including features of the following—probably incomplete—list:

Central Nervous System

- Intracerebral abscess
  i. Ring-enhancing mass
  ii. Vasogenic edema
  iii. Mass effect
  iv. Hypodense area
- Cerebritis
- Encephalitis
- Subdural abscess
- Epidural abscess
- Calcification
- Ventricular compression
- Sulcal effacement
- Midline shift
- Granulomatous disease
- Cysticercosis
- Toxoplasmosis
- Mycotic aneurysma
- Postinfectious vasculitis
- White matter disease

Spine

- Osteomyelitis
- Discitis
- Intervertebral discitis

- Bone erosion
- End-plate erosion
- Sclerosis
- Pott's disease

Head and neck

- Sinusitis
  i. Mucosal thickening
  ii. Sinus opacification
- Periorbital infection
- Mastoiditis
- Soft tissue neck infection

Chest

- Pneumonia
- Necrotizing pneumonia
- Bronchopneumonia
- Aspiration pneumonia
- Localized empyema
- Pulmonary emboli
- Lung abscess
- Atypical pneumonia
- Interstitial inflammation
- Interstitial infiltrate
- Pneumocystis jiroveci pneumonia (PCP)
- Fungal pneumonia
- Aspergillosis
- Tuberculosis
- Parapneumonic effusion
- Pleural thickening
- Pleural effusion
- Lobar consolidation
- Segmental consolidation
- Apical fibrosis
- Air–Crescent sign
- Halo sign
- Diffuse pulmonary infiltrate
- Pulmonary nodules
- Cavitation
- Ground-glass attenuation
- Mediastinitis
- Adenopathy

Abdomen

- Solid organ abscess
  i. Hepatic abscess
  ii. Splenic abscess
  iii. Pancreatic abscess
  iv. Renal abscess
- Perinephritic abscess
- Subphrenic abscess
- Peritoneal abscess
- Pyelophlebitis
- Appendicitis
- Cholecystitis
- Diverticulitis
- Inflammatory bowel disease
- Necrotic pancreatitis
- Gas formation
- Bowel wall thickening
  i. Colitis
  ii. Enteritis
- Gallbladder wall thickening
- Fistula

Soft tissue and osteoarticular infection

- Gas edema
- Gas formation
- Osteopenia
- Scalloping of the cortical bone
- Sequestration
- Periostal deviation
- Reactive bone formation
- Osteoblastic change
- Bone demineralization
- Periarticular soft-tissue swelling
- Widening of the joint space
- Vascular graft infection

General

- Whole body scan
- White blood cell scan
- Cellular labeling
- Antigranulocyte monoclonal antibodies
- Inflammatory response imaging
  i. Increased blood flow
  ii. Increased capillary permeability
  iii. Recruitment of white blood cells

Bibliography

1. Petersdorf RP (1980) Important consideration in infectious disease. In: Isselbacher KJ, Adams RD, Braunwald E et al Harrison's principles of internal medicine. 9th edn. McGraw-Hill, Auckland, p 541
2. Bone RC, Sprung CL, Sibbald WJ (1992) Definitions for sepsis and organ failure. Crit Care Med 20:724–726
3. Levy MM, Fink MP, Marshall JC et al (2003) 2001 SCCM/ESICM/ACCP/ATS/SIS international sepsis definition conference. Intensiv Care Med 29:530–538
4. World Health Report 2003 ▶http://www.who.int/whr/2003/en/

Infectious Myositis

►Infection, Soft Tissue

Infiltrating Ductal Carcinoma

►Carcinoma, Ductal, Invasive

Infiltrating Epitheliosis

►Radial Scar, Breast

Infiltrating Lobular Carcinoma (ILC)

►Carcinoma, Lobular, Invasive

Infiltrating Papillary Carcinoma

►Carcinoma, Other, Invasive, Breast

Inflammation

►Oral Cavity, Inflammatory Diseases

Inflammation, Chronic, Nose, and Paranasal Sinus

Silvio Mazziotti
Department of Radiological Sciences, University of Messina, Messina, Italy
smazziotti@unime.it

Definitions

Rhinosinusitis is defined as the inflammation of the nasal cavity and the adjacent paranasal sinuses and is most often the result of a viral infection (typically a cold) that causes the mucous membrane of the nose to become inflamed, blocking the drainage from the sinuses into the nose and throat. It may develop as a result of nasal allergies or other conditions that obstruct the nasal passages. However, any factor that causes the mucous membrane to become inflamed may lead to ►sinusitis. Bacteria and fungi are more likely to grow in sinuses that are unable to drain properly. Bacterial or fungal infections in the sinuses often cause more phlogosis and are more likely to last longer and worsen with time.

The terms acute, recurrent acute, subacute, and chronic rhinosinusitis have been used to define the illness by its duration (1).

Acute rhinosinusitis has a relatively rapid onset and is normally of 4 weeks duration or less and symptoms totally resolve. Resolution of symptoms usually occurs within 5 to 7 days, and patients usually recover without medical intervention.

Recurrent acute rhinosinusitis is defined as four or more episodes of acute disease within a 12-month period, with resolution of symptoms between each episode.

Subacute rhinosinusitis is basically a low-grade continuum of acute infection of more than 4 but less than 12-weeks duration.

Chronic rhinosinusitis is distinguished by symptoms that persist for 12 weeks or more or occurs more than four times a year with symptoms persisting for more than 20 days. The most frequent complications of inflammatory rhinosinusitis are ►Polyps Nasal and cysts. Chronically obstructed sinus secretions can accumulate and a ►mucocele can develop.

Pathology/Histopathology

Rhinosinusitis is inflammation or infection of the mucous membranes that line the inside of the nose and sinuses. The evoked completely reversible inflammatory changes in acute disease are swelling of the turbinates, thickening of mucosae in the nasal fossae and sinuses due to submucosal edema, and variable amount of sinus secretions. In acute sinusitis, fluid often collects in the sinus cavity, giving rise to an air-fluid level.

The chronic disease can result in an atrophic, sclerosing, or hypertrophic polypoid mucosa. These different mucosal alterations often coexist with one another and with areas of acute inflammations of either an allergic or an infectious etiology. The bony sinus walls surrounding a chronically infected sinus frequently

become thickened and sclerotic with reactive new bone formations. Epithelial hyperplasia and mucosal infiltration of leukocytes are common features of chronic rhinosinusitis.

Nasal polyps are outgrowths of nasal mucosa made up of edema fluid with sparse fibrous cells, a few mucus glands and a surface epithelium invaded by some inflammatory cells. Inflammatory polyps may be present in the nose and/or paranasal sinuses. Polyps are gelatinous in appearance, rarely bleeding, mobile, and insensitive to manipulation. They have a characteristic gray color that allows to distinguish them from the normal pink nasal mucous membrane.

A ▶retention cyst is a spherical mucoid-filled cyst that forms when a mucous gland of the sinus mucosa becomes obstructed; its walls are thus defined by the epithelium of a mucous gland and duct itself, not by the walls of the sinus. There is almost always air still surrounding the retention cyst, while bony expansion and remodeling of the sinus do not often occur.

A sinus mucocele is defined as a mucous collection of mucoid secretions lined by the mucus-secreting epithelium of a paranasal sinus. It occurs when a sinus ostium or a compartment of a septated sinus becomes obstructed, thus causing the sinus cavity to be mucous-filled and airless. The obstruction is often inflammatory in nature, but may also be due to tumor, trauma, or surgical manipulation. It is the most common expansile lesion of the paranasal sinuses and leads to outward expansion with bony remodeling. Initially, the bony structures remain intact, but with further expansion deossification may occur.

Clinical Presentations

In acute sinusitis, nasal congestion and discharge are almost always present. The discharge is typically thick and contains pus that is yellowish to yellow–green. Severe headache occurs and there is pain or pressure in specific areas in the face. The symptoms of recurrent acute and chronic sinusitis tend to be vague and generalized, last longer than 8 weeks, and occur throughout the year, even during nonallergic seasons. Nasal congestion and obstruction are common. Chronic cough, yellowish discharge, bad breath, and postnasal drip may occur. Sufferers do not usually experience facial pain unless the infection is in the frontal sinuses: in this case, it usually results in a dull, constant ache. Facial tenderness or pressure, however, may be present. Sinusitis complicated by the presence of polyps will not resolve until the polyps have been reduced in size, either medically or surgically. Signs and symptoms of a mucocele may last from a few days to years and are most often due to mass effect. A mucocele in the frontal sinuses typically leads to frontal headaches and inferolateral proptosis with diplopia. Additionally, a superomedial orbit mass may develop, and the voice may be nasal in quality. A mucocele in the ethmoidal sinuses frequently presents as lateral proptosis as well as nasal congestion. A mucocele in the maxillary sinuses causes upward displacement of the eye, a cheek mass, and nasal congestion. A mucocele in the sphenoid sinuses can lead to suboccipital headaches and visual loss.

Imaging

Conventional Sinus Radiographs

The plain radiographic examination for rhinosinusitis can include Caldwell (antero-posterior view), Waters (occipito-dental view), and lateral view. The Caldwell and Waters views best demonstrate the frontal and maxillary sinuses. The lateral view is the best choice for visualization of the sphenoid sinus and adenoidal tissue in children. Nevertheless, these views do not allow a good evaluation of ethmoidal cells (2, 3). Opacification, moderate-to severe mucosal thickening, or air-fluid levels in patients with persistent symptoms are generally considered suggestive of sinusitis. Such abnormalities are easily detected in maxillary and frontal sinuses by standard radiographs. Isolated polyps may be visualized by plain radiography but their precise localization often requires further imaging procedures. Although standard sinus radiographs are often considered useful in the diagnosis and monitoring of acute sinusitis, they are of limited value in the evaluation of chronic unremitting disease (2, 3). Low cost and small radiation dosage are advantages of this technique, and the possibility of portable examination can be helpful in the intensive care setting. The major drawback of plain radiography is its low sensitivity in the diagnosis of rhinosinusitis; in fact, interpretation of standard radiographs may be controversial: overlay of anatomical structures may mimic mucosal thickening or air-fluid levels and a hypoplastic sinus may be misinterpreted as pathologic opacification. Standard radiographs are inadequate for determination of the need for, or guidance of, endoscopic sinus surgery in both children and adults.

Computed Tomography

CT is currently the modality of choice for the evaluation of the regional anatomy of the nasal cavity and the paranasal sinuses (4). In contrast with plain radiographs, CT excellently demonstrates the anterior ethmoid cells, the upper two-thirds of the nasal cavity and the frontal recess. There is also strong evidence that CT is the gold standard for precise delineation of inflammatory sinus

disease secondary to obstruction of the ostiomeatal complex. Axial views parallel to the hard palate can provide important anatomical data. Optimal demonstration of the anterior ethmoid sinuses and ostiomeatal channels requires CT imaging in coronal planes that, in addition, closely correlate with the surgical approach. Ideally, coronal and axial 1.5 mm slices are performed with a helicoidal CT scan, which allows for a 3D reconstruction. Highly contrasting densities identify air within the bony sinuses, fat within the orbit and soft tissues outlined by air in the nasal cavity.

The primary role of CT scans is to aid in the diagnosis and management of recurrent and chronic sinusitis, or to define the anatomy of the sinuses prior to surgery. The characteristics of chronic inflammatory disease on CT are mucoperiosteal thickening, soft tissue mass, and osteitis of the ethmoid bony architecture. Bony erosion is unusual and is more frequently associated with more invasive processes such as mucocele, polyposis, or a neoplastic lesion. The region most frequently involved with inflammatory disease is the middle meatus. Associated maxillary sinus mucoperiosteal disease and, to a lesser extent, frontal sinus disease are frequently found.

It is well known that sinusitis may originate from or be perpetuated by local factors predisposing to sinus ostial obstruction. Current surgical strategy aims to remove the causative disease and reestablish ventilation and mucus clearance. In this respect, coronal CT offers an optimal view of the components of the ostiomeatal complex and enables the detection of significant anatomical variants: Haller's cells, agger nasi cells, paradoxical curvature of the middle turbinate, bulla ethmoidalis, deformities of the uncinate process, or concha bullosa. In terms of preoperative assessment, coronal CT serves as an anatomical map for the surgeon and it has been demonstrated that it greatly improves the planning and the safety of functional endoscopic surgery.

CT scan is the preferred imaging technique for the diagnosis of polyps and the evaluation of the extent of polyposis. Solitary polyps can be detected by CT imaging, although they cannot be differentiated from mucous retention cysts as both entities are shown as homogeneous soft-tissue masses with smooth and outwardly convex borders (Fig. 1). However, this is of little consequence, as any treatment for these common benign entities is the same.

In more severe polyposis, the major CT features are polypoid masses associated with complete pansinus opacification and infundibular widening; bony changes assume a destructive appearance that, in more advanced cases, suggests malignant tumors or granulomas (Fig. 2).

The CT finding of an expanded, airless sinus cavity filled with secretions characterized by rather homogeneous mucoid attenuation is characteristic of a mucocele (Fig. 3).

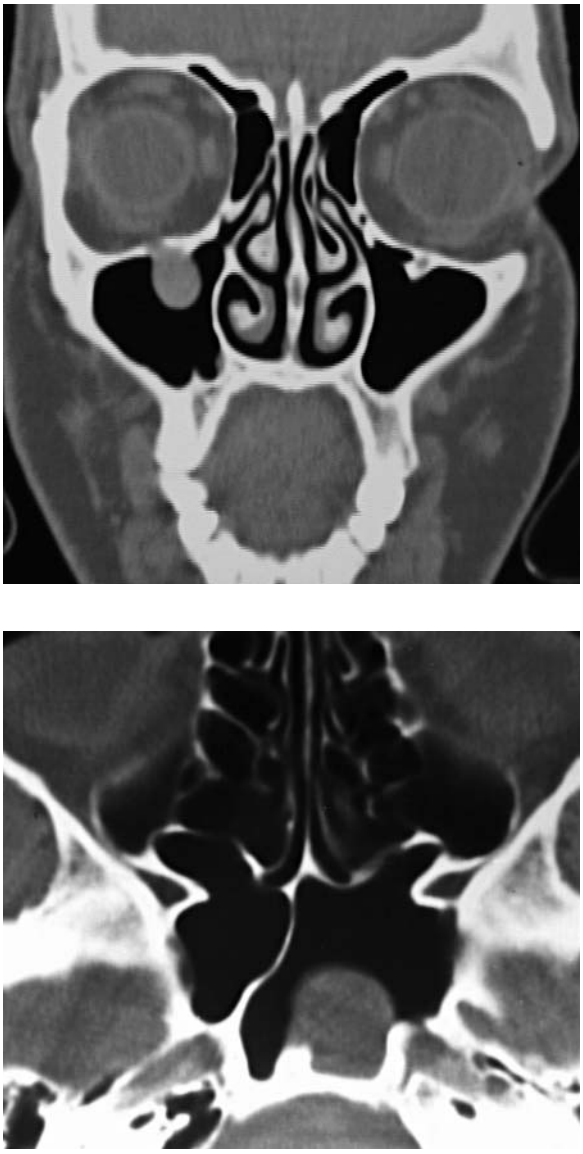

Inflammation, Chronic, Nose, and Paranasal Sinus. Figure 1 Coronal (a) and axial (b) CT scans. In (a) there is a solitary retention cyst or polyp in the right maxillary sinus. In (b) there is a retention cyst or polyp in the left sphenoid sinus. The sinuses are otherwise normal.

Magnetic Resonance Imaging

MR provides better imaging of soft tissues than CT, but it is less suited to imaging the bony anatomy of this region, and more particularly that of the ostiomeatal complex (4, 5). Because bone and air yield similar signal intensities on MRI, resolution of bony structures is poor and it is difficult to perceive anatomical characteristics critical for the surgeon. Furthermore, in the patient with extensive inflammatory disease mainly involving the ethmoid sinuses, the signal intensity on T2-weighted images of

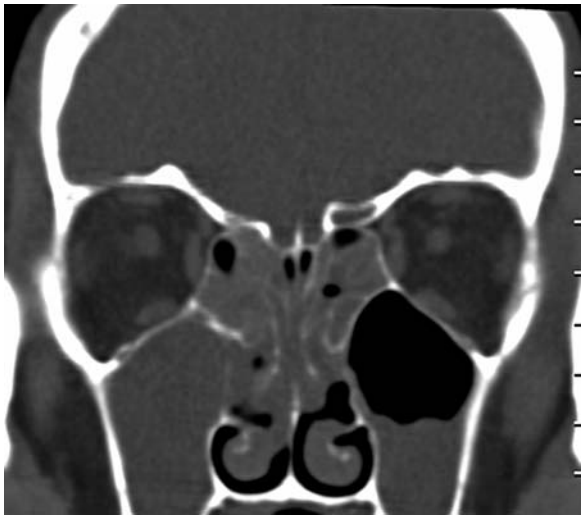

Inflammation, Chronic, Nose, and Paranasal Sinus. Figure 2 Coronal CT scan shows diffuse pansinusitis with the evidence of mucosal thickening and polyposis. Bony changes with a destructive appearance are also evident.

the pathologic process is indistinguishable from the appearance of the normal mucosa in the edematous phase of the nasal cycle. Although MRI has significant limitations in the definition of anatomy, it is extremely sensitive in evaluation of paranasal sinus mucosal disease in the frontal, maxillary, and sphenoid sinuses because the mucosa in these sinuses does not suffer the cyclic edema.

The etiology of certain disease processes and other sinus lesions may be better differentiated by MR. MR is often useful in the differential diagnosis between inflammatory diseases and malignant tumors. Bacterial and viral inflammations have high signal intensity on T2-weighted images, whereas neoplastic processes demonstrate an intermediate bright signal on T2-weighted images. Fungal concretions have very low signal intensity on T2-weighted images similar to that of air. MRI with Gadolinium contrast is useful for cases complicated by orbital or intracranial extension.

Nuclear Medicine

Nuclear medicine has a limited role in the assessment of rhinosinusitis. Rhinoscintigraphy may be a quick and reliable imaging method for evaluating the ciliary activity of nasal mucosa and the nasal mucociliary clearance function in patients with sinusitis.

Diagnosis

Clinical judgment with a careful history and physical examination should generally suffice in the diagnosis of

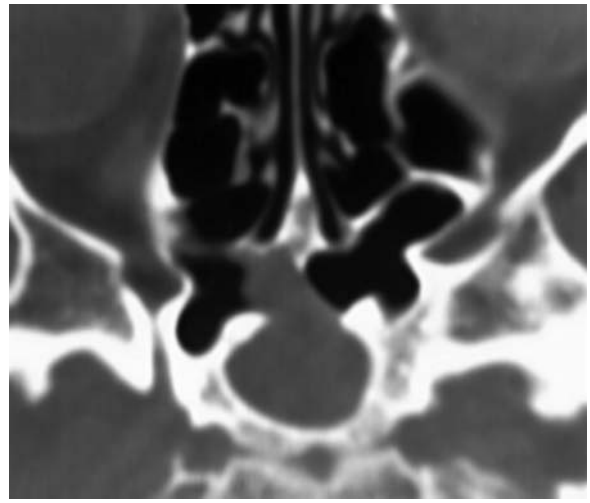

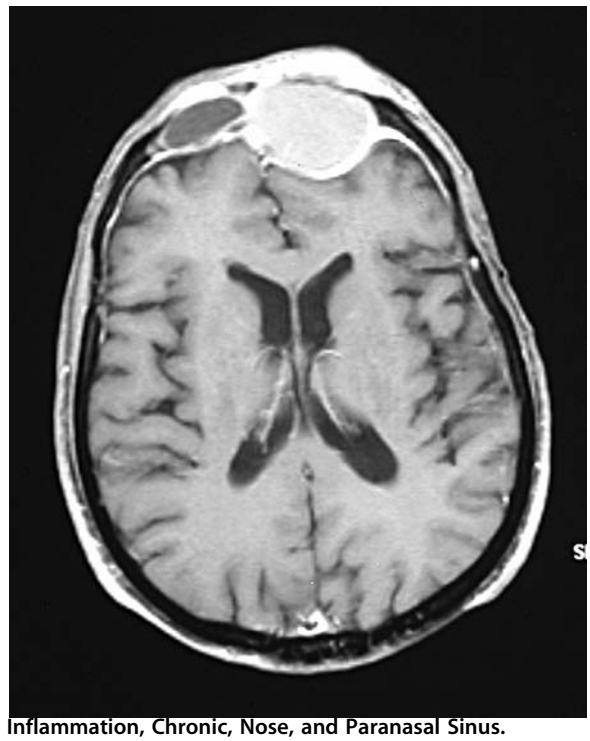

Inflammation, Chronic, Nose, and Paranasal Sinus. Figure 3 Mucocele. Axial CT scan (a) shows an expanded airless sphenoid sinus cavity filled with fairly homogeneous mucoid attenuation secretions. The sinus walls are remodeled. Axial T1-weighted MR image (b) shows bilateral expansive frontal sinus masses. On the right side has low signal intensity, on the left one it is hyperintense due to the high protein content of the entrapped secretions.

uncomplicated acute or subacute rhinosinusitis. Therefore, in these cases confirmatory plain radiography, given its low sensitivity, is rarely necessary.

However, when symptoms are recurrent or refractory despite adequate treatment, further diagnostic

evaluations may be indicated. In patients requiring confirmation of sinusitis, simple axial and coronal CT images can be adequate for screening purposes. In clinical practice, diagnosis of sinonasal polyposis is usually assessed by endoscopy but CT scan is frequently performed to help evaluate the disease.

Given the cost, the longer acquisition time, and the poor delineation of bony anatomy by MRI, it should only be used in rare cases of suspected sinonasal neoplasia, fungal sinusitis, or supposed intracranial or orbital complications of rhinosinusitis.

CT and MR should not be used in the initial diagnostic stages of patients with uncomplicated rhinosinusitis.

Bibliography

1. Willett LR, Carson JL, Williams JW Jr (1994) Current diagnosis and management of sinusitis. J Gen Intern Med 9:38–45
2. Kuhn JP (1986) Imaging of the paranasal sinuses: current status. J Allergy Clin Immunol 77:6–8
3. Skinner DW, Richards SH (1991) A comparison between sinus radiographic findings and the macroscopic appearances of the paranasal sinus mucosa. Ear Nose Throat J 70:169–172
4. Jorissen M (1996) Recent trends in the diagnosis and treatment of sinusitis. Eur Radiol 6(2):170–176
5. Rao VM, El-Noueam KI (1998) Sinonasal imaging. Radiol Clin North Am 36:921–939

Inflammatory Carcinoma

▶Carcinoma, Other, Invasive, Breast

Inflammatory Lesion

▶Oral Cavity, Inflammatory Diseases

Inflammatory Mass of Ovaries and Fallopian Tubes

▶Abscess TuboOvarian

Inflammatory Pseudotumor

Most common mass lesion of the lung with unclear origin.

▶Neoplasms, Chest, Childhood

Infrainguinal Arterial Obstruction

▶Occlusion, Artery, Popliteal
▶Occlusion, Artery, Femoral

Infrainguinal Arterial Occlusion

▶Occlusion, Artery, Femoral

Inframesocolic Peritoneal Compartment

This extends between the transverse mesocolon and the pelvis and between the anterior abdominal wall and the anterior perirenal space. It is subdivided into left-right paracolic gutters and left-right inframesocolic cavities by the descending-ascending mesocolon and the small bowel mesentery, respectively.

▶Peritoneal Collections

Insufficiency, Acute, Renal

Patrice Taourel
Service d'Imagerie Médicale, Hôpital Lapeyronie,
371 avenue du Doyen Gaston Giraud,
34295 Montpellier, Cedex 5
p-taourel@chu-montpellier.fr

Definition

Acute renal insufficiency is the sudden rapid deterioration in renal function. There is no clearly defined set of biochemical criteria that characterize renal insufficiency. In some forms of renal insufficiency, known as renal failure, the renal function is insufficient to maintain homeostasis.

Pathology

The causes of acute renal insufficiency can be divided into three main categories: prerenal or functional causes, renal causes, and postrenal causes.

Prerenal causes constitute the most common causes of acute renal insufficiency and are associated with renal hypoperfusion. Such conditions include congestive heart failure, diuretic use, sepsis, dehydration due to gastrointestinal causes (diarrhea, vomiting), renal or respiratory loss, hemorrhage, burns, cirrhosis with ascites, and diabetic ketoacidosis. Renal artery stenosis, when treated by angiotensin-converting enzyme inhibitor, represents a rare but interesting model of functional cause of renal failure due to a decrease of the glomerular filtration pressure by an excessive vasodilatation of the postglomerular arteriole.

Renal causes may result from damage to any portion of the kidney: the tubule, the glomerulus, the blood supply, or the interstitium. Tubular nephropathy includes acute obstruction of the tubules mainly due to precipitation of urate in patients receiving chemotherapy or to precipitation of Bence Jones proteins, and acute tubular necrosis, which constitutes the most common renal cause of acute renal insufficiency. Acute tubular necrosis is due to two mechanisms: hypoperfusion of the kidney with decreased glomerular filtration and increased pressure in the tubules. The renal involvement is reversible with treatment of the cause. A large number of conditions are reported in relation to acute tubular necrosis, including burns, sepsis, snake bites, toxins, transfusion, incompatible transfusion, dehydration, peritonitis, and pancreatitis; some of these are the same as for functional renal failure, explaining why these two conditions may be associated and that their differential diagnosis is difficult.

The vascular nephropathy responsible for acute renal insufficiency includes acute renal vein thrombosis, renal artery occlusion, and disease of the intrarenal arteries, such as collagen vascular diseases (polyarteritis nodosa, Wegener's granulomatosis, and systemic lupus erythematous), scleroderma, and intravenous drug abuse.

Acute interstitial nephritis is underestimated in frequency, and diagnosis is difficult because it is not revealed by any clinical finding such as edema or hypertension and because the diuresis is preserved for a long time. It may occur in association with a variety of drugs, such as penicillin, sulfonamide derivatives, or nonsteroidal anti-inflammatory agents, or with a number of nonrenal infectious processes; it may be due to tumoral infiltration of the two kidneys in lymphoma, for instance; or it may arise in an idiopathic form. Glomerular damage constitutes less than 5% of acute renal insufficiency as a result of acute glomerulonephritis, drug toxicity, Goodpasture's syndrome, or systemic lupus erythematosus.

Postrenal causes refer to the onset of acute renal insufficiency due to acute obstruction. Although acute obstruction accounts for only 15% of acute renal insufficiency, it is the most commonly sought cause because it is the one most easily reversed under appropriate treatment.

Clinical Presentation

Uremia may result in symptoms related to a number of different organ systems including the gastrointestinal tract (nausea, vomiting), the cardiovascular system (hypertension, cardiac arrhythmias, pericarditis), the nervous system (personality changes, seizures, somnolence), and the hematopoietic system (anemia, bleeding diathesis). However, clinical findings are more often due to the cause of the acute renal failure and to the hydroelectrolytic changes than to the consequences of uremia.

Imaging

Ultrasound

Ultrasound (US) is the best available imaging study for patients with renal failure. It permits clinicians to know the size of the kidney as evaluated by its maximum length, which has become the standard parameter because it is simple and correlates well with renal volume. (The average renal length is 11 cm in adults.) US also allows measurement of the cortical thickness from the outer border of the medullary pyramids to the renal capsule (which normally measures about 10 mm) and analysis of the outline of the kidney, which may be rounded, lobulated, or dented.

US permits study of the cortical echogenicity, which is most often inferior to the liver echogenicity. Although the echogenicity of the renal cortex and liver may be the same in a minority of healthy subjects, a renal cortex more echogenic than the liver is clearly abnormal past the age of 6 months and indicates renal disease.

Corticomedullary differentiation must be analyzed. Prominently hypoechoic medullary pyramids usually indicate increased cortical echogenicity (Fig. 1), whereas

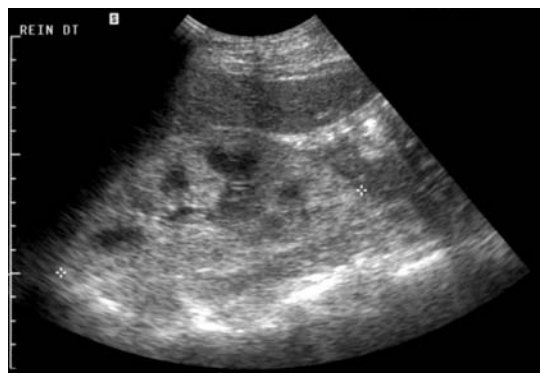

Insufficiency, Acute, Renal. Figure 1 Acute renal insufficiency due to glomerulopathy. The cortex of the kidney is hyperechoic, making the medulla appear very hypoechoic.

hyperechoic pyramids indicate medullary disease. But the main use of US is to seek dilated fluid-filled calyces in the renal sinus that may be differentiated from venous engorgement and peripelvic cysts.

US is an useful tool to differentiate acute from chronic renal insufficiency because in acute renal insufficiency, the kidneys have a normal size or are enlarged whereas in chronic insufficiency, they are more often decreased in size with decreased thickness of the renal cortex, which is considered the most sensitive finding. However, renal size is conserved or increased in glomerulopathy and diabetic nephropathy. Consequently, in the clinical context of renal insufficiency, normal kidney size does not affirm the acute character of the affliction, whereas a decrease in kidney size, as well as in the thickness of the cortex, rules it out.

The main task of US is to look for an obstruction. However, in the clinical setting of two native kidneys, acute obstructive renal failure is rare except in patients with bilateral iatrogenic postoperative obstruction. The lack of calyceal dilatation effectively rules out obstruction as a cause of acute renal failure. For diagnosing non-obstructive causes of acute renal insufficiency, US may provide limited but interesting information regarding the nature of the underlying renal disease and must be integrated to the clinical setting. Swelling of the renal cortex in conjunction with a history of an inciting event or the presence of granular casts in the urine indicates acute tubular necrosis, whereas enlarged, echogenic kidneys in conjunction with hematuria are indicative of nephritis. In a patient with nephrotic syndrome and acute renal failure, swollen, echogenic kidneys may instead indicate renal vein thrombosis, particularly if there is new-onset hematuria or the renal vein is prominent with luminal echoes. Unilateral cortical atrophy with hypertension and unremarkable urinary sediment should raise suspicion for renovascular disease.

Doppler

Doppler improves the sonographic assessment of renal dysfunction. In the setting of acute renal failure, its principal use is to demonstrate the patency of the renal arteries and veins and to look for thrombosis.

Arterial thrombosis may lead to acute renal failure in patients with a single kidney. In other cases, it may decompensate a chronic renal insufficiency in acute failure in patients with nephroangiosclerosis and severe atherosclerosis. Thrombosis of the renal artery occurs most commonly as a complication of severe atherosclerosis or transluminal angioplasty. The most common Doppler finding is absence of an intrarenal arterial signal. If there is incomplete occlusion or if collateral vessels are present, a severe tardus-parvus abnormality is detected. In some patients, US may demonstrate a proximal renal artery stump.

Thrombosis of the renal vein is usually caused by an underlying abnormality of hydration, the clotting system, or the kidney itself. In infants it is mainly due to dehydration, whereas in adults the most common cause is membranous glomerulonephritis. Color Doppler may image the renal vein thrombosis, and spectral analysis may show abnormality of the arterial wave with a shift in the anterograde frequency and reversal of flow during diastole.

The clinical role of Doppler for differentiating renal disease by the resistive index (RI) is more controversial. Classically, patients with isolated glomerular disease have normal RI values, whereas subjects with vascular or arterial disease have markedly elevated RI values. However, these data indicate rather a trend, and there is no cut off to differentiate disease in a given patient.

Computed Tomography

Computed tomography (CT) is not recommended for exploring the cause of renal insufficiency because such exploration needs intravenous contrast except for the search for a ureteral stone. However, it may sometimes be performed when the renal function is unknown or when dialysis is scheduled. Analysis of the CT nephrogram gives some information. When bilateral, global absence means a total lack of renal function; when unilateral, it is most often seen with blunt abdominal trauma with renal pedicle injury. Segmental absence is attributable to focal renal infarction (Fig. 2), most likely due to arterial emboli. Global persistence may be unilateral, caused by renal artery stenosis, renal vein thrombosis, urinary tract obstruction, systemic hypotension, intratubular obstruction, or abnormalities in tubular function. A striated nephrogram is caused by ureteric obstruction, acute pyelonephritis, contusion, renal vein

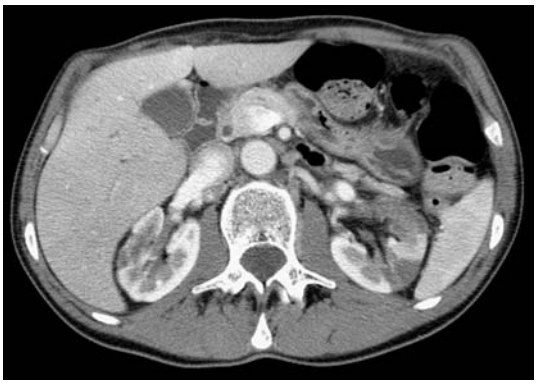

Insufficiency, Acute, Renal. Figure 2 Bilateral renal infarcts complicating a spontaneous dissection of the renal arteries

thrombosis, tubular obstruction, hypotension, or autosomal recessive polycystic disease. The rim pattern is most often associated with renal infarction and occasionally with acute tubular necrosis and renal vein thrombosis.

Magnetic Resonance Imaging

Magnetic resonance imaging (MRI) has great potential in the noninvasive evaluation of important functional renal parameters such as glomerular filtration, renal perfusion, tubular concentration, renal diffusion, and the oxygenation state of the kidneys. To date, however, MRI is used more in research than in clinical practice.

Nuclear Medicine

Because the excretion of radiopharmaceuticals depends on renal function, they cannot be used to evaluate all patients with renal failure. This is particularly true concerning products excreted primarily by glomerular filtration (technetium). Products excreted by tubular secretion may demonstrate the kidneys even when renal dysfunction is relatively advanced. In clinical practice, radionuclide studies usually only help exclude arterial occlusion because images are difficult to interpret when renal function is markedly impaired.

Diagnosis

An acute renal insufficiency may be diagnosed in a clinical setting that makes obvious the cause of the renal failure, or it may be discovered by clinical findings of hyperuremia or by biochemical results. The goals of imaging are the following:

1. To differentiate acute renal failure from chronic failure
2. To understand the mechanism of the renal failure: functional, postobstructive, or due to nephropathy
3. To seek the cause of the nephropathy: tubular, glomerular, interstitial, or vascular

Most often, the diagnosis of the causes of the renal failure is obvious in the clinical context because several causes may be involved; for instance, in the clinical setting of shock, functional insufficiency and acute tubular necrosis may explain the renal failure and may be related. In the lack of clinical orientation, the imaging strategy is based on US rather than on Doppler. US is used to look for a dilatation of the calyces and seek for findings of chronic renal insufficiency by showing kidneys with decreased size. Doppler is used to look for a thrombosis of the renal artery or veins or a bilateral stenosis of the renal arteries. Other parameters, including kidney echogenicity and the RI, have only an orientation value and do not substitute for renal biopsy.

Insufficiency, Chronic, Renal

Patrice Taourel
Service d'Imagerie Médicale, Hôpital Lapeyronie,
371 avenue du Doyen Gaston Giraud,
34295 Montpellier, Cedex 5
p-taourel@chu-montpellier.fr

Definition

Chronic renal insufficiency is the gradual progressive loss of renal function. The renal dysfunction is attributable to the loss of functioning renal parenchyma and, as such, is irreversible. Consequently, in most cases, the process of chronic renal insufficiency results in the need for dialysis or renal transplantation

Pathology

The causes of chronic renal insufficiency may be divided into three main categories: prerenal causes, renal causes, and postrenal causes:

Prerenal chronic renal insufficiency is due to medical conditions that cause continuous hypoperfusion of the kidneys, leading to kidney atrophy (shrinking), loss of nephron function, and chronic renal failure. These conditions include poor cardiac function, chronic liver failure, and atherosclerosis of the renal arteries.

Renal chronic renal insufficiency may result from damage to any portion of the kidney: the gomerulus, the tubule, the blood supply, or the interstitium.

- The main cause of glomerulopathy that is responsible for renal failure is diabetes, and diabetic nephropathy is the most common cause of chronic renal failure in industrialized countries. It occurs as a result of glomerular hyperperfusion that leads to glomerular hypertension, which results in glomerular sclerosis. Other causes of secondary glomerulopathies include amyloidosis, systemic lupus erythematosus, or primary glomerulopathies when there is no extrarenal finding. Theoretically, glomerulopathies are slowly evolutive; however, in some cases the evolution to terminal renal failure may be fast, in particular in the context of HIV nephropathy.
- The tubulo-interstitial involvement in nephropathy may be due to drugs, infection, tumoral infiltration by lymphoma or leukemia, or precipitation of urate or calcium in the metabolic causes of nephropathies.
- The vascular nephropathies represent a cause of chronic renal failure increasing in frequency. The disease may be a

result of three mechanisms: nephrosclerosis due to hypertension which constitutes the second leading cause of chronic renal failure, distal renal infarct due to emboli, or ischemia of the kidneys by bilateral stenosis of the renal arteries.

- Constitutional diseases, such as polycystic disease or Alport's syndrome, are responsible for about 10–15% of cases of chronic renal failure.

Postrenal chronic renal insufficiency is due to obstruction of the normal flow of urine, leading to obstructive uropathy, progressively reduced renal blood flow, and glomerular filtration and damage to the nephrons. Abnormalities that may hamper urine flow and cause postrenal chronic renal insufficiency include bladder outlet obstruction due to an enlarged prostate gland or bladder stone, neurogenic bladder, kidney stones in both ureters, obstruction of the tubules, retroperitoneal fibrosis of any cause, and vesicoureteral reflux.

Clinical Presentation

Patients with mildly diminished renal reserve are asymptomatic, and renal dysfunction can be detected by laboratory testing. A patient with mild to moderate renal insufficiency may have only vague symptoms. Nocturia is noted, principally due to a failure to concentrate the urine during the night. Lassitude, fatigue, and decreased mental acuity are often the first manifestations of uremia. Neuromuscular features then follow including twitches, peripheral neuropathies, muscle cramps, and convulsions. Anorexia, nausea, vomiting, stomatitis, and an unpleasant taste in the mouth are almost uniformly present. The skin may appear yellow–brown and there are bony lesions of renal osteodystrophy. Malnutrition is very common. In advanced renal failure, gastrointestinal ulcerations and bleeding are common. Hypertension related to hypervolemia is present in 80% of patients, and cardiomyopathy and pericarditis are not rare.

Imaging

Ultrasound

Ultrasound (US) is the best available imaging study for patients with renal failure. The size of the kidney can be evaluated using its maximum length, which has become the standard parameter because it is simple and correlates well with renal volume. Average renal length is 11 cm in adults. US also allows measurement of the cortical thickness from the outer border of the medullary pyramids to the renal capsule, which normally measures about 10 mm, and it allows analysis of the outline of the kidney that may be rounded, lobulated, or dented. The cortical echogenicity can be studied with US, which is most often inferior to the echogenicity of the liver. Although the echogenicity of the renal cortex and the liver is the same in minority of healthy subjects, a renal cortex more echogenic than the liver is clearly abnormal past the age of 6 months and indicates renal disease. The corticomedullary differentiation must be analyzed. Prominently hypoechoic medullary pyramids usually indicate increased cortical echogenicity, whereas hyperechoic pyramids indicate medullary disease and particularly medullary nephrocalcinosis for which the most common causes are medullary sponge kidney (Fig. 1), renal tubular acidosis type 1, and hypercalcemic states. With US, one can search for dilated fluid-filled calyces in the renal sinus (Fig. 2) that may be differentiated from venous engorgement and from peripelvic cysts.

US is a useful tool with which to differentiate acute from chronic renal insufficiency, since in acute renal insufficiency the kidneys have a normal size or are enlarged, whereas they are more often decreased in size

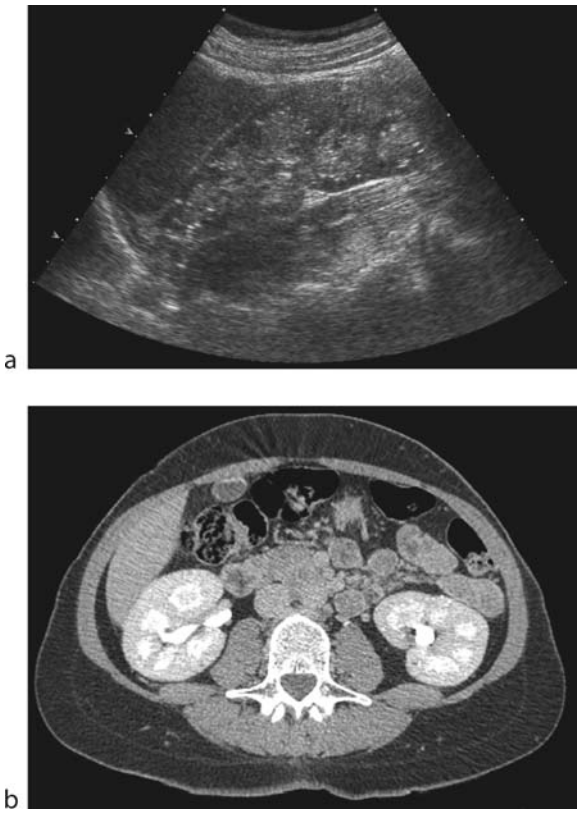

Insufficiency, Chronic, Renal. Figure 1 Medullary nephrocalcinosis due to medullary sponge kidney. (a) US shows hyperechoic renal pyramids without obvious shadowing; (b) CT at the excretory phase shows stasis of urine in the dilated distal collecting tubes.

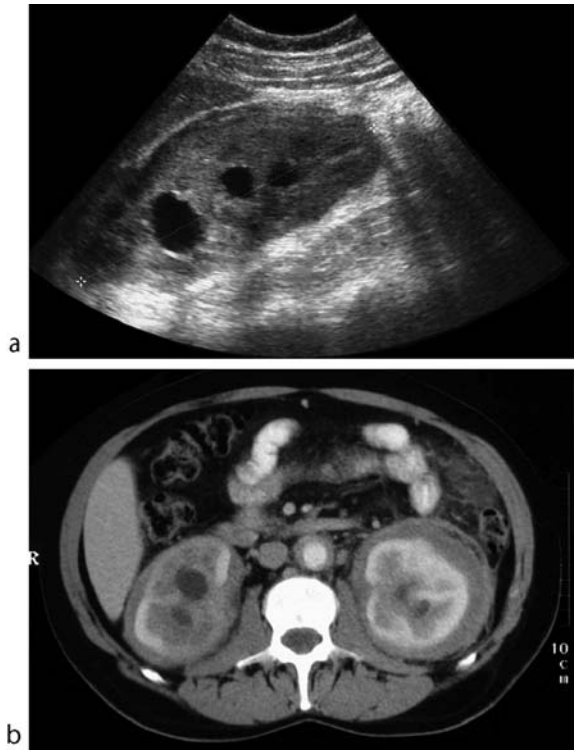

Insufficiency, Chronic, Renal. Figure 2 Bilateral perirenal fibrosis. (a) US shows dilatation of the calices; (b) CT clearly shows the perirenal fibrosis responsible for the obstruction.

with a decreased renal cortex thickness that is considered the most sensitive finding. However, renal size is conserved or increased in glomerulopathy or in diabetic nephropathy. Consequently, in the clinical context of renal insufficiency, a decrease in the size of the kidney, as well as in the thickness of the cortex, may confirm chronic disease, although a normal-sized kidney does not rule it out.

US is mainly used to look for an obstruction. Chronic obstruction produces increasing dilatation of the ureter and the collecting system proximal to the obstruction lesion. The amount of dilatation varies from case to case. In general, the dilatation increases both with the duration of obstruction and as a direct function of the intraluminal pressure. The most severe dilatation therefore does not occur with very mild obstruction or with complete obstruction after which urine formation tends to cease, but rather at an intermediate state in which the degree of obstruction increases intraluminal pressure but does not cause immediate severe oliguria.

In chronic renal failure, the size of the kidney and the thickness of the cortex are most often decreased. A very thin cortex indicates severe, irreversible renal disease. However, enlarged, very echogenic kidneys suggest amyloidosis, HIV nephropathy, or nephritis. Normal-sized or moderately enlarged kidneys that are echogenic are suggestive of glomerulopathies, such as diabetic nephropathy, immunoglobulin A nephropathy, or membranous nephropathy. Renal size is preserved even in advanced diabetic nephropathy, often with only a modest increase in cortical echogenicity, an appearance that is distinctly unusual in advanced renal failure from other causes. Cortical irregularity with a history of multiple urinary tract infections suggests the diagnosis of chronic pyelonephritis, particularly if dilatation of the calyces is present. In the absence of such a history, cortical scarring could represent vascular disease with previous infarcts. In polycystic kidney disease, US easily shows a huge and bilateral renal enlargement due to numerous cysts of variable size.

Doppler

Doppler improves the sonographic assessment of renal dysfunction. In the setting of chronic renal failure without cause, the principal interest is to look for a stenosis of the renal arteries by showing an increased peak systolic frequency shift at stenosis and a poststenotic spectral broadening with a decrease of the resistive index within the intrarenal arteries.

The clinical role of Doppler for differentiating renal disease using the resistive index (RI) is controversial. Some studies suggest that an increased RI of the renal arteries is associated with the severity of systemic atherosclerosis and that the intrarenal vascular resistance differs depending on the underlying renal disease, with a greater increase in diabetic nephropathy than in chronic glomerulonephritis and nephrosclerosis. However, these data indicate a trend, and there is no cut-off for differentiating disease in a given patient.

Computed Tomography

Computed tomography (CT) is not recommended in the exploration of the cause of renal insufficiency, because such exploration needs intravenous contrast agents, except when searching for a ureteral stone. However, in cases where the renal function is not known or because dialysis is scheduled CT can be performed. The analysis of the CT nephrogram gives some information. A global absence when bilateral means a total lack of renal function. Segmental absence is attributable to focal renal infarction, most likely due to arterial emboli. Global persistence may be unilateral, caused by renal artery stenosis, renal vein thrombosis, or urinary tract obstruction, or due to systemic hypotension, intratubular obstruction, or abnormalities in tubular function. Striated nephrograms are caused by ureteric obstruction, acute pyelonephritis, contusion, renal vein thrombosis, tubular obstruction, hypotension, and autosomal recessive polycystic disease.

Magnetic Resonance Imaging

Magnetic resonance imaging (MRI) has a great potential in the noninvasive evaluation of important functional renal parameters such as glomerular filtration, renal perfusion, tubular concentration, the oxygenation state of the kidneys, and renal diffusion. However, to date, the evaluation of these parameters is more in the field of research than in clinical practice. The main clinical interest of MRI in the daily clinical evaluation of patients with renal failure is to permit the morphological evaluation of the kidneys and the urinary tree after noniodinated contrast enhancement.

Nuclear Medicine

Because the excretion of radiopharmaceuticals depends on renal function, they cannot be used to evaluate all patients with renal failure. This is particularly true for products (Technetium) excreted primarily by glomerular filtration, whereas products excreted by tubular secretion may demonstrate the kidneys even when renal dysfunction is relatively advanced. In clinical practice, radionuclide studies usually only help exclude arterial occlusion, because images are difficult to interpret when renal function is markedly impaired.

Diagnosis

In most cases, the cause of the renal failure is known (diabetic nephropathy, uropathy, polycystic kidney disease) and the goals of imaging will be to look for an aggravating factor (obstacle, stenosis of the renal artery).

In some cases, the renal failure is discovered after clinical findings of hyperuremia or is more often revealed by biochemical test results. In these cases the goals of imaging are

- To differentiate acute renal failure from chronic failure;
- To seek the cause of the nephropathy: tubular, glomerular, interstitial, or vascular. This diagnostic step is crucial because (a) some diagnoses are obvious on imaging (polycystic kidney disease, bladder outlet obstruction), (b) in some cases it may be possible to treat the cause (surgery of a uropathy, dilatation of a stenosis of the renal artery), (c) the prognosis depends on the cause, (d) some renal diseases (glomerulopathy) may recur on the renal transplant;
- To look for factors worsening the renal failure (obstacle).

The imaging strategy is based on US. US will provide some clues of the cause of nephropathy, based on the size of the kidney, the presence of cysts, the outline of the kidneys, their symmetry, and the corticomedullary differentiation. In patients with a suspicion of vascular nephropathy, Doppler will look for findings of stenosis of the renal artery. Renal biopsy, often guided by imaging, is used to discover the cause of the renal failure when the size of the kidney is preserved and when the calyces are not dilated.

Intermediate ARM

ARM where the rectal pouch enters the sling of the puborectalis muscle; depending on the gender, either rectobulbar or rectovaginal fistulas can exist.

▶Anorectal Malformation

Intermittent Imaging

Imaging of ultrasound contrast media at a low frame rate (typically one image every second or every few seconds) to minimize bubble destruction caused by the ultrasound itself.

▶Time Intensity Curves

Internal Derangement, Temporomandibular Joint

Bodo Kress[1], Marc Schmitter[2]
[1]Department of Neurology, University of Heidelberg Medical Section, Heidelberg, Germany
[2]Department of Prosthodontic, Department of Neurology, University of Heidelberg Medical Section, Heidelberg, Germany
bodo_kress@med.uni-heidelberg.de

Synonyms

Temporomandibular arthropathy; Temporomandibular joint disorders

Definition

Internal derangement is caused by an abnormal movement and/or position of the disc. Naturally, the disc with its posterior attachment is located in closed-mouth position on the zenith of the condyle. During the opening of the mouth, the condyle and the disc slide on the tuberculum articulare. In joints presenting a disc displacement, the disc is located in front of the condyle. If the patient opens

the mouth, the condyle might slide on the disc and consequently, the condyle–disc relation normalises during mouth opening (anterior disc displacement with reduction). This action is clinically associated with a click during opening and closing.

In other cases, the condyle might not slide on the disc during mouth opening (anterior disc displacement without reduction). Thus, the disc–condyle relation remains pathological in the opened-mouth position. Consequently, there is often a limitation of the mouth opening in combination with pain as the disc closes the condyle in its movement. However, many subjects present an anterior disc displacement without suffering from any clinical signs or symptoms (the data vary between 7% and 35%).

Anatomy

The main components of the temporomandibular joint (TMJ) are the head of the mandible, the tubercle, the mandibular fossa and the articular disc. The disc has a posterior attachment to the ligamentous apparatus (the superior and inferior strata of the bilaminar zone). The articular disc plays a major role in TMJ function. It consists of an avascular anterior part, which is composed of fibrocartilage and a vascularised posterior part. The anterior part includes an anterior band, an intermediary zone and a posterior band. Under physiological conditions, the biconcave disc separates the TMJ into two compartments, which coordinate rotational movements (lower portion) and translational movements (upper portion). The face of a clock can be used for describing the anatomical location of the disc in relation to the condyle with the head of the mandible in the middle. When the mouth is closed, the posterior attachment of the disc is located at a position between 11 and 12 o'clock in the sagittal plane (Fig. 1a) (3).

When the mouth is open, the disc is interposed between the head of the mandible and the tubercle in the sagittal plane (Fig. 1b). Portions of the articular disc are not infrequently located medial to the head of the mandible in the coronal plane (Fig. 2a–c).

The head of the mandible is homogeneously structured without bony attachments and/or conspicuous flat areas. Under physiological conditions there is (almost) no fluid within the joint.

Pathology/Histopathology

Internal Derangement (Sagittal View)

Partial anterior displacement is diagnosed if the posterior attachment of the disc is located at a position between 10 and 11 o'clock or if anterior displacement cannot be seen on all slices.

Complete anterior displacement is diagnosed if the posterior attachment of the disc cartilage is located at a position below 10 o'clock on all slices or if it has no contact with the condyle (Fig. 3a). Anterior displacement is the most common type of internal derangement. The distinction between partial and complete anterior displacement in the closed-mouth position has no clinical relevance. What is clinically important is whether the disc resumes its normal position relative to the condyle when patients open their mouths (anterior disc displacement with reposition) or whether the disc remains anterior to the condyle on mouth opening (anterior disc displacement without reposition, Fig. 3b). Whereas anterior disc displacement with reposition is often accompanied by clicking sounds on opening and closing the mouth, anterior disc displacement without reposition is char-

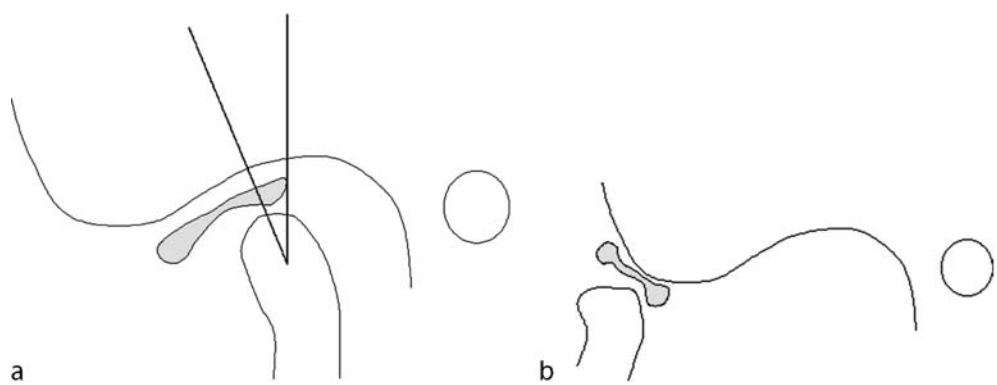

Internal Derangement, Temporomandibular Joint. Figure 1 Schematic drawing of a normal disc in the closed mouth (a) and opened mouth position, sagittal view (b). In the closed-mouth position the posterior attachment of the disc is located at a position between 11 and 12 o'clock, in the opened mouth position at a position between the condyle and the tubercle.

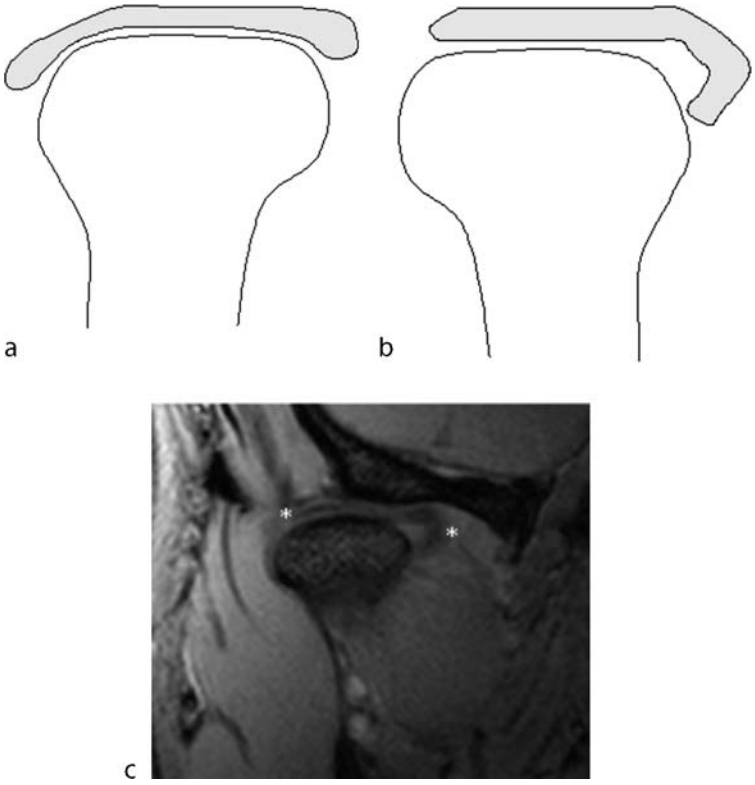

Internal Derangement, Temporomandibular Joint. Figure 2 MR image and schematic drawing of a normal disc (coronal view). Coronal T1-weighted FLASH 2D sequence with the mouth closed (a) and opened (b, c).

acterised by a limitation of mouth opening. Posterior disc displacement is relatively rare.

Internal Derangement (Coronal View)

While there is an extensive literature on the pathology of internal derangement in the sagittal plane, very few studies have focused on the coronal view. Normal and abnormal disc positions in the coronal plane, for example, have not yet been sufficiently defined. A review of the literature shows that there is only one prospective study that describes disc positions in a population of symptom-free subjects (Fig. 2a–c) (5). Medial displacement of the disc on mouth opening has been described as a pathological condition in many publications but appears to be within the range of normal variation. By contrast, the absence of a medial orientation seems to be a pathological finding. In addition, the coronal view can help avoid false-negative results in patients evaluated for disc position in the sagittal plane. A further systematic scientific analysis of coronal disc positions (especially in association with the clinical presence of clicking sounds and unremarkable sagittal MR images) might in the future offer useful diagnostic information (Table 1).

Clinical Presentation and Examination

The main clinical symptom is unilateral arthrogenous pain and/or a limited mandibular range of motion. For the clinical examination of the stomatognathic system, standardised criteria should be used and applied by calibrated examiners to obtain a higher reliability (1). A basic distinction should be made between arthrogenic and myogenic changes, which is often difficult, especially in patients with limited mouth opening. The importance of this distinction and the associated difficulties are explainable when the proximity of the TMJ to the surrounding muscles is taken into consideration. Diagnosis is facilitated by detailed information about clinical findings and their diagnostic significance.

Functional disorders are multi-factorial in origin. For this reason, the approach to the patient should include an assessment of psychosocial factors, although arthrogenic disorders are less commonly associated with psychosocial findings than myogenic disorders. The research diagnostic criteria for temporomandibular disorders (RDC/TMD) (1) is an examination protocol that meets all relevant requirements and is used worldwide for the assessment of functional disorders.

The clinical examination for patients suffering from TMD (e.g. the RDC/TMD) includes palpation of muscles (e.g. the masseter and temporal muscles) and portions of the TMJ (e.g. the lateral and posterior poles of the condyle) and documentation of sites painful to palpation. In addition, the range of motion of the mandible is assessed by measuring (maximum) mouth opening as well as lateral and protrusive movements. An additional clinical item to be considered is the assessment of joint sounds since grinding sounds, for example, may be indicative of changes in the shape of the condyle. The fluctuating character of TMJ sounds, however, must be considered in the examination.

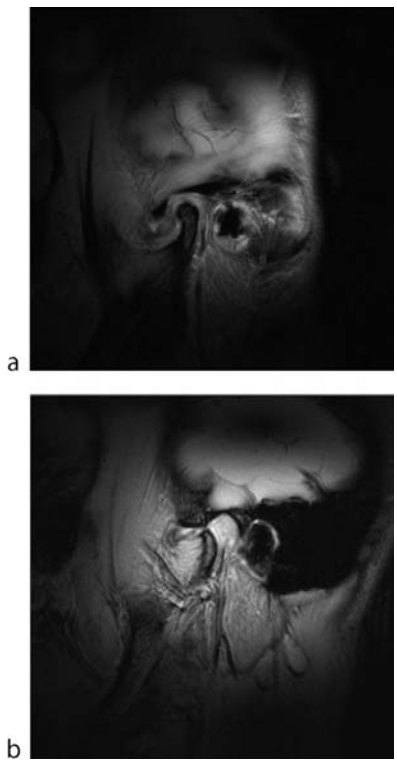

Internal Derangement, Temporomandibular Joint.
Figure 3 MR image and schematic drawing of complete anterior disc displacement (a) without reposition (b). Sagittal T1-weighted FLASH 2D sequence with the mouth closed (a) and opened (b).

Imaging of the Temporomandibular Joint

As the clinical assessment of the TMJ condition is sometimes unreliable because of fluctuating joint sounds, psychosocial aspects and the overlap of muscular and arthrogenous findings, imaging of the TMJ is necessary in some cases.

Magnetic resonance imaging offers high soft-tissue contrast and is therefore ideally suited for visualising tumourous, inflammatory and degenerative conditions of the TMJ. CT and X-ray only show bony structure and have a role in trauma (2).

The critical structures of the TMJ, such as the posterior attachment of the disc are very small. In addition, the accuracy of MRI findings depends not only on image resolution and quality but also on the anatomical knowledge of the radiologist. The higher the image quality, the higher will be inter-rater reliability or in other words, the level of agreement between the examiners with regard to disc position (4). For this reason, high image resolution and a good signal-to-noise ratio are important. Further factors that make image acquisition difficult are the pain that most patients feel when opening their mouth and the movements of the mandible that are associated with swallowing. This limits the examination time and requires the use of magnetic resonance systems with a field strength of 1.5 T and bilateral surface coils. These surface coils should have a diameter not exceeding 10 cm and should be placed over the TMJ. When MRI is used for evaluating patients suspected of having internal derangement, a TMJ positioning device that can be adjusted steplessly to each patient should be used in order to achieve a maximal opening of the mouth. This helps minimise mandibular movements during imaging.

Magnetic Resonance Imaging Protocol

The advantages and disadvantages of the various types of sequences must be carefully considered in selecting the most appropriate sequences. Spin echo sequences offer high soft-tissue contrast but are associated with a long imaging time at a relatively low resolution. The

Internal Derangement, Temporomandibular Joint. Table 1 MRI protocol for diagnosing internal derangement

		TE (msec)	TR (msec)	Field of view	Matrix	Slice thickness (mm)	Acquisition time (min)
Coronal oblique	PD FLASH 2D	10.2	208	120×120	256×256	3	3.32
Sagittal oblique	PD FLASH 2D	10.2	208	120×120	256×256	3	3.32
Coronal oblique	T2 TSE	112	5290	120×120	256×256	3	3.41

advantages of gradient-echo sequences are a short imaging time, high resolution and small slices. Although these sequences offer less contrast, they are widely used for functional MRI. We use a modified FLASH 2D sequence. PD-weighted sequences have proved to be effective in diagnostic imaging of other joints. With a reduced flip angle, the modified FLASH 2D sequence allows us to obtain images similar to PD-weighted scans. This sequence makes it possible to delineate the head of the mandible, the disc and the dorsal ligamentous apparatus. For this reason, we use it in object-oriented coronal and sagittal planes in the closed-mouth and open-mouth positions. Cine mode MRI at different openings of the mouth is not required since it does not provide additional information of clinical relevance and offers images of poor quality. The protocol also includes a coronal T2-weighted sequence that is used for imaging joint effusion and bone oedema.

The administration of an intravenous contrast agent is not necessary when internal derangement is suspected but may be required for diagnostic imaging of patients with tumours. In these cases, a T1-weighted fat-saturated sequence should be used.

Joint Effusion

An abnormal fluid collection within the TMJ is always a pathological condition that is not necessarily accompanied by pain. By contrast, minimal amounts of fluid in the lateral and medial recesses serve as physiological conditions.

Joint Contour

The head of the mandible usually has a smooth surface. Arthrotic osteophytes of the head of the mandible may be indicative of degeneration. It should be noted, however, that healthy joints can also show minimal shape changes within the range of normal variation. Depending on their extent, these changes can cause deformation of the condyle. They must be distinguished from mutilating abnormalities of the TMJ, which can be a sign of arthritis especially in young patients and should not be diagnosed as arthrotic changes. The administration of a contrast agent is not necessary since contrast enhancement of the synovial membrane must be expected in the presence of such marked joint lesions. Instead, patients should be advised to consult a rheumatologist and undergo serological testing.

In addition, cartilage lesions are found in the TMJ as in other joints. Cortical or osteochondral defects with loose fragments can occur.

Under normal physiological conditions, the disc has a biconcave shape but often adopts a different shape in the course of disc displacement, for example, it becomes biconvex. In the late stage of disc degeneration it is no longer possible to delineate the contours of the disc.

Range of Motion

Range of motion in the anterior–posterior direction depends on mouth opening capacity and thus shows individual differences. Asymmetries, where one mandibular head moves further in the ventral direction than the other one, are pathological conditions. In healthy test subjects, the condyle not infrequently (in more than 40% of cases) slides over the tubercle. Hypomobility is a pathological condition that is associated with the limitation of mouth opening and is characterised by a limited range of motion of the condyle in relation to the tubercle. It is often accompanied by an asymmetric opening of the mouth and occurs together with anterior disc displacement without reduction.

Diagnosis

Anterior displacement: Posterior attachment is below 10 o'clock position in closed mouth,
With reposition: Disc is in the normal position on mouth opening,
Without reposition: Disc is in front of the condyle on mouth opening,
Posterior displacement (very rare): Posterior attachment is dorsal to 1 o'clock position in closed mouth,
Hypomobility: Limitation of mouth opening and is characterised by a limited range of motion of the condyle in relation to the tubercle,
Joint effusion: An abnormal fluid collection within the TMJ.

Bibliography

1. Dworkin SF, LeResche L (1992) Research diagnostic criteria for temporomandibular disorders. J Craniomandib Disord 6:301–355
2. Katzberg R (1989) Temporomandibular joint imaging. Radiology 170:297–307
3. Rammelsberg P, Pospiech P, Jäger L et al (1997) Variability of disk position in asymptomatic volunteers and patients with internal derangements of the TMJ. Oral Surg Oral Med Oral Pathol Oral Radiol Endod 83:393–399
4. Schmitter M, Kress B, Hahnel S et al (2004) The effect of quality of temporomandibular joint MR images on interrater agreement. Dentomaxillofac Radiol 33:253–258
5. Schmitter M, Kress B, Ludwig C et al (2005) Temporomandibular joint disk position in the coronal MRI plane in symptom-free subjects. Radiology 236:559–564

Internal Hernia

The protrusion of bowel through a defect in its mesentery, but where the abnormally positioned bowel lies within the abdominal cavity.

▶Small Bowel, Postoperative

Internal Rectal Prolapse – Intussusception

▶Pelvic Floor Dysfunction, Anorectal Manifestations

Internal Urethrotomy

Surgical procedure that involves incising a urethral stricture transurethrally using endoscopic equipment. The incision is made under direct vision with an urethrotome and allows release of scar tissue. Care must be taken not to injure the corpora cavernosa because this could lead to erectile dysfunction.

▶Urethra, Stenosis

Intersex

▶Ambiguous Genitalia

Intersexuality

▶Ambiguous Genitalia

Interspinous Distance

Narrowest distance on an axial section between the ischial spines.

▶Pelvimetry, Magnetic Resonance

Interstitial Lung Diseases, Known Causes or Association

David M Hansell[1], Nicola Sverzellati[2]
[2]Department of Radiology, Royal Brompton Hospital, London, UK
[1]Department of Clinical Sciences, Section of Radiology, University of Parma, Italy
d.hansell@rbh.nthames.nhs.uk
nicolasve@tiscali.it

Synonyms

Diffuse parenchymal or interstitial lung disease from known causes or association

Definition

Many factors may produce diffuse predominantly interstitial infiltration of the lung. These entities comprise: hypersensitivity pneumonitis (HP), smoking-related interstitial lung disease, collagen vascular diseases, pulmonary vasculitis, drug toxicity, and radiation induced lung fibrosis.

Pathology/Histopathology

Hypersensitivity Pneumonitis

Hypersensitivity pneumonitis is an immunologically induced inflammatory disease of the lung parenchyma and terminal airways as a consequence of repeated inhalation of a variety of organic dusts and other agents in a sensitized host. The classic histopathology of HP features the triad of cellular bronchiolitis, a lymphoplasmocytic interstitial infiltrate, and poorly formed nonnecrotizing granulomas. However, pathologic features may vary with disease stage and a fibrotic pattern very similar to usual interstitial pneumonia (UIP) or nonspecific interstitial pneumonia (NSIP) is frequently seen in chronic, fibrotic HP.

Smoking-Related Interstitial Lung Disease

The increasing recognition that Langerhans cell histiocytosis (LCH), respiratory bronchiolitis-interstitial lung disease (RB-ILD), and desquamative interstitial pneumonia (DIP) form a spectrum of interstitial patterns in response to smoking-related lung injury has led to the proposal of the term "smoking-related interstitial lung

disease" to cover these entities. The variety of interstitial lung diseases associated with cigarette smoking is wider than generally appreciated and these often coexist (1). Respiratory bronchiolitis (RB) is a histopathologic lesion, characterized by the presence of pigmented intraluminal macrophages within respiratory bronchioles, whereas RB-ILD disease occurs when RB is extensive enough to cause symptoms and physiologic evidence of interstitial lung disease. LCH in adults results from the accumulation of specific histiocytic cells known as Langerhans cells in the lung, and is strongly associated with cigarette smoking.

Collagen Vascular Diseases

The collagen vascular disorders can affect many parts of the lung: the pleura, alveoli, interstitium, vasculature, lymphatic tissue, or airways. Most of the parenchymal manifestations of collagen vascular diseases are similar to those found in lone idiopathic interstitial pneumonias (IIPs).

Pulmonary Vasculitis

Pulmonary vasculitis may occur in the context of a systemic vasculitis or may be associated with other underlying diseases such as collagen or drug induced lung diseases. Principally small-vessel primary vasculitis, which causes alveolar hemorrhage and/or inflammatory infiltrates more reminiscent of diffuse interstitial lung disease (2).

Miscellaneous Causes of Pulmonary Fibrosis

Drug Toxicity

Numerous agents including cytotoxic (such as bleomycin, methotrexate, and cyclophosphamide) and noncytotoxic drugs (such as nitrofurantoin, sulfasalazine, and amiodarone) have the potential to cause pulmonary toxicity damage. The spectrum of the abnormalities includes mainly diffuse alveolar damage (DAD), nonspecific interstitial pneumonia, organizing pneumonia (OP), eosinophilic pneumonia, and pulmonary hemorrhage (3). Granulomatosis-like reactions as well as pulmonary vasculitis may also be caused by drug toxicity.

Radiation Induced Lung Fibrosis

Radiation effects on the lung are commonly seen within 6–8 weeks of starting treatment, and peak 3–4 months after completing treatment. After the early transient radiation, pneumonitis fibrosis progresses, consolidates, and contracts over the following months.

Clinical Presentation

Hypersensitivity Pneumonitis

The clinical features of HP are classically divided into three stages, based on the duration of the patient's symptoms: acute, subacute, and chronic. However, significant clinical and radiological overlap can often occur between these nominal phases.

Smoking-Related Interstitial Lung Disease

Patients with RB are usually asymptomatic whereas most patients with RB-ILD have mild symptoms that are not disabling. Cough and dyspnea are the most common presenting symptoms, though pneumothorax may be the presenting complaint in patients affected by LCH.

Collagen Vascular Diseases

The lung disease associated with collagen vascular disease may precede the clinical presentation of the collagen disease by 5 years or more. The pulmonary symptoms resemble mainly those of patients with other interstitial lung diseases.

Pulmonary Vasculitis

Wegener's Granulomatosis

At presentation, upper airway involvement with sinusitis and rhinitis is the most common clinical feature in patients affected by Wegener's granulomatosis. The pulmonary symptoms include hemoptysis, cough, chest pain, and dyspnea.

Churg-Strauss Syndrome

The diagnosis of Churg-Strauss syndrome is made in the presence of the following findings: (1) asthma, (2) eosinophilia greater than 10%, (3) neuropathy, (4) transient or migratory pulmonary opacities.

Microscopic Polyangitiis

A nongranulomatous necrotizing systemic vasculitis is usually responsible for the pulmonary–renal syndrome. Hence, important features that distinguish it clinically from any other vasculitis are the presence of glomerulonephritis and the frequency of pulmonary hemorrhage.

Miscellaneous Causes of Pulmonary Fibrosis

Drug Toxicity

Recognition of drug-induced lung disease can be difficult because the clinical manifestations are often nonspecific, and may be attributed to infection, radiation pneumonitis, or recurrence of the underlying disease.

Radiation Induced Lung Fibrosis

If any symptoms (dyspnea, cough, and fever) related to pulmonary irradiation occur, they are mainly seen in the acute phase. In chronic phase, if fibrosis is not severe and extensive, patients are usually asymptomatic.

Imaging

Hypersensitivity Pneumonitis

Chest radiography, in the acute or subacute phase, is often nonspecific; ground-glass opacification (GGO) or a nodular/reticulonodular pattern may be present. In chronic HP reticular opacities and volume loss occur.

A variety of high resolution computed tomography (HRCT) patterns have been described in HP. GGOs, mosaic attenuation, nodules, and reticular abnormalities may all be found in acute or subacute or chronic forms of the disease since significant clinical and radiological overlap can often occur between these nominal phases. Diffuse or patchy GGO with a geographic distribution is the most common finding in the acute phase, although HRCT is rarely obtained at this stage. The nodules are the most distinctive HRCT feature, and they are often seen in the subacute stage; they are centrilobular, poorly defined, of GG attenuation in contrast to the nodules of most other inhalational diseases. A mosaic pattern, due to small airways involvement with expiratory air-trapping, provides supportive evidence for the diagnosis, especially when it occurs in association with GGOs and nodules (Fig. 1) (4). Findings of fibrosis, such as reticular opacities, honeycombing, and traction bronchiectasis are only present in the chronic phase; at this stage, the predominant mid-lung distribution of the abnormalities in association with areas of air-trapping may help to differentiate chronic HP from other fibrotic lung diseases such as nonspecific interstitial pneumonia and usual interstitial pneumonia.

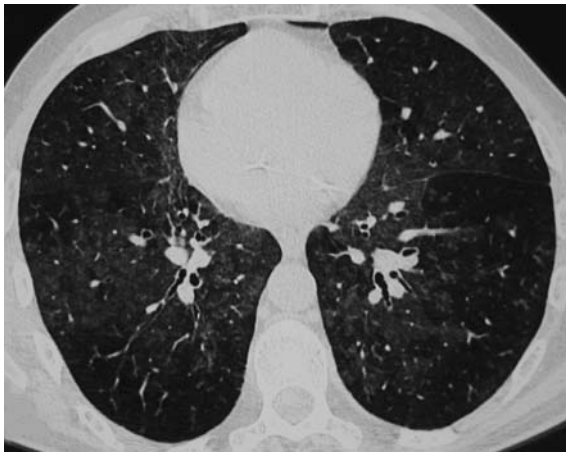

Interstitial Lung Diseases, Known Causes or Association. Figure 1 Subacute hypersensitivity pneumonitis (farmer's lung). Inspiratory HRCT shows mosaic attenuation, with areas of poorly defined ground-glass nodular opacities superimposed on a background of decreased attenuation.

Smoking-Related Interstitial Lung Disease

It is unusual to be able to diagnose RB-ILD by chest radiography alone. The HRCT features of both RB and RB-ILD are essentially represented by hazy centrilobular nodules predominating in the upper lobes and small patches of GG attenuation; in RB-ILD these abnormalities are more widespread and often associated with a background of emphysema and bronchial wall thickening. Interlobular septal thickening due to interstitial fibrosis may be seen in RB-ILD, but is rarely a prominent feature. Knowledge of a smoking history is clearly important, and may help to distinguish RB/RB-ILD from subacute HP which is usually not associated with this habit. RB-ILD differs from DIP in that GG attenuation of RB-ILD is usually less extensive, patchier, and more poorly defined.

Chest radiography in LCH shows nodular, cystic, reticular, or reticulonodular lesions, almost invariably involving the middle and upper lung zones, and frequently sparing the costophrenic sulci. Pneumothorax is a recognized feature of Langerhans cell histiocytosis. The HRCT appearance is a cystic-nodular pattern involving mostly the upper lobes. Nodules are usually <5 mm in diameter, have a peribronchiolar and centrilobular distribution, and may cavitate. Cysts are usually <10 mm in diameter but may coalesce becoming >20mm and leading to bizarre-shaped spaces with a bilobed, clover-leaf, or branching appearance. Nodules and cysts can occur independently of each other, but in the majority of patients they are found concomitantly. Occasionally, patchy or diffuse GGOs may be seen, probably related to areas of RB and DIP (1).

Collagen Vascular Diseases

Rheumatoid Arthritis

The chest radiograph of a patient affected by RA is usually normal but may show hyperinflation, reticulonodular

pattern, or pleural effusions. The "rheumatoid lung," interstitial inflammatory, and fibrotic pulmonary disease occur in a minority of patients; however; such term seems to be of little use as a descriptor, since lung biopsies show a wide range of abnormalities, including interstitial pneumonia, lymphoid hyperplasia, OP, and DAD, and HRCT more accurately reflects these changes than chest radiography. Although UIP and less frequently NSIP are the most frequent by encountered patterns, airway diseases including bronchiectasis and bronchiolectasis (even away from the fibrotic areas) and obliterative bronchiolitis (which causes a mosaic pattern) are not uncommon. It should be kept in mind that patients with rheumatoid arthritis often receive chronic drug therapy so that there may be coexistent drug-induced disease.

Systemic Sclerosis

As with other fibrosing lung diseases, the initial radiographic abnormalities may be subtle and consist of fine reticulation; as the disease progresses, the lower zone reticulation become coarser and more extensive.

The HRCT features of lung disease in patients with systemic sclerosis closely resemble those in patients with idiopathic nonspecific interstitial pneumonia. The finding of pulmonary arterial enlargement out of proportion to the severity of the lung fibrosis may indicate an independent vasculopathy akin to primary pulmonary hypertension. The presence of a dilated esophagus may also suggest of systemic sclerosis (Fig. 2).

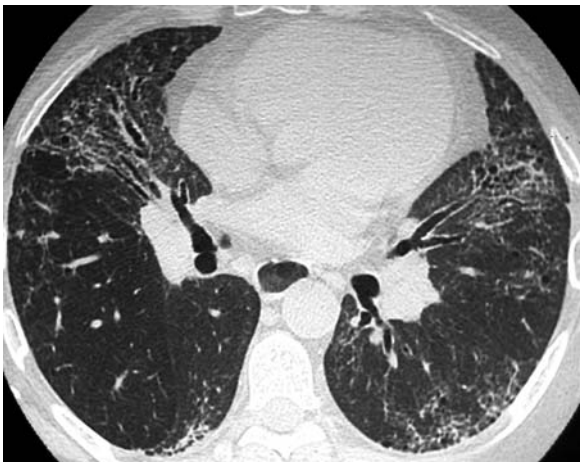

Interstitial Lung Diseases, Known Causes or Association. Figure 2 A 55-year-old patient with systemic sclerosis. HRCT through the lung bases shows fine reticulation and ground-glass opacity with a patchy distribution, consistent with a nonspecific interstitial pneumonia (NSIP) pattern (note the esophageal dilatation).

Systemic Lupus Erythematosus

Pleuropulmonary involvement of some sort occurs in approximately one-half of patients with systemic lupus erythematosus (SLE). The most common radiographic findings (not usually coexistent) consist of pleural effusion, cardiovascular changes, elevation of the diaphragm associated with basal atelectasis, and parenchymal consolidations and/or GGO pattern. The latter may reflect infection, pulmonary hemorrhage, lymphoproliferative infiltrate, or rarely of acute lupus pneumonitis characterized histologically by changes of DAD; moreover, fibrotic interstitial lung disease (NSIP, UIP, and OP subtypes) is generally regarded as an unusual manifestation of SLE.

Polymyosistis/Dermatomyositis

Radiographic changes in the lungs usually consist of symmetric reticulonodular opacity; more acute cases may show areas of airspace opacity. The HRCT changes are consistent with the pathologic findings, and represent OP and/or NSIP. Bilateral multifocal consolidation tends to occur in the lower zones with a subpleural and bronchovascular predilection, usually accompanied by linear opacities or GGO. In time, a fine honeycombing pattern equivalent to usual interstitial pneumonia may develop.

Pulmonary Vasculitis

Wegener's Granulomatosis

Chest radiographs typically show bilateral, multiple rounded opacities which may cavitate. The CT findings, although variable, consist mainly of subpleural or peribronchovascular nodules or masses; central cavitation usually occurs in nodules measuring greater than 2 cm in diameter, and the walls of cavitated lesions are often thick and irregular. Predominant bilateral air-space consolidation due to pulmonary hemorrhage is an infrequent but serious complication. Bronchial abnormalities, including bronchiectasis and bronchial wall thickening, have been reported in about 40% of cases. Tracheal narrowing is an important and relatively common manifestation of Wegener's granulomatosis.

Churg-Strauss Syndrome

The main HRCT features of Churg-Strauss syndrome consist of air-space consolidation or GGOs, nodules, and septal lines: these findings reflect the presence of air-space eosinophilic infiltrates as well as OP, and interstitial edema (which may be secondary to cardiac dysfunction) (5). Airway changes, in particular bronchial wall thickening, may be ascribed to the underlying asthma (Fig. 3).

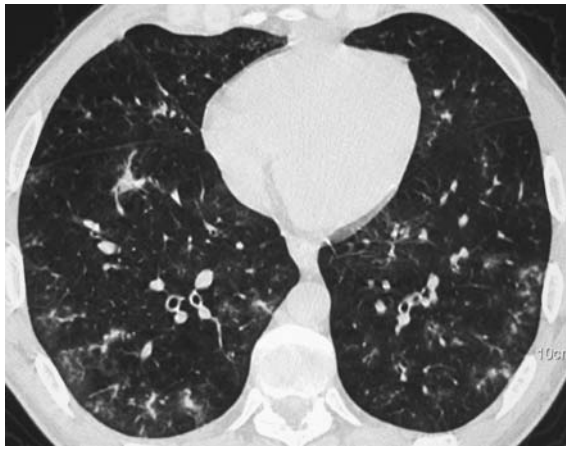

Interstitial Lung Diseases, Known Causes or Association. Figure 3 A 28-year-old man with Churg-Strauss syndrome. HRCT shows patchy ground-glass attenuation and poorly defined nodules with a peripheral distribution. Areas of decreased attenuation and bronchial wall thickening are also present, reflecting the underlying asthma.

Microscopic Polyangitiis

The HRCT findings are mostly related to ▶diffuse alveolar hemorrhage caused by capillaritis. Thus, consolidation as well as patchy GGO may be seen.

Miscellaneous Causes of Pulmonary Fibrosis

Drug Toxicity

The spectrum of abnormalities seen on HRCT in patients with drug-induced lung disease reflects the underlying histopathological findings including mainly DAD, NSIP, OP, eosinophilic pneumonia, and pulmonary hemorrhage (3). Some drugs can produce more than one pattern of histopathological involvement, and amiodarone toxicity is arguably the only condition in which CT can be used to make a definitive diagnosis by virtue of the high-attenuation values of amiodarone deposits in the lung.

Radiation Induced Lung Fibrosis

The earliest radiographic finding is a diffuse haze in the irradiated region with obscuration of vascular margins; scattered consolidations appear, and these areas may coalesce into a geometric area of pulmonary opacity. At this stage, CT findings are GGO and consolidation with a geographic distribution. With time the opacities become more linear or reticular and distort adjacent structures. 3D conformal radiotherapy can produce atypical findings, sometimes suggesting residual tumor or relapse.

Nuclear Medicine

Radiation Induced Lung Fibrosis

Fluoro-deoxyglucose positron emission tomography (FDG PET) imaging is more accurate than chest radiographs, and CT for distinguishing persistent or recurrent tumor from posttreatment scarring or fibrosis.

Diagnosis

Hypersensitivity Pneumonitis

Clinical and HRCT features often are characteristic enough to make the diagnosis. If the diagnosis remains equivocal, bronchoscopy may be helpful by demonstrating lymphocytosis on bronchoalveolar lavage or granulomas on transbronchial biopsy.

Smoking-Related Interstitial Lung Disease

A firm histological confirmation generally requires an open or thoracoscopic lung biopsy. However, the identification of Birbeck granules on electron microscopic evaluation of the cell pellet from a bronchoalveolar lavage can be diagnostic for LCH.

Collagen Vascular Diseases

Many of these diseases are characterized by the presence of a specific type of autoantibody, which may greatly assist specific diagnosis. Careful evaluation of the chest radiograph and CT can yield some useful clues to the presence of collagen vascular disease.

Pulmonary Vasculitis

Their diagnosis is based on clinical, radiographic, and histopathalogic findings. Although this group of diseases eludes a precise clinical or histological diagnosis, an increasing array of HRCT features can be used to corroborate pulmonary vasculitis as the dominant pathologic process.

Miscellaneous Causes of Pulmonary Fibrosis

Drug Toxicity

Diagnosis of drug-induced lung disease requires careful correlation of the history of drug exposure, compatible radiological findings, exclusion of alternative diagnoses, and improvement after withdrawal of offending agent.

Radiation Induced Lung Fibrosis

Radiological manifestations typically have a characteristic temporal relationship to the completion of therapy. Knowledge of this temporal relationship and an understanding of the expected patterns of radiation fibrosis associated with different radiation therapy techniques is needed to suggest a diagnosis of radiation induced lung fibrosis and to differentiate it from recurrent tumor or superimposed infection (6).

Bibliography

1. Hansell DM, Nicholson AG (2003) Smoking-related diffuse parenchymal lung disease: HRCT-pathologic correlation. Semin Respir Crit Care Med 24:377–392
2. Marten K, Schnyder P, Schirg E et al (2005) Pattern-based differential diagnosis in pulmonary vasculitis using volumetric CT. AJR Am J Roentgenol 184:720–733
3. Erasmus JJ, McAdams HP, Rossi SE (2002) High-resolution CT of drug-induced lung disease. Radiol Clin North Am 40:61–72
4. Patel RA, Sellami D, Gotway MB et al (2000) Hypersensitivity pneumonitis: patterns on high-resolution CT. J Comput Assist Tomogr 24:965–970
5. Silva CI, Muller NL, Fujimoto K et al (2005) Churg-Strauss syndrome: high resolution CT and pathologic findings. J Thorac Imaging 20:74–80
6. Choi YW, Munden RF, Erasmus JJ et al (2004) Effects of radiation therapy on the lung: radiologic appearances and differential diagnosis. Radiographics 24:985–997

Interstitial Lung Diseases, Unknown Etiology

Nicola Sverzellati[1], David M Hansell[2]
[1]Department of Clinical Sciences, Section of Radiology, University of Parma, Parma, Italy
[2]Department of Radiology, Royal Brompton Hospital, London, UK
nicolasve@tiscali.it

Synonyms

Diffuse interstitial lung disease from unknown causes; Diffuse parenchymal lung disease from unknown causes; Idiopathic interstitial lung diseases

Definition

The term "idiopathic interstitial lung diseases" is applied to a group of disorders with distinct histological and radiological appearances and without a known cause. These disorders essentially include sarcoidosis, ►lymphangioleiomyomatosis, ►pulmonary alveolar proteinosis, eosinophilic pneumonia, and idiopathic interstitial pneumonias (IIPs).

Idiopathic Interstitial Pneumonias

Pathology/Histopathology

The evolution of the classification of the IIPs over time has culminated in seven entities: idiopathic pulmonary fibrosis (IPF), corresponding to the pathology of usual interstitial pneumonia (UIP); nonspecific interstitial pneumonia (NSIP); desquamative interstitial pneumonia (DIP); respiratory bronchiolitis-associated interstitial lung disease (RBILD); cryptogenic organizing pneumonia (COP), formerly known as bronchiolitis obliterans organizing pneumonia; acute interstitial pneumonia (AIP); and lymphocytic interstitial pneumonia (LIP) (1).

The histological diagnosis of UIP is based on temporal and spatial heterogeneity of the fibrotic lesions (variegated appearance with scattered areas of normal lung, fibroblastic foci, honeycombing, etc.) with patchy involvement and normal lung adjacent to severely fibrotic lung. In contrast to UIP, the pathologic findings of NSIP are spatially and temporally uniform and consist primarily of interstitial inflammation or fibrosis. The main pathologic finding of COP consists of polypoid masses of granulation tissue within peripheral airways, extending into the alveoli and associated with interstitial and peribronchial cellular infiltration. Although DIP is currently classified as an IIP (1), its usual association with cigarette smoking has led it to be considered part of a spectrum of smoking-related lung diseases. DIP is characterized by spatially homogeneous thickening of alveolar septa, associated with intraalveolar accumulation of macrophages. AIP is a rapidly progressive form of interstitial pneumonia that is histologically identical to acute respiratory distress syndrome (ARDS). LIP occurs almost exclusively in patients who either have a connective tissue disorder (particularly Sjögren syndrome), immunodeficiency or Castleman disease. Though not usually idiopathic, it was included in the classification of IIPs (1) largely because it is important in the histological differential diagnosis of the IIPs. LIP is characterized by marked infiltration of the interstitial space by a monotonous sheet of lymphocytes.

Clinical Presentation

The most frequent presenting symptoms of patients affected by IIPs are progressive dyspnea, nonproductive cough, and (more commonly in COP) an influenza-like illness. Less common symptoms include nonspecific chest pain and constitutional symptoms such as weight loss and

fatigue, whereas patients with AIP and dyspnea progress rapidly to respiratory failure.

Imaging

Almost all patients affected by IIPs have abnormal chest radiographs characterized mostly by a variety of nonspecific patterns, most frequently a reticular pattern; however, consolidations and patchy abnormalities may predominate, especially in COP and AIP.

UIP. Abnormalities are predominantly basal, often patchy, with a strikingly peripheral distribution. The typical high-resolution computed tomography (HRCT) image is characterized by the presence of reticular opacities, within which are cystic airspaces (honeycombing), and traction bronchiectasis (Fig. 1). Ground-glass opacity (GGO) is usually present but is less extensive than the reticular pattern. Mediastinal adenopathy is a frequent accompaniment.

A rapid development of new areas of GGO and/or consolidation raises the possibility of an accelerated phase of the disease, an opportunistic infection, or pulmonary edema. Other complications include pneumothorax, pneumomediastinum, lung neoplasms, pulmonary hypertension, and cardiac failure.

NSIP. The CT features of NSIP consist mainly of GGO and reticular opacities involving the lower zones, with a peripheral and/or a peribronchovascular distribution. GGO occurs as an isolated finding in about one-third of patients but is more commonly associated with reticular abnormality or consolidation, which may represent foci of organizing pneumonia. Honeycombing, if present, is limited in extent compared with UIP.

Even though no single feature or combination of CT features can be identified as being entirely specific for a histological diagnosis of NSIP, a summary of the CT findings, particularly the extent of the disease, is very important for the evaluation of patients with NSIP. There is a better correlation between response in terms of disease extent on CT than the absolute histopathological subtype of disease, presumably due to the global assessment of the lung provided by CT in contrast to the inherent sampling of lung biopsy (2).

COP. CT shows consolidations that are usually bilateral, patchy, asymmetric, peripheral, and migrating; the lower lung zones are more frequently affected (Fig. 2). GGOs are present in about 60% of cases (3). Other CT findings include small centrilobular nodules, irregular lines, and ill-defined perilobular densities. COP in its usual radiological manifestation may spontaneously resolve or respond to steroid therapy, but some cases associated with reticular opacities may progress to irreversible fibrosis. When considering the dominant feature of COP on CT – namely consolidation – other entities, such as infections, bronchioalveolar carcinoma, lymphoma, and vasculitis, should be excluded.

DIP. The main feature on CT is the presence of GGO, which is usually bilateral and symmetrical. The distribution is basal and peripheral. Small thin-walled cysts may occur within the areas of GGO, whereas signs indicating architectural distortion (irregular linear opacities, honeycombing) are seen in about one-third of cases.

AIP. The earliest CT appearances are bilateral and patchy GGOs, often associated with consolidation in the

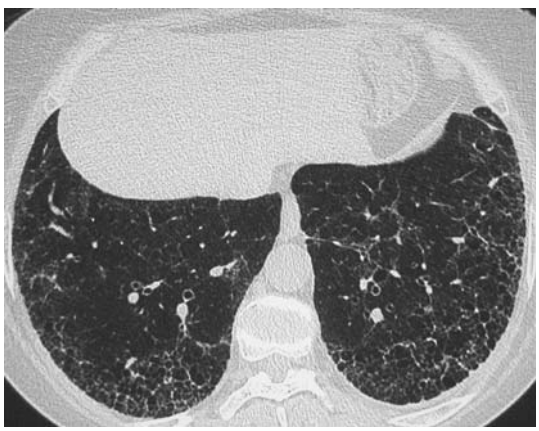

Interstitial Lung Diseases, Unknown Etiology. Figure 1
A 63-year-old man with usual interstitial pneumonia. High-resolution computed tomography shows peripheral honeycomb lung destruction and reticular abnormality in the lower lobes.

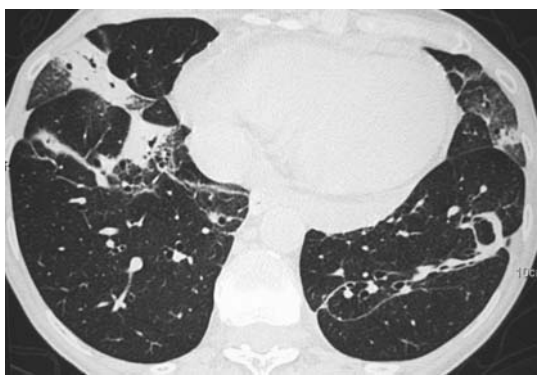

Interstitial Lung Diseases, Unknown Etiology. Figure 2
A 52-year-old man with recurrent migratory consolidation due to cryptogenic organizing pneumonia. The consolidation has a predominant peribronchovascular distribution.

dependent lung. In surviving patients, CT shows a progressive change from GG attenuation to traction bronchiectasis, cystic lesions, and reticular opacities, predominantly in the nondependent lung.

Patients with AIP are more likely to have a symmetric bilateral distribution of the lesions with lower lung predominance compared with patients with ARDS (1). Other differential diagnoses include acute exacerbation of an underlying chronic idiopathic fibrosis or systemic disease (connective tissue diseases and vasculitis), infections, pulmonary edema, and pulmonary hemorrhage.

LIP. The concomitant presence of GGOs, poorly defined nodules (centrilobular or subpleural) and scattered thin-walled cysts can help differentiate LIP from other IIPs on HRCT but the range of CT appearances of the rare IIP is wide, and a confident HRCT diagnosis is unusual. Other common findings are lymphadenopathy and interlobular septal thickening.

Nuclear Medicine

To date, nuclear medicine techniques such as positron emission tomography (PET) and lung scanning have no well-documented clinical role in the diagnosis, management, or prognosis of most diffuse lung processes.

Diagnosis

HRCT assumes a central role in defining the morphologic pattern of the IIPs, particularly in distinguishing between UIP from the other IIPs. Because UIP has a worse prognosis than the other forms of IIPs, it is important to clearly separate those patients who have the pattern of UIP on HRCT from those with other patterns. However, the HRCT features of each IIP may not be characteristic, and there is overlapping as well as coexistence of these entities.

When the HRCT pattern is typical, UIP can be confidently diagnosed in more than half of cases. Nevertheless, a confident diagnosis of UIP on HRCT is not straightforward in about one-third of patients with biopsy-confirmed UIP; in such cases, the honeycombing is less pronounced and the GGO may predominate, resembling an HRCT appearance of NSIP.

In all the other cases of IIPs, surgical biopsy is usually warranted to secure a definite diagnosis.

Sarcoidosis

Pathology/Histopathology

Sarcoidosis is a systemic disease of unknown etiology characterized by noncaseating granulomatous inflammation. Although known to affect any organ system, the lungs and its associated lymph nodes are involved in 90% of patients. Pathologic findings in sarcoidosis consist of noncaseating granulomas with epithelioid cells and large, multinucleated giant cells. In the lungs, granulomas are predominantly distributed along lymphatic pathways, being characteristically found along bronchovascular bundles, interlobular septa, and pleura. Although granulomas may remain stable for a long time or resolve spontaneously (or in response to treatment), in a minority of cases a centripetal fibrosis tends to obliterate the granulomas, leading to an extensive interstitial fibrosis with destruction and distortion of the lung architecture.

Clinical Presentation

Sarcoidosis most commonly presents between 20 and 40 years of age. Presentation as an incidental radiographic finding occurs in about 50% of cases. Respiratory illness, erythema nodosum, and ocular symptoms represent the other common presentations. Acute onset with erythema nodosum or asymptomatic bilateral hilar lymphadenopathy usually heralds a self-limiting course with spontaneous resolution, whereas insidious onset, especially with lung involvement or multiple extrapulmonary lesions, may be followed by progressive fibrosis of the lung and other organs (4). Sarcoidosis occurring in blacks is later in onset, is more likely to involve peripheral nodes, and to become chronic and disseminated; in general, the prognosis of sarcoidosis is worse in blacks than in whites. Although patients with sarcoidosis usually have a restrictive defect, an obstructive impairment can be surprisingly related to the extent of the reticular pattern depicted on HRCT or to small airway involvement and air trapping.

Imaging

Frequently, the diagnosis is first brought to attention by incidental findings on chest radiography, and staging of the disease is traditionally based on chest radiograph findings: stage O = no demonstrable abnormality; stage I = nodal enlargement only; stage II = nodal enlargement associated with parenchymal abnormality; stage III = pulmonary opacity not associated with node enlargement or evidence of fibrosis; stage IV = lung fibrosis (parenchymal distortion, lobar volume loss, etc.). Generally, the abnormalities on chest radiography mostly consist in hilar (typically symmetric) and mediastinal adenopathy, profuse bilateral small nodules, rounded or irregular, associated with linear and irregular opacities in the middle and upper zones. Symmetry is an important diagnostic feature of the hilar adenopathy associated with sarcoidosis because symmetric adenopathy is unusual in lymphoma, tuberculosis, and metastatic disease.

Hilar and mediastinal lymphadenopathy is seen more frequently on CT, which can also allow a more detailed analysis of nodal calcification. Because of their typical "perilymphatic" distribution, the nodules depicted on HRCT are clustered along the bronchovascular bundles, interlobular septa, interlobar fissures, adjacent to the costal pleural (sometimes mimicking small pleural plaques), and also in the centrilobular regions (Fig. 3) (5). Nodules tend to predominate in perihilar regions with relative sparing of the lung periphery and may be grouped unilaterally or bilaterally in small areas. Nodules of sarcoidosis typically measure 1–5 mm, but rarely, multiple ill-defined large nodules (ranging in diameter from 1 to 4 cm) can be observed on chest radiography. In approximately 10% of patients with sarcoidosis, a confluence of granulomas may cause compression of the alveoli and result in poorly defined bilateral parenchymal consolidations containing an air bronchogram; both parenchymal consolidations or large nodules can, although rarely, cavitate. Innumerable small interstitial granulomas (beyond the resolution of CT) may cause patchy GGOs on HRCT.

Although the parenchymal abnormalities are often reversible, pulmonary fibrosis occurs in approximately 20–25% of cases. Classic changes include linear opacities (radiating laterally from the hilum), fissural displacement, bronchovascular distortion (bronchiectasis), and honeycombing concentrated in the upper zones of the lungs. Finally, HRCT can also help demonstrate other specific complications (pulmonary hypertension, bronchial stenosis, etc.) and comorbidities (such as aspergilloma colonization of the cavities).

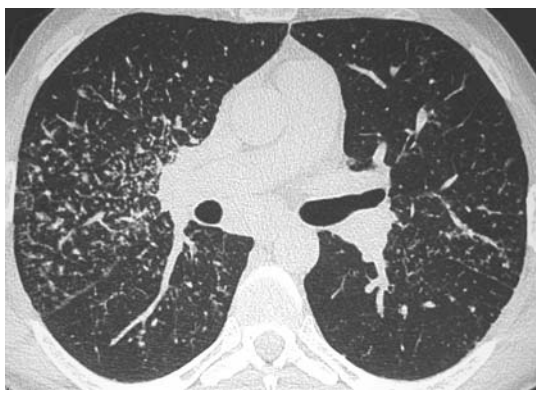

Interstitial Lung Diseases, Unknown Etiology.
Figure 3 Sarcoidosis. High-resolution computed tomography shows small nodules along interlobular septa, pulmonary vessels, and visceral pleura (e.g., the left oblique fissure).

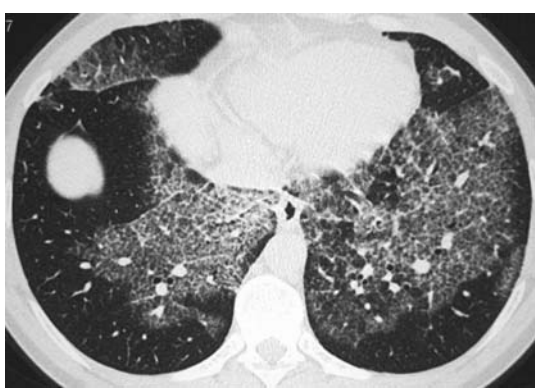

Interstitial Lung Diseases, Unknown Etiology.
Figure 4 Pulmonary alveolar proteinosis. High-resolution computed tomography shows extensive bilateral ground-glass opacity with a geographic distribution and a fine reticular pattern with interlobular as well as intralobular septal thickening superimposed (crazy-paving pattern).

Nuclear Medicine

Only PET scanning with various markers has shown utility in detecting occult disease activity in patients affected by sarcoidosis.

Diagnosis

The definitive diagnosis of sarcoidosis requires clinical and imaging features compatible with the diagnosis, as well as confirmation of the presence of noncaseating granulomas. Laboratory investigations may show various nonspecific derangements such as high serum levels of angiotensin converting enzyme (ACE), hypercalcemia, and a decreased CD4:CD8 ratio in the blood serum. Chest radiography still plays an important role in diagnosis of sarcoidosis, while CT is superior for demonstrating subtle mediastinal lymphadenopathy and associated parenchymal involvement. Histological confirmation of the presence of granulomas is critical in the diagnosis of sarcoidosis; transbronchial biopsy has a high diagnostic yield because of the predominantly peribronchovascular distribution of the granulomas.

Bibliography

1. American Thoracic Society/European Respiratory Society (2002) International multidisciplinary consensus classification of the idiopathic interstitial pneumonias. Am J Respir Crit Care Med 165:277–304
2. Screaton NJ, Hiorns MP, Lee KS et al (2005) Serial high resolution CT in non-specific interstitial pneumonia: prognostic value of the initial pattern. Clin Radiol 60:96–104
3. Lynch DA, Travis WD, Muller NL et al (2005) Idiopathic interstitial pneumonias: CT features. Radiology 236:10–21
4. Koyama T, Ueda H, Togashi K et al (2004) Radiologic manifestations of sarcoidosis in various organs. Radiographics 24:87–104
5. Nishimura K, Itoh H, Kitaichi M et al (1993) Pulmonary sarcoidosis: correlation of CT and histopathologic findings. Radiology 189:105–109

Intertuberous Distance

Narrowest distance on an axial section between the ischial tuberosities.

►Pelvimetry, Magnetic Resonance

Interval Cancer

An interval cancer is a malignant tumor that presents clinically during the interval between routine screenings and that was not visible or not suspected on review. This type must be distinguished from missed cancers that were overlooked on prospective initial studies, but were visible on review.

►Carcinoma, Ductal, Invasive

Interventional Hepatic Procedures

Riccardo Lencioni, Marzio Perri
Department of Diagnostic and Interventional Radiology University of Pisa, Pisa, Italy
lencioni@med.unipi.it

Several image-guided interventional procedures, including percutaneous and intra-arterial therapies, have been developed to treat primary and secondary liver malignancies. Percutaneous techniques of tumour ablation consist in the direct application of chemical agents (ethanol or acetic acid) or thermal agents, including heating (radiofrequency, laser and microwaves) and freezing (cryoablation) to a focal tumour (1). In intra-arterial therapies, chemotherapeutic and/or embolizing agents are delivered into the hepatic arterial system.

Techniques

Ethanol Injection

►Percutaneous ethanol injection (PEI) has been the most widely used tumour ablation technique (2, 3). PEI induces local tumour necrosis as a result of cellular dehydratation, protein denaturation and chemical occlusion of tumour vessels. Since it allows a real-time control, US guidance is the best option for PEI administration enabling a faster procedure time, precise centring of the needle in the target, and continuous monitoring of the injection. Fine non-cutting needles, with either a single end hole or multiple side holes, are commonly used for PEI. PEI may be performed under local anaesthesia and patient hospitalization is not required. The treatment schedule typically includes four to eight session performed once or twice weekly. However, number of session and amount of ethanol to inject may vary according to the size of the lesion, intra-tumour ethanol distribution and patient's compliance.

Radiofrequency Ablation

Percutaneous ► radiofrequency (RF) ablation works on the principle that alternating current operated within the radiofrequency range can produce focal thermal injury in tissues (2, 3). The thermal damage caused by RF heating is dependent on both the tissue temperature and the duration of heating and when a 90–105°C temperature throughout the entire target volume is achieved and maintained for at lest 4–6 min, a large area of coagulative necrosis can be obtained. In RF ablation, the patient is part of a closed-loop circuit that includes an RF generator, an electrode needle, and a large dispersive electrode (ground pads). In each treatment session the electrode needle is placed within the liver tumour under US, CT or MR, guidance. Grounding is achieved by attaching large ground pads and the electrode is then attached to the RF generator. Since the dimension of RF thermal lesions is related not only to tissue-anatomic characteristics (heat conduction and heat lost *via* circulation) but also to technical elements (current intensity and size of the needle electrode), several technological improvements have been introduced in order to optimize RF results. Particularly, modified electrodes, such as cooled-tip electrode needles and expandable electrode with multiple retractable lateral-exit prongs on the tip, allow to obtain a larger volume necrosis and to make the procedure more effective. With any technology, each insertion lasts 10–20 min, since after this time the impedance rise induced by coagulative necrosis not allow further heat diffusion in the tumour. RF treatment may be performed by using local anaesthesia or conscious sedation.

Laser Ablation

►Laser ablation uses laser light produced by a neodymium yttrium albuminium garnet (Nd:YAG; wavelength 1,064 nm) delivered through a quartz fibre optic with a diameter of 400 μm with diffuse light emission. Laser light is converted into heat in the target area with an ensuing coagulative necrosis, secondary degeneration and

atrophy, and tumour shrinkage with minimal damage to surrounding structures. The dimension of the coagulative necrosis laser induced depends on laser power, laser irradiation time and the optical and thermal tissue characteristics (4).

Microwave Ablation

►Microwave ablation is an electromagnetic method of inducing tumour destruction by using devices with frequencies greater than or equal to 900 kHz (5). In microwave ablation a microwave generator and needle electrodes are employed. The microwave energy is transmitted *via* a flexible cable and delivered by the electrodes. Microwaves cause vibration and rotation of molecular dipoles, predominantly water, resulting in a thermal coagulation of tissues.

Cryoablation

►Cryotherapy is defined as local tumour destruction *in situ* by freezing. The resulting freeze process causes irreversible cellular damage and tissue necrosis is obtained (3–5). Different methods, including repeated freeze cycles, temporary hepatic inflow occlusion and multi-needle probe systems, have been developed to increase the size of cryolesion.

Transcatheter Arterial Embolization and Chemoembolization

►Transcatheter arterial embolization (TAE) consists in a temporary or permanent peripheral occlusion of the hepatic artery. It requires catheterization of the segmental hepatic artery supplying the liver tumour following by intra-arterial injection of embolic materials. ►Transcatheter arterial chemoembolization (TACE) combines peripheral occlusion and local deposition of chemotherapeutic agents, consisting in intra-hepatic arterial injection of chemotherapeutic agents followed by embolic agents. The anti-tumour effect depends on the synergy between the actions of chemotherapy and ischemia, since the occlusion of the tumour arterial supply advantageously follows the controlled infusion of the chemotherapeutic drug. TACE can be performed by using several different techniques, including conventional and segmental catheterism. Conventional TACE is performed by injecting an anticancer-in-oil emulsion followed by embolic material at the level of the proper hepatic artery while in segmental and subsegmental technique a microcatheter is inserted into the more distal branches of the hepatic artery, and the drug as well as the embolic material are injected solely in the feeding artery of the tumour. This allows a more strong anticancer effect, sparing at the same time the non-cancerous liver parenchyma (3). A large variety of chemotherapeutic drugs and embolic agents have been used.

Clinical Applications

Radiological interventional procedures have been employed in the treatment of either primary or secondary unresectable hepatic malignancies. A robust evidence concerning the clinical value of these techniques is currently available for the use of ethanol injection, radiofrequency ablation and TACE. An appropriate use of each treatment technique can only be done when the therapeutic strategy is decided by a multidisciplinary team and is tailored to the individual patient and to the features of the disease (2, 3).

Ethanol Injection

PEI is cheap, easy to perform, repeatable and has been the most widely used ablation technique in HCC patients. It is a well-tolerated treatment, with a high anti-tumoural efficacy in small solitary, nodular-type HCC (3 cm or less). Since HCC nodules have a soft consistency and are surrounded by a firm cirrhotic liver, injected ethanol diffuses within tumour tissue easily and selectively, leading to complete tumour necrosis in a great number of small lesions (2). The injected ethanol does not always accomplish complete necrosis in HCC nodules because of its inhomogeneous distribution within the lesion, especially in the presence of intra-tumoural septa, and repeated treatment session are usually required. In hepatic metastases the hard consistency of the neoplastic tissue impairs an adequate diffusion of ethanol resulting in a poor tumour control.

Radiofrequency Ablation

RF ablation is an effective treatment both in primary and metastatic liver tumour and represents the most widely used method for percutaneous thermal ablation. RF ablation seems to be more effective than PEI in the treatment of small HCC. Particularly, RF can achieve a more effective local tumour control than PEI with fewer treatment sessions. However, despite RF may provide marginal anti-tumour benefits also in lesions larger than 3 cm in diameter, where PEI is unable to disrupt the intra-tumoural septa, the treatment of large HCC is still problematic (2). RF is also effective in the treatment of hepatic metastases and to date it represents a valuable option in unresectable, solitary and small hepatic metastases arising from colorectal adenocarcinoma (3, 4). Although more invasive than PEI, RF ablation is considered to be safe, with a relatively low complication rate. Particularly, RF treatment of lesion adjacent to the gallbladder or to the hepatic hilum as well as

of lesions located along the surface of the liver is associated with a higher risk of complications.

Transcatheter Arterial Chemoembolization

TACE may be an effective method of controlling hepatic disease in many patients with liver-dominant neoplasms, such as HCC, colorectal metastases and neuroendocrine tumours (3). Particularly, TACE remains a valuable approach for HCCs in the intermediate stage.

Moreover, TACE can also be used as an adjuvant to other forms of therapy and, since the absence of tumour seeding risk, it represents the first therapeutic option in HCC patients waiting for liver transplantation.

TACE has also been proved to be effective in the treatment of hepatic metastases arising from neuroendocrine tumours and colorectal cancer.

Bibliography

1. Goldberg SN, Charboneau JW, Dodd GD III et al (2003) International Working Group on Image-Guided Tumor Ablation Image-guided tumor ablation: proposal for standardization of terms and reporting criteria. Radiology 228(2):335–345
2. Lencioni R, Cioni D, Crocetti L et al (2004) Percutaneous ablation of hepatocellular carcinoma: state-of-the-art. Liver Transpl 10(2):S91–97
3. Bartolozzi C, Lencioni R (eds) (1999) Liver Malignancies. Springer-Verlag, Berlin Heidelberg, New York
4. Vogl TJ, Muller PK, Mack MG et al (1999) Liver metastases: interventional therapeutic techniques and results, state of the art. Eur Radiol 9(4):675–684
5. Ng KK, Lam CM, Poon RT et al (2003) Thermal ablative therapy for malignant liver tumors: a critical appraisal. J Gastroenterol Hepatol 18(6):616–629

Interventional Procedures

Procedures which treat disease states by open surgery or minimally invasive methods.

▶Aneurysm, Aortic and Thoracic

Intervertebral Disk Degeneration

Degenerative changes in the intervertebral disk usually begin with dehydration of the nucleus pulposus and annular tears. Dehydration is easily diagnosed on sagittal T2-weighted MR images as decreased signal of the disc. This can be accompanied by narrowing the intervertebral space due to the decreased height of the intervertebral disk, which may be seen on plain films, sagittal reformatted CT images and sagittal T2-weighted MR images. Other features of disk degeneration are vacuum phenomenon (the presence of the gas in the disk due to the production of the nitrogen during the degenerative process) and calcifications; both are excellently visible on CT examination, may be also seen on plain films and MR gradient-echo images. Degeneration of the intervertebral disk is often associated with disk bulging and may lead to disk herniation. On the other hand it is almost always combined with degenerative changes of the adjacent vertebral endplates and very often-with degeneration of the other structures of the disco-somatic unit.

▶Degenerative Conditions, Spine

Intestinal Angina

Abdominal pain related to transient intestinal ischemia, appearing 20–30 min after a meal.

▶Vascular Disorders, the Gastrointestinal Tract

Intra-Axial Brain Tumors

▶Neoplasms, Brain, Intraaxial

Intra- and extracranial, (cervical) cysts

Intra- and extracranial, (cervical) cysts are epithelial lined, well circumscribed, fluid filled non-neoplastic benign lesions. Depending on their location, adjacent stuctures may be displaced or compressed. Clinical symptoms vary with cyst location.

▶Cyst, Cerebral and Cervical, Childhood

Intra-dural Extra-medullary Space

This space is limited by the surface of the cord and the dura and is filled by cerebrospinal fluid. The cord is covered by pia matter and arachnoid membrane. In the spinal canal the arachnoid and pia matter form separate layers. The subarachnoid space separates them everywhere except where it is traversed by the nerve roots and the spinal

ligaments. The dura is separated from the vertebral canal by a layer of tissue that contains the internal vertebral venous plexus and a deposit of adipose tissue that lies in a dorsal recess between the ligamenta flava.
▶Tumors, Spine, Intradural, Extramedullary

Intracellular Reporter System

Intracellular reporter systems utilize gene products that are present within the cells
▶Reporter Systems

Intracystic Papillary Carcinoma

Variant of intraductal papillary carcinoma, located within a cyst.
▶Cyst, Breast

Intracystic Papillary Carcinoma with Invasion

▶Carcinoma, Other, Invasive, Breast

Intracystic Papilloma

Benign papillary tumor inside a cyst.
▶Cyst, Breast

Intrahepatic Suppuration

▶Abscess, Hepatic

Intralesional Tumor Resection

When the surgical margins are within the tumor margins, thus making residual tumor and recurrent tumor more common and associated with a poorer prognosis.
▶Neoplasms, Soft Tissues, Malignant

Intraosseous Lipoma

Intraosseous lipoma is a benign bone lesion composed of mature adipose tissue, which in most cases originates from the medullary portion of bone. Rarely, lipomas can develop in cortical or periosteal locations.
▶Neoplasms, Bone, Benign

Intraparenchymal Hematoma, Splenic

A collection of clotted blood within the disrupted splenic parenchyma. It represents a possible finding in cases of splenic parenchymal or vascular lesion.
▶Trauma, Splenic

Intraperitoneal Chemohyperthermia

In addition to surgery, local chemotherapy is applied in the peritoneal cavity with optimal biological effects in a hyperthermic stage. Arterial vascularization of a neoplasm is used as a route for locoregional application of chemotherapeutic agents.
▶Chemoperfusion

Intrarenal Abscess

▶Abscess, Renal

Intrauterine MRI

▶Fetal Imaging

Intravascular Contrast Media

▶Contrast Media, MRI, Blood Pool Agents

Intravenous Urography

Recently nonionic contrast agents are administered intravenously, which are excreted by the kidney into the renal pelvis, ureters, bladder, and urethra (at miction). IVU is useful for the diagnosis of obstruction, trauma, tumors, congenital malformation, and infection. It can assess kidney function, intra- and extraluminal pathology, and differentiate stones from other abdominal calcifications. It can differentiate nonmalignant from malignant causes of obstruction, haematuria, and pain. Radiopaque calculi projecting inside the collecting system, independent of the patient's position, can be less, equal or more opaque as surrounding contrast, while radiolucent calculi present as a filling defect. IVU confirms the diagnosis of acute stone obstruction also if KUB is inconclusive by assessing secondary signs of obstructing calculi: delayed excretion, persisting nephrographic effect, extravasations in spontaneous forniceal rupture, mild and local dilatation. After obtaining a KUB, 20 min postcontrast films are proposed in obstruction. In carefully conducted IVU, stones or other pathology can be assessed within the time of examination in the majority of cases using solely four images. The application of prone or slightly oblique standing projections, when necessary to opacify the collecting system to the level of obstruction, under fluoroscopic control, reduces the examination time and number of films. Rarely delayed films are required.

▶Colic, Acute, Renal
▶Medullary Sponge Kidney

Intrinsic Brain Tumor

▶Neoplasms, Brain, Supratentorial, Pediatric

Intussusception

The invagination or "telescoping" of a loop of bowel within itself, most commonly occurring as an ileo-colic intussusception but also including ileo-ileal and ileo-ileo-colic.

▶GI Tract, Pediatric, Specific Problems

Intussusception

▶GI Tract, Pediatric, Specific Problems

Invasive Ductal Carcinoma

An invasive carcinoma is a tumor with extension of tumor cells through the ductal basement membrane. A spiculated mass with irregular margins, sometimes with amorphous or pleomorphic microcalcifications, is a typical sign of invasive ductal carcinomas.

▶Carcinoma, Ductal, Invasive

Involucrum

An involucrum is a layer of reactive, vital bone that has been formed around dead bone in chronic osteoneyelitis in an attempt to confine the ongoing infection.

▶Osteomyelitis

Involucrum, Sequestrum, Cloaca

When bone infection has been untreated or inadequately treated for weeks, the periosteal reaction forms a sheath, the involucrum, around the devitalized shaft, the sequestrum, with pus from the marrow discharging through a hole in the sequestrum, the cloaca (from the Latin word for sewer).

▶Osteomyelitis, Neonates, Childhood

IOCM

▶Iso-Osmolality Contrast Media

IPSID

▶Immunoproliferative Small Intestinal Disease

Ipsilateral Breast Tumor Recurrence

▶Recurrent Neoplasms, Breast

Iron Overload

Iron overload can be subdivided into two types: parenchymal cell iron deposition in hemochromatosis, cirrhosis, intravascular hemolysis, and iron deposition in cell of the reticulo-endothelial system, also called hemosiderosis, which is seen most commonly after multiple transfusions or in diseases with extravascular hemolysis. Iron deposition in hepatocytes causes cellular damage, while iron deposition in reticulo-endothelial cells (Kupffer cells in the liver) does not produce a significant organ dysfunction.

▶Diffuse Infiltrative Diseases, Hepatic
▶Hemochromatosis, Skeletal

Ischemia

In ischemia, oxygen deprivation is accompanied by an inadequate removal of metabolites due to reduced perfusion. During the ischemic condition, an imbalance occurs between oxygen supply and demand, which may manifest as anginal discomfort, deviation of the ST segment on electrocardiography, or impairment of the regional or global left ventricular function.

▶Ischemic Heart Disease, Nuclear Medicine

Ischemia, Brachial

Elias N. Brountzos
Department of Radiology,
Athens University, Medical School, Greece
ebrountz@cc.uoa.gr

Synonyms

Acute upper extremity ischemia

Definition

Acute arterial insufficiency of the upper extremity

Pathology

Embolization is the most common cause of acute upper-limb ischemia. Embolization of the upper-limb arterial bed represents 15–32% of all peripheral emboli (3). The heart is the source of emboli in 90% of the cases. Other sources of emboli are shown in Table 1. The brachial artery is more frequently embolized (60%), followed by the axillary artery (23%), the subclavian artery (12%), and the forearm and digital arteries (5%). Iatrogenic trauma to the upper extremity arteries occurs during arterial cannulation for angiography or monitoring. Thrombosis of the brachial artery is common after arteriotomy for cardiac catherization (0.3–28%). Percutaneous brachial artery catheterization is more often complicated with local complications compared to femoral catheterization. Because of the collateral supply, many patients remain asymptomatic. Nevertheless immediate surgical intervention with thrombectomy is recommended because many initially asymptomatic patients develop symptoms of ischemia later. Axillary artery thrombosis complicates transaxillary arteriography in 0.8% of the patients. Immediate thrombectomy is required. Radial artery thrombosis occurs in 40% of the patients undergoing radial artery cannulation for monitoring, but ischemic symptoms develop in only 0.5%. Other iatrogenic injuries are encountered during blind placement of central venous catheters.

Non-iatrogenic arterial trauma of upper extremities is not rare. Of all arterial injuries in civilian experience, the axillary artery is injured in 5–9%, the brachial artery in 30%, and the forearm arteries in 7–20%. The causative agents are missiles or sharp objects. Other mechanisms include stretch injuries from falls or those occurring during shoulder dislocation. Brachial artery injury is a complication of fractures and dislocations of the elbow.

Clinical presentation: The presentation is similar to that of the lower extremity acute ischemia with pulseness, palor, pain, paresthesias, and paralysis. Usually it involves the hand and the fingers. Mild symptoms are not rare with the patient complaining of only a cold hand (1). The clinical picture of embolization maybe dramatic or symptoms may develop over the course of several hours. Physical examination is essential to access the level of obstruction.

Ischemia, Brachial. Table 1 Acute upper extremity ischemia. Etiology

1. Iatrogenic injury (axillary, brachial, radial artery cannulation)
2. Non iatrogenic trauma
3. Embolization
a. Cardiac origin
b. Proximal artery ulcerated plaque
c. Aneurysms (ascending aorta, innominate, subclavian, axillary, brachial, ulnar)
d. Thoracic outlet syndrome
e. Fibromuscular disease
4. Steal phenomenon after arteriovenous fistula formation
5. Aortic dissection

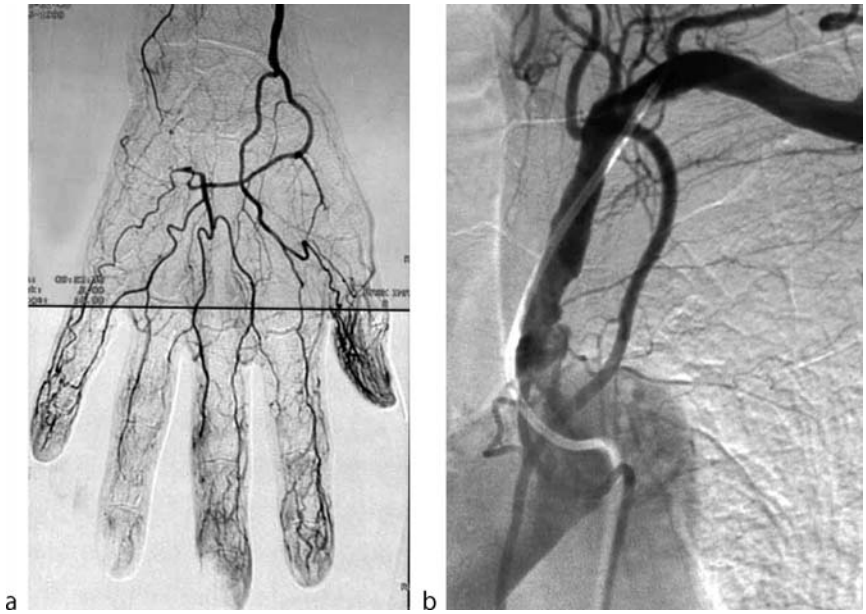

Ischemia, Brachial. Figure 1 (a) Hand DSA in a patient with acute onset of left-hand ischemia depicts atherosclerotic disease of the hand arteries, absence of the ulnar artery and the deep palmar arch, and filling defects of the digital arteries suggestive of peripheral embolization. (b) Selective DSA of the left subclavian artery depicts ulcerated occlusive lesion of the left subclavian artery.

Imaging and Diagnosis

If embolization is suspected, color Doppler sonography or other noninvasive imaging modalities can evaluate large arteries, but may fail to provide detailed information on the hand arterial pathology. Angiography is recommended to rule out proximal arterial embolic source. Imaging from the arch to the digits should be performed. The proximal arteries should be evaluated for aneurysm containing thrombus or atherosclerotic lesions. With digital embolization, luminal defects are depicted in the involved vessels (Fig. 1). In non-iatrogenic trauma the diagnosis is obvious in the presence of active arterial hemorrhage, expanding hematoma, ischemia, or absence of pulses. Sometimes the patient has to go immediately to surgery. Imaging is mandatory to rule out subclinical vascular injury. Angiography is the recommended imaging modality as it can be used in the same session for interventional treatment. Findings include spasm, intimal flaps, thrombosis, laceration, frank exsanguination, and pseudoaneurysm.

Interventional treatment

Surgical exploration with thrombo-embolectomy is the treatment of choice for acute ischemia of the upper limb. Intra-arterial thrombolysis has promising results. When the source of emboli is a proximal ulcerated plaque, stent placement can be used as an alternative to surgical reconstruction. Following arterial trauma, extravasation or pseudoaneurysms can be treated by embolization.

References

1. Kaufman JA (2004) Upper-extremity arteries. In: Kaufman JA and Lee MJ (eds) The Requisites. Vascular and Interventional Radiology. Philadelphia, Mosby, pp 142–162
2. Porter JM, Edwards JM (2000) Occlusive and vasospastic diseases involving distal upper extremity arteries—Raynaud's syndrome. In: Rutherford RB (ed) Vascular Surgery, Denver Colorado, WB Saunders, pp 1170–1183
3. Whitehouse WM, Jr (2000) Upper extremity revascularization. In: Rutherford RB (ed) Vascular Surgery, Denver Colorado, WB Saunders, pp 1162–1170
4. Connell DA, Koulouris G, Thorn DA et al (2002) Contrast-enhanced MR angiography of the hand. Radiographics 22:583–599
5. Brountzos EN, Petersen B, Binkert CA et al (2004) Primary stenting of subclavian and innominate artery occlusive disease: a single center experience. Cardiovasc Inter Rad 27:616–623

Ischemia, Limb, Acute

Dierk Vorwerk
Klinikum Ingolstadt, GmbH, Direktor des Institues für diagnostische und interventionelle Radiologie, Krumenauerstraße 25, 85049 Ingolstadt
dierk.vorwerk@klinikum-ingolstadlt.de

Synonyms

Acute arterial occlusion; Acute ischemic limb

Definition

Acute leg ischemia is mainly a result of embolic disease either from the heart or from ulcerating atherosclerotic lesions that may induce thrombus formation and consecutive thrombus induction. It may also be of iatrogenic origin due to invasive studies or percutaneous interventions such as vascular recanalization.

True thrombosis may occur in the case of a thrombophilic state or due to physical rest such as long-distance flights or long car driving. If thrombosis occurs in an artery that allows sufficient collateral flow onto a preexisting lesion, a sufficient collateralization, symptoms may be less severe. Thus, diagnosis may be made late leading to the state of subacute or chronic thrombosis.

Pathology/Histopathology

Acute ischemia of a peripheral limb is caused by acute embolic embolization of clot material of mainly cardiac origin, acute thrombosis from preexisting arterial lesions, or, rarely, coagulation problems.

Clinical Presentation

In general, the duration of symptoms of up to 4 weeks is classified as acute, between 1 and 3 months as subacute, and longer than 3 months as chronic thrombosis of the artery. This classification is of practical importance since treatment – both surgically and percutaneously – is influenced by the age of the occlusion. A simple mechanical removal of the embolus/thrombus becomes more difficult the longer an occlusion exists.

Clinically, acute ischemia is classified into four different states: stage I, with mild symptoms and no tissue or nervous deficits representing acute limb threatening; stage IIa, with minimal sensory loss, no muscle weakness but inaudible arterial Doppler signals; stage IIb, with extended sensory loss, mild to moderate muscle weakness, and inaudible arterial signal; and stage III, with profound anesthesia of the limb, muscular paralysis, and inaudible venous and arterial signals (1).

Clinical examination, pulse status, and duplex sonography are valuable tools for making the diagnosis of an acute leg ischemia. The patient's history is important for analyzing potential risk factors such as arrhythmias or heart valve disease.

Imaging

Duplex sonography and angiography are the principle imaging modalities that are used to make the diagnosis. Magnetic resonance (MR) angiography and computed tomography (CT) angiography may play a role in the future, but the painful state and the acuteness of the event lead to agitation of the patient, preventing lengthy imaging protocols which require full cooperation.

Angiographic imaging is frequently required to analyze the extent and the location of thrombotic occlusions (Fig. 1a–f). An ipsilateral antegrade approach is recommended if the ipsilateral femoral pulse is present and normal. An antegrade puncture is preferred so as to continue with a percutaneous intervention if possible. A contralateral retrograde approach is performed if the ipsilateral femoral pulse is abnormal. The diagnostic catheter is introduced into the iliac artery *via* a cross-over maneuver if the proximal iliac artery is patent. If involvement of the common or profound femoral arteries is suspected, sonography or duplex sonography may be added as a simple diagnostic tool.

Hand injection of dye and a 4 to 5 F access are usually sufficient to establish the diagnosis.

To date, other imaging modalities such as MR angiography or CT angiography do not play a major role in the diagnosis of acute ischemia as the potential combination of the diagnostic and interventional procedure in one step favors direct transarterial imaging.

In the case of renal insufficiency or contrast media intolerance, carbon dioxide or MR contrast agents may be used as alternative contrast media for catheter-directed angiography. Carbon dioxide is, however, frequently very painful in acute ischemic limbs limiting the imaging quality by movement artifacts.

Nuclear Medicine

Nuclear medicine plays no particular role in the diagnosis of acute ischemia.

Diagnosis

Diagnosis based on the clinical and angiographic findings is usually easy to make. It is more difficult to detect the underlying source of acute occlusion, the extent of the thrombosed arterial segment, and the best appropriate therapeutic approach.

Interventional Radiological Treatment

According to the TASC document (1), treatment of acute ischemia depends on the clinical stage. In stage I and IIa, surgical treatment with open embolectomy or thrombectomy by use of Fogarty embolectomy balloons and its

derivatives as well as thrombolysis by use of thrombolytic agents including rtPA and urokinase are accepted concepts. In stage IIb, Fogarty embolectomy is the treatment of choice, while thrombolysis is not recommended due to potential complications that may result from bleeding into revascularized tissue, resulting in a compartment syndrome. In early stage III, surgical thrombectomy may be tried; however, in advanced stage III cases, only amputation remains the principal option.

As usual, a correct diagnosis in time and rapid onset of treatment are mandatory for limb salvage and they need to be implemented in each center dealing with acute disease. It is, however, true that acute ischemic states are frequently overseen or neglected also by the patient. The

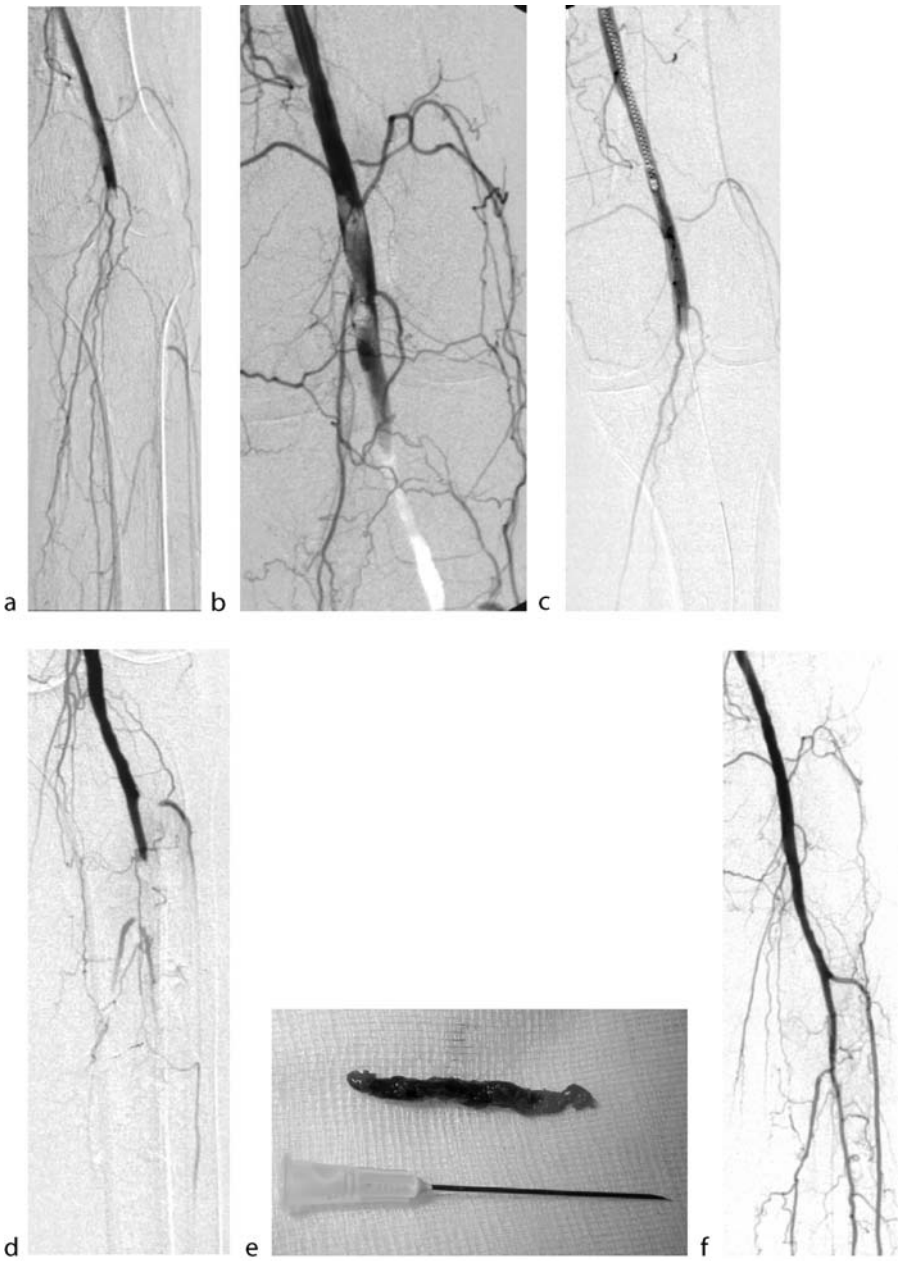

Ischemia, Brachial. Figure 1a–f Acute ischemia of the lower left leg. (a) Acute embolic occlusion of the poplietal artery at the level of the joint. (b) Aspiration fails to clear the popliteal artery but demasks a large thrombus. (c/d) After rotational thrombectomy by a Rotarex catheter, the popliteal lumen has ben reopened but there is still occulsion of the distal popliteal artery and the trifurcation. (e) Aspiration removes a larger clot from the distal popliteal artery. Trifurcation is now reperfused.

time factor is crucial for the success of a surgical approach as well as for percutaneous interventions.

To achieve a successful and enduring result, at least one lower limb artery or a major collateral has to be reopened down to the foot in order to establish a sufficient outflow situation and to avoid early rethrombosis. Follow-up medication is an important part of the treatment concept.

Thrombolysis has some drawbacks that prevent its widespread use in subacute and acute thrombosis and embolic disease. It is relatively time consuming and a rapid revascularization is rare. In particular, in advanced stages a treatment duration of up to 24 h may worsen the clinical situation with an unpredictable outcome. Local bleeding may occur at the entry site, complicating an adjunctive surgical approach – if required. Reduced clotting abilities after thrombolysis also interfere with surgery. Furthermore, the subset of patients with acute ischemia are frequently of older age and their comorbidities often contraindicate the use of thrombolytic agents.

Two different trials – the STILE and TOPAS trials – have advocated thrombolysis to be equivalent to surgery. The TOPAS trial found a limb salvage rate of 72% after 6 months for the urokinase group vs. 75% in the surgical group. The STILE trial found a similar outcome at 30 days for both treatments. Earnshaw et al., however, found that patients with a neurosensory deficit and acute ischemia had a significantly lower limb salvage rate (31%) compared to those treated by surgery (59%) (2). Berridge et al., performing an analysis of randomized data available on thrombolysis vs. surgery in acute ischemia, found no significant difference with regard to limb salvage for up to 1 year and with regard to overall survival, but found a significant increase in stroke rate, major hemorrhage, and distal embolization at 30 days in patients undergoing initial thrombolysis (Berridge).

Fogarty embolectomy *via* a femoral or popliteal approach is a quick method in the case of circumscribed thrombi, but it may become difficult in concomitant atherosclerotic stenoses or extensive thromboses including the lower limb arteries.

In older thrombi, wall adhesion of the occluding clots can complicate removal of clots by use of Fogarty embolectomy balloons and sometimes additional instruments are required.

Instruments for Mechanical Thrombectomy

Mechanical removal of thrombosis *via* a percutaneous approach is an old dream of interventional radiologists who – like surgeons – prefer a quick, elegant, and effective solution to the problem instead of going through lengthy procedures, which thrombolysis certainly can turn out to be. Many different mechanical devices were developed with enthusiasm, introduced into clinical practice, tested as insufficient and have disappeared from the market. The Kensey catheter is an early example of this not-too-small family of disappointed hopes.

In the meantime, however, some valid instruments and techniques are available which allow successful and relatively safe and timely removal of clot material.

They include:

- Manual aspiration
- Hydrodynamic thrombectomy
- Rotational thrombectomy
- Atherectomy
- Stent placement

In addition, a number of other devices or treatment options are under development and evaluation and their number is still growing.

References

1. TASC working group TASC: (2000) Management of peripheral arterial disease. Transatlantic intersociety consensus. Int Angiol 19 (Suppl. 1) 152:161–163
2. Ouriel K, Veith FJ, Sasahara AA (1998) A comparison of recombinant urokinase with vascular surgery as initial treatment for acute arterial occlusion of the legs. Thrombolysis or Peripheral Arterial Surgery (TOPAS) Investigators. N Engl J Med. Apr 16;338 (16): 1105–1111
3. [No authors listed] (1994) Results of a prospective randomized trial evaluating surgery versus thrombolysis for ischemia of the lower extremity. The STILE trial. Ann Surg Sep;220(3):251–266
4. Earnshaw JJ, Gregson RH, Makin GS et al (1989) Acute peripheral arterial ischemia: a prospective evaluation of differential management with surgery or thrombolysis. Ann Vasc Surg. Oct;3(4):374–379
5. Berridge DC, Kessel D, Robertson I (2002) Surgery versus thrombolysis for acute limb ischaemia: initial management. Cochrane Database Syst Rev (3):CD002784. Review
6. Starck EE, McDermott JC, Crummy AB et al (1985) Percutaneous aspiration thromboembolectomy. Radiology Jul;156(1):61–66
7. Sniderman KW, Bodner L, Saddekni S et al (1984) Percutaneous embolectomy by transcatheter aspiration. Work in progress. Radiology Feb;150(2):357–361
8. Wagner HJ, Starck EE, Reuter P (1994) Long-term results of percutaneous aspiration embolectomy. Cardiovasc Intervent Radiol Sep–Oct;17(5):241–246
9. Canova CR, Schneider E, Fischer L et al (2001) Long-term results of percutaneous thrombo-embolectomy in patients with infrainguinal embolic occlusions. Int Angiol Mar;20(1):66–73
10. Henry M, Amor M, Henry I et al (1998) The Hydrolyser thrombectomy catheter: a single-center experience. Endovasc Surg Feb;5(1):24–31
11. Kasirajan K, Gray B, Beavers FP et al (2001) Rheolytic thrombectomy in the management of acute and subacute limb-threatening ischemia. J Vasc Interv Radiol Apr;12(4):413–421
12. Görich J, Rilinger N, Sokiranski R et al (1998) Mechanical thrombolysis of acute occlusion of both the superficial and the deep femoral arteries using a thrombectomy device. AJR Am J Roentgenol May;170(5):1177–1180

13. Hopfner W, Bohndorf K, Vicol C et al (2001) Percutaneous hydromechanical thrombectomy in acute and subacute lower limb ischemia. Rofo Mar;173(3):229–235. German
14. Zeller T, Frank U, Burgelin K et al (2002) Long-term results after recanalization of acute and subacute thrombotic occlusions of the infra-aortic arteries and bypass-grafts using a rotational thrombectomy device. Rofo Fortschr Geb Rontgenstr Neuen Bildgeb Verfahr Dec;174(12):1559–1565
15. Reekers JA (1998) A balloon protection sheath to prevent peripheral embolization during aortoiliac endovascular procedures. Cardiovasc Intervent Radiol Sep–Oct;21(5):431–433

Ischemia, Mesenteric, Acute

Stefan Müller-Hülsbeck
Department of Radiology, University Hospital Schleswig-Holstein, Campus Kiel, Kiel, Germany
muehue@rad.uni-kiel.de

Synonyms

Acute mesenteric arterial embolus (AMAE); Acute mesenteric arterial thrombosis (AMAT); Acute mesenteric infarction; Acute mesenteric ischemia; Acute mesenteric occlusive disease; Acute mesenteric venous thrombosis; Mesenteric vascular occlusion; Nonocclusive mesenteric ischemia (NOMI); Occlusive mesenteric arterial ischemia (OMAI)

Definitions

Acute mesenteric ischemia is the acute interruption of blood flow to the small or large intestine. The word "ischemia" means decrease in oxygen supply. Mesenteric ischemia is a condition in which the mesenteric arteries do not deliver enough blood and oxygen to the small and large intestines. This makes it difficult for the intestines to digest food and can cause segments of the intestine to die. "Occlusion of the mesenteric vessels is apt to be regarded as one of those conditions of which the diagnosis is impossible, the prognosis hopeless, and the treatment almost useless" (1). Antonio Beniviene first described mesenteric ischemia in the fifteenth century. It was studied more intensively in the mid-nineteenth century after case reports by Virchow and others.

Pathology/Histopathology

In practice, acute mesenteric ischemia (AMI) is divided into four different primary clinical entities: (1) acute mesenteric arterial embolus (AMAE), (2) acute mesenteric arterial thrombosis (AMAT), (3) nonocclusive mesenteric ischemia (NOMI), and (4) mesenteric venous thrombosis (MVT). Occlusive mesenteric arterial ischemia (OMAI) includes both AMAE and AMAT.

Typically, the celiac artery trunk (CAT) supplies the foregut, hepatobiliary system, and spleen; the superior mesenteric artery (SMA) supplies the midgut (i.e., small intestine and proximal mid-colon); and the inferior mesenteric artery (IMA) supplies the hindgut (i.e., distal colon and rectum). However, multiple anatomic variants are observed. Venous drainage is through the superior mesenteric vein (SMV), which joins the portal vein.

AMI arises primarily from problems in the SMA circulation or its venous outflow. Collateral circulation from the CA and IMA may allow sufficient perfusion if flow in the SMA is reduced because of occlusion, low-flow state (NOMI), or venous occlusion. The inferior mesenteric artery is seldom the site of lodgment of an embolus. Only small emboli can enter this vessel because of its smaller lumen. When lodgment occurs, the embolus lodges at the site of division of the inferior mesenteric artery into the left colic, sigmoidal, and superior hemorrhoidal arteries. In such instances, collateral flow from the middle colic and middle hemorrhoidal arteries (through the vascular arcades of the inferior mesenteric artery distal to the embolus) may sustain the perfusion of the left colon (2).

Insufficient blood perfusion to the small bowel and colon may result from arterial occlusion by embolus or thrombosis (AMAE or AMAT), thrombosis of the venous system (MVT), or nonocclusive processes such as vasospasm or low cardiac output (NOMI). Embolic phenomena account for approximately 50% of all cases, arterial thrombosis for about 25%, NOMI for roughly 20%, and MVT for less than 10% (3). Hemorrhagic infarction is the common pathologic pathway, whether the occlusion is arterial or venous.

Embolic AMI is usually caused by an embolus of cardiac origin. Typical causes include mural thrombi after myocardial infarction, atrial thrombi associated with mitral stenosis and atrial fibrillation, vegetative endocarditis, mycotic aneurysm, and thrombi formed at the site of atheromatous plaques within the aorta or at the sites of vascular aortic prosthetic grafts interposed between the heart and the origin of the SMA. Most often, emboli lodge about 6–8 cm beyond the SMA origin, at a narrowing near the emergence of the middle colic artery.

Damage to the affected bowel portion may range from reversible ischemia to transmural infarction with necrosis and perforation.

The mucosal barrier becomes disrupted as the ischemia persists, and bacteria, toxins, and vasoactive substances are released into the systemic circulation. This can cause death from septic shock, cardiac failure, or multisystem organ failure before bowel necrosis actually occurs. As hypoxic

damage worsens, the bowel wall becomes edematous and cyanotic. Fluid is released into the peritoneal cavity, explaining the serosanguinous fluid sometimes recovered by diagnostic peritoneal lavage. Bowel necrosis can occur in 8–12 h from the onset of symptoms.

Thrombotic AMI is a late complication of preexisting visceral atherosclerosis. Symptoms do not develop until two of the three arteries (usually the CA and SMA) are stenosed or completely blocked (4, 5).

Clinical Presentation

Symptoms are initially nonspecific, before evidence of peritonitis is found (6–8). Thus, diagnosis and treatment are often delayed until the disease is far advanced; the key to diagnosis lies in a high index of suspicion. Patients with advanced ischemia present with diffuse peritonitis, shock, and severe metabolic derangements. The diagnosis will become obvious at the time of surgery. Often these patients cannot be salvaged; the mortality is reported to be between 70 and 90%. While the prognosis is grave for patients in whom the diagnosis is delayed until bowel infarction has already occurred, patients who receive the appropriate treatment in a timely manner are much more likely to recover. In the early stage of ischemia the patient complains of severe abdominal pain (due to vasospasm) in the absence of peritoneal findings. This scenario has been described by clinicians as "pain out of proportion to the physical findings." Symptoms often found are: severe abdominal pain out of proportion to physical examination findings, pain initially of a visceral nature and poorly localized, nausea, vomiting, diarrhea, gastrointestinal bleeding may be present.

Imaging

A flow-chart for the diagnosis and treatment of patients at risk of AMI is given in Fig. 1(9).

- Plain abdominal films (abnormal in 20–60% of cases)

Findings on plain films of the abdomen are often normal in the presence of AMI. However, plain films are warranted to exclude identifiable causes of abdominal pain such as perforated viscus with free intraperitoneal air. Therefore, all patients should have an upright and supine plain film of the abdomen in order to rule out visceral perforation or bowel obstruction.

Positive findings are usually late and nonspecific (ileus, small bowel obstruction, edematous/thickened bowel walls, and paucity of gas in the intestines). More specific signs, such as pneumatosis intestinalis—i.e., submucosal gas, thumbprinting of bowel wall, and portal vein gas—are late findings.

- Computed tomography scan

Computed tomography (CT) scan helps to evaluate AMI and to exclude other causes of abdominal pain. CT angiography has a sensitivity of 71–96% and a specificity of 92–94% (10). Although still not considered the gold standard compared with classic angiography, CT angiography is noninvasive, readily available, and the preferred modality for MVT (90% sensitivity). Moreover, with recent multidetector CT scanners, accuracy is expected to be much higher, close to 100%.

CT scan may also show pneumatosis intestinalis, portal vein gas, bowel wall, and/or mesenteric edema, abnormal gas patterns, thumbprinting, streaking of mesentery, and solid organ infarction. Bowel wall edema is the most common finding on CT scan. Arterial occlusion may show nonenhancement of the vessels (Fig. 2). MVT usually shows a thrombus in the SMV or portal vein. Finally, intraluminal thrombus in involved vessel is well detected (11).

- Angiography

This was the gold standard for diagnosis and presurgical planning and is often an important part of treatment. To promptly diagnose patients with true AMI, a low threshold for obtaining early angiographs should be adopted for patients at risk. Sensitivity is reported to be 88% for AMI. Nowadays, multidetector CT is equal or even more adequate in presenting vascular anatomy and surrounding tissue, such as in the bowel.

- Ultrasonography

Duplex sonography studies are highly specific (92–100%) but not as sensitive (70–89%) as angiography (12). The examination cannot detect clots beyond the proximal main vessels nor can it be used to diagnose NOMI. Ultrasound is considered a second-line study for AMI. It is often less useful in the presence of dilated fluid-filled loops of bowel.

Some studies show that the usefulness of duplex scanning is similar to that of CT scanning if it is performed for MVT. It may show a thrombus or absent flow in the involved arteries or veins. Other possible findings include portal vein gas, biliary disease, free peritoneal fluid, thickened bowel wall, and intramural gas.

- Magnetic resonance imaging/magnetic resonance angiography

Magnetic resonance imaging (MRI) and magnetic resonance angiography (MRA) provide findings similar to CT scan in AMI. Sensitivity of MRA is 100% and specificity is 91%. MRA is particularly effective for evaluating MVT; however, in emergency situations MR should not be the first choice.

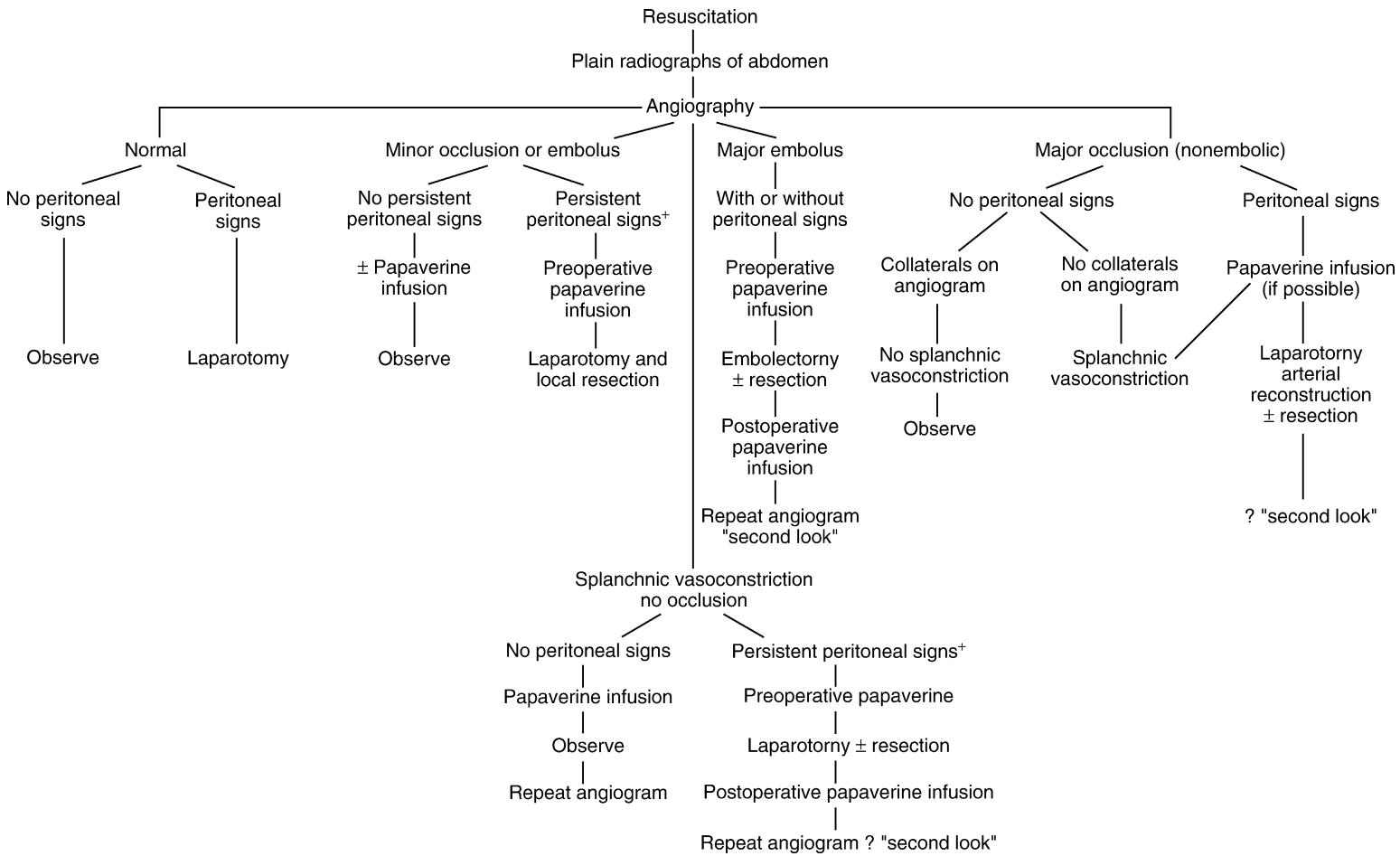

Ischemia, Mesenteric, Acute. Figure 1 A flow-chart for the diagnosis and treatment of patients at risk of AMI (modified from Oldenburg WA, Lau LL, Rodenberg TJ et al (2004) Acute mesenteric ischemia—A clinical review. Arch Int Med 164:1054–1062.

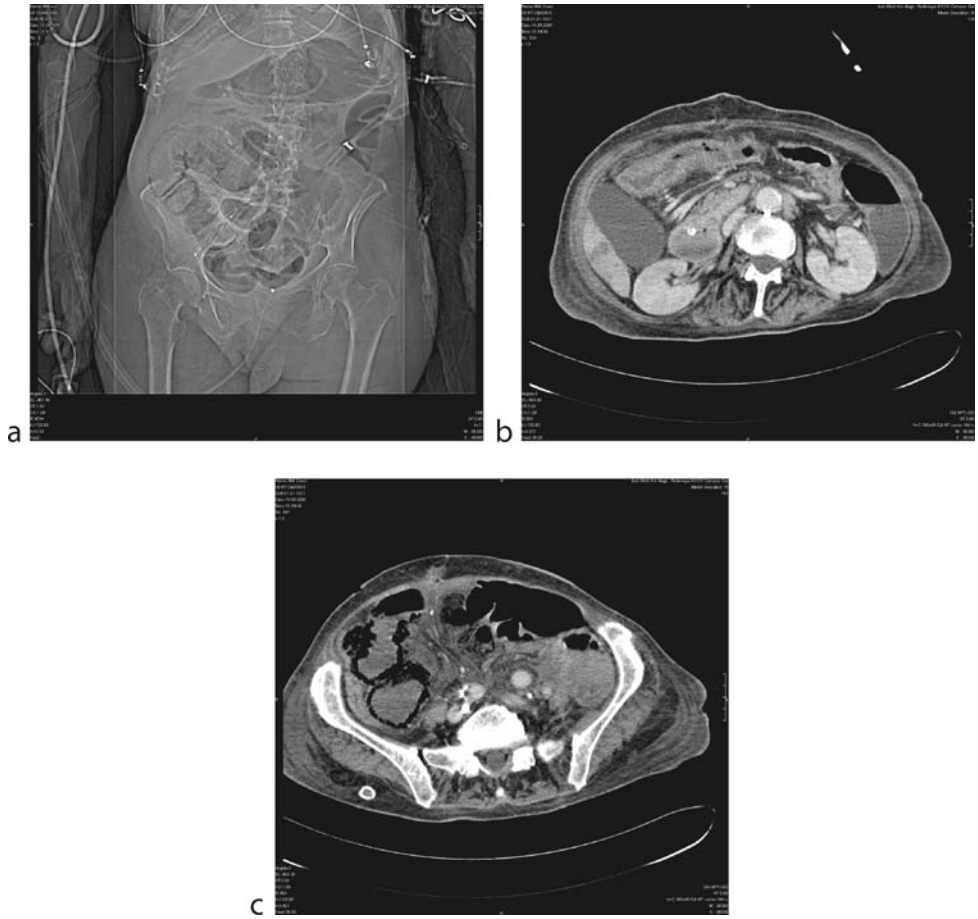

Ischemia, Mesenteric, Acute. Figure 2 CT scan of a patient suffering from AMI. Celiac trunk is severely stenosed and SMA is partially occluded by calcified plaque material. On CT scout view, pneumatosis intestinalis is visible (a). The bowel is edematous and thickened (b), clear signs of pneumatosis intestinalis are often seen in advanced acute mesenteric ischemia (AMI) with gangrenous bowel proven by surgery (c).

Nuclear Medicine

It is not of importance for the diagnosis of AMI.

Diagnosis

Clinical sequelae in combination with typical imaging findings make the diagnosis clear.

Interventional Radiological Treatment

- Angiographically infused papaverine (Vasodilator therapy)

Catheter-directed papaverine infusion in the affected vessel following angiography is useful for all arterial forms of AMI. It relieves reactive vasospasm in occluded arterial vessels and is the only treatment for NOMI other than resection of gangrenous bowel.

After angiography, an infusion of 30 mg/h should be started, and the dose should be adjusted up to 60 mg/h for a clinical response. This is continued for at least 24 h for a maximum of 5 days. If the catheter slips into the aorta, significant hypotension can occur (13). Papaverine is incompatible with heparin (crystallization)

- Angiographically infused thrombolytics

Thrombolytics infused through the angiogram catheter can be a life-saving therapy for selected patients with embolic AMI (14).

Bleeding is the main complication. Thrombolytic administration is risky and should only be undertaken if peritonitis or other signs of bowel necrosis are absent. It must be started within 8 h of symptom onset. If symptoms do not improve within 4 h or if peritonitis develops, the

perfusion should be stopped and surgery should be performed.

- Angioplasty after thrombolysis

A very select group of patients who have atherosclerotic plaques at the origin of the SMA after thrombolysis are eligible for angioplasty. Angioplasty can be technically difficult because of the anatomy of the SMA. The use of low-profile Monorail devices (0.014 or 0.0018 in. compatible) might enhance technical success rates. Restenosis rates are 20–50% (15).

- Heparin for MVT

Heparin anticoagulation is the main treatment for MVT. If no signs of bowel necrosis exist, the patient may not even need an operation. Heparin may increase the chance of bleeding complications. An avenue of study for possible future clinical trials may be the use of enoxaparin (Lovenox) or other low-molecular-weight heparins as a potential substitute for heparin in the treatment of MVT.

Heparin should be administered as a bolus of 80 U/kg, not to exceed 5,000 U, and then as an infusion at 18 U/kg/h until full conversion to oral warfarin. Appropriate monitoring of anticoagulation using activated partial thromboplastin time (aPTT) is mandatory.

Surgery

Thrombectomy/embolectomy, arterial bypass, and resection of necrotic bowel are typical procedures (16–18).

- Complications: Sepsis/septic shock, multiple system organ failure, death
- Mortality: 70–90% overall; from arterial embolism: 60–80%, from arterial thrombosis: 70–100%, from nonocclusive mesenteric ischemia: 40%, from mesenteric venous thrombosis: 25–30%

Bibliography

1. Cokkinis AJ (1961) Intestinal ischaemia. Proc R Soc Lond B Biol Sci 54:354–356
2. Rosenblum JD, Boyle CM, Schwartz LB (1997) The mesenteric circulation. Anatomy and physiology. Surg Clin North Am 77:289–306
3. Bassiouny HS (1997) Nonocclusive mesenteric ischemia. Surg Clin North Am 77:319–326
4. Cognet F, Ben Salem D, Dranssart M et al (2002) Chronic mesenteric ischemia: imaging and percutaneous treatment. Radiographics 22:863–879
5. AbuRahma AF, Stone PA, Bates MC et al (2003) Angioplasty/stenting of the superior mesenteric artery and celiac trunk: early and late outcomes. J Endovasc Ther 10:1046–1053
6. Fink S, Chaudhuri TK, Davis HH (2000) Acute mesenteric ischemia and malpractice claims. South Med J 93:210–214
7. Boley SJ, Brandt LJ, Sammartano RJ (1997) History of mesenteric ischemia. The evolution of a diagnosis and management. Surg Clin North Am 77:275–288
8. Mansour MA (1999) Management of acute mesenteric ischemia. Arch Surg 134328–330; discussion 331
9. Oldenburg WA, Lau LL, Rodenberg TJ et al (2004) Acute mesenteric ischemia—A clinical review. Arch Int Med 164:1054–1062
10. Kirkpatrick ID, Kroeker MA, Greenberg HM et al (2003t), Biphasic CT with mesenteric CT angiography in the evaluation of acute mesenteric ischemia: initial experience. Radiology 229: 91–98
11. Kumar S, Sarr MG, Kamath PS (2001) Mesenteric venous thrombosis. N Engl J Med 345:1683–1688
12. Nicoloff AD, Williamson WK, Moneta GL et al (1997) Duplex ultrasonography in evaluation of splanchnic artery stenosis. Surg Clin North Am 77:339–355
13. Kozuch PL, Brandt LJ (2005) Review article: diagnosis and management of mesenteric ischaemia with an emphasis on pharmacotherapy. Aliment Pharmacol Ther 21:201–215
14. Yamaguchi T, Saeki M, Iwasaki Y et al (1999) Local thrombolytic therapy for superior mesenteric artery embolism: complications and long-term clinical follow-up. Radiat Med 17:27–33
15. Mohammed A, Teo NB, Pickford IR (2000) Percutaneous transluminal angioplasty and stenting of coeliac artery stenosis in the treatment of mesenteric angina: a case report and review of therapeutic options. J R Coll Surg Edinb 45:403–407
16. Hansen KJ, Deitch JS (1997) Transaortic mesenteric endarterectomy. Surg Clin North Am 77:397–407
17. Hladak P, Raupach J, Lojak M et al (2005) Treatment of acute mesenteric thrombosis/ischemia by transcatheter thromboaspiration. Surgery 137:122–123
18. Klempnauer J, Grothues F, Bektas H (1997) Long-term results after surgery for acute mesenteric ischemia. Surgery 121:239–243

Ischemia, Mesenteric, Chronic

Stefan Müller-Hülsbeck
Department of Radiology, University Hospital Schleswig-Holstein, Kiel, Germany
muehue@rad.uni-kiel.de

Definitions

Chronic mesenteric ischemia (CMI), first described as "abdominal angina" by Councilman in 1894 (1), Goodman in 1918 (2) and as entity by Dunphy in 1936 (3), is a rare disorder that is often diagnosed late. CMI is a condition caused by narrowing of the arteries to the intestines. There are three main arteries to the intestines and, in general, two of them must be narrowed to cause symptoms.

Pathology/Histopathology

Because of the extensive collateral arterial network of the gut, chronic mesenteric ischemia is relatively uncommon. The incidence of CMI is estimated to be at 1 in 100,000 (4), although autopsy studies of an unselected population demonstrated mesenteric atherosclerosis in 35% to 70% of the cases (5). It is usually related to extensive mesenteric atherosclerosis. In more than 95% of patients, the

cause of mesenteric ischemia is diffuse atherosclerotic disease, which decreases the flow of blood to the bowel. Symptoms of CMI arise when transient episodes of inadequate, usually postprandial blood flow in the mesenteric arteries are not able to assuage the physiological demand in the intestines. Stenoses in visceral arteries commonly are caused by atheroma, mainly in the proximal segments of the vessels. Fatty infiltration in the arterial wall results in stenosis or finally occlusion of one or more visceral arteries. As the atherosclerotic disease progresses, symptoms worsen. The number of involved arteries before symptoms occur is still debated. So, at least two vessels of the celiac trunk, the superior mesenteric artery and the inferior mesenteric artery, should be stenosed or occluded for the diagnosis of CMI with abdominal angina (6, 7). The presence of a stenosis in a single visceral vessel collateral flow may allow patients to be asymptomatic. Usually, all three major mesenteric arteries are occluded or narrowed.

The pathophysiologic mechanism by which ischemia produces pain is still not completely understood.

Chronic mesenteric ischemia is a rare diagnosis. No reports of the actual incidence have been published. Moawad searched 20 years of literature and found only 330 cases. Because many cases are not reported, the true prevalence could be much higher. Autopsy studies support this theory, with findings of stenosis in up to 30% of selected patients with a history of abdominal pain.

Clinical Presentation

Patients classically present with chronic postprandial pain, nausea, diarrhea and obvious weight loss, which often results in "food fear" in patients. CMI is caused by intermitting transient episodes of inadequate intestinal blood supply, usually concurring with the increased metabolic demand at digestion (7). As no sensitive and specific tests are available to diagnose CMI, accurate acquisition of medical history and exclusion of other conditioning gastrointestinal causes are essential (8). Patients with the diagnose of CMI are usually over 60-year-old. However, most patients do not present with "classic" symptomatology and are frequently misdiagnosed for other diseases. In some patients, if untreated, the narrowing in the arteries leads to clotting causing severe abdominal pain and death.

Imaging

- Ultrasound

Ultrasonography (US) uses sound waves to generate images of internal organs on a monitor. A special ultrasound (Doppler) of the celiac, superior mesenteric and inferior mesenteric arteries can help your doctor determine if there is decreased blood flow, which indicates a likelihood of chronic mesenteric ischemia.

Mesenteric duplex ultrasonography is a non-invasive method of analyzing flow through the vessels. Unfortunately, intraperitoneal gas, respiratory movements, obesity and any previous abdominal surgeries limit results.

Besides duplex sonography as an accurate non-invasive technique of detecting significant stenoses in mesenteric vessels (9), computed tomography angiography and magnetic resonance angiography have been established for pretreatment evaluation of the celiac artery and superior mesenteric artery. With duplex sonography as the easiest to perform screening and follow-up tool, intraarterial digital subtraction angiography (DSA) remains the most precise technique for the evaluation of the degree of the stenosis.

Based on currently available literature, MRI and computerized tomography (CT) should be performed as second step for diagnostic imaging; if anything remains open, DSA should be performed in order to start interventional treatment during the same session.

We currently perform multi-detector CT with 3D reformatting in all patients with suspected acute or chronic mesenteric ischemia. In our experience, CT has eliminated the need for additional imaging studies such as Doppler US or diagnostic angiography. However, further investigation is necessary to determine the scope of utility of multi-detector row CT in this clinical setting (10).

Nuclear Medicine

Not of importance for the diagnosis of AMI.

Diagnosis

Clinical sequelae in combination with typical imaging findings makes the diagnosis clearer.

Interventional Radiological Treatment

Until the 1990s, open surgery was considered the treatment of choice; percutaneous transluminal angioplasty (PTA) was reserved for patients for whom surgery carried a high risk. Many surgical procedures have been described with various results. The blockage in the involved arteries is removed, and the arteries reconnected to the aorta. Alternatively, a bypass around the blockage, usually with a prosthetic plastic tube graft, is performed. Endarterectomy and aortovisceral bypass have been employed. Until today, surgical revascularisation has been the method

of choice for treatment of patients with CMI (7). Surgical procedures such as endarterectomy and aortoceliac and aortomesenteric bypass grafting are associated with relatively high peri-operative major complications (15–33%) and mortality (0–17%) (11–13). Thus, there has been a demand for a less invasive technique. As an alternative method, PTA and stenting was established in the early 1980s. However, only few studies have been performed since then to prove the safety and durability of percutaneous angioplasty and stenting with results for periprocedural major complications of up to 25% and mortality of up to 13%, most of them with inhomogeneous collectives of both PTA and stenting in one study (6, 11–19).

More recently, balloon angioplasty has appeared to provide good results with a less invasive approach. In order to obtain good long-term results with acceptable recurrence rate, we gather minimal invasive PTA, and stent procedures should only be performed by experienced physicians.

Therefore, we recommend after diagnosing CMI to plan interdisciplinarily (gastroenterologist, surgeon and interventionalist/radiologist) the optimal therapeutic approach towards the management of the stenosed arteries for each affected individual. However, there are no definite recommendations for the planning of the right procedure, since only descriptive studies, blind experience and case reports and no type I data (i.e., randomized trials) or type II data (i.e., nonrandomized controlled trials) have been available so far (7, 12). In general, open vascular surgery was the method of choice for patients with CMI, whereas

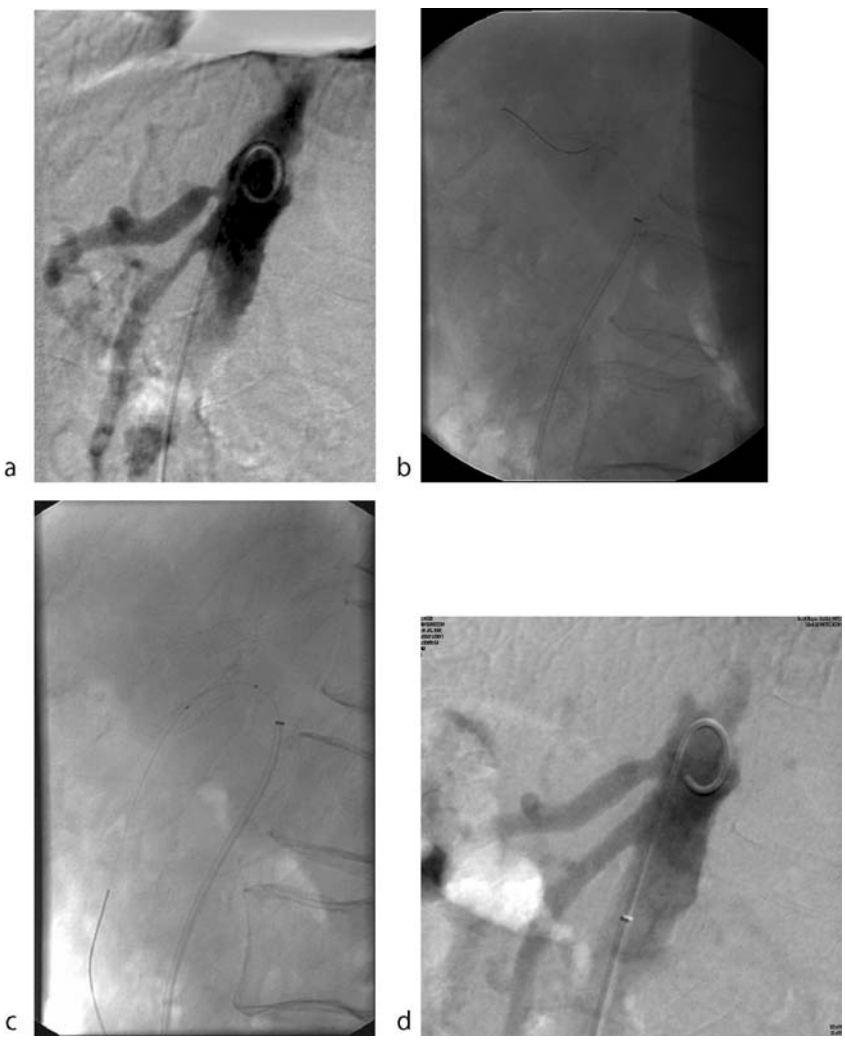

Ischemia, Mesenteric, Chronic. Figure 1 (a) DSA presenting a severe stenosis involving the origin of the celiac artery and the superior mesenteric artery. (b) In order to treat symptoms of CMI in the 62-year-old patient stent placement was performed in the celiac artery (6 × 18 mm) and the superior mesenteric artery (5 × 18 mm) during the same approach, so-called rapid-exchange/monorail devices were used. (c) The fluoroscopic view shows unfolded stents in a proper position. (d) The final angiography reveals patent arteries, with a remaining light luminal narrowing of the celiac artery.

endovascular therapy with or without stent implacement was reserved for patients with multi-morbidity and at high operative risk. For surgical revascularization, excellent long-term patency ranges from 70 to 93% (mean 84%), but an overall perioperative morbidity rate of 29% and mortality rate of 7% gives rise to concern (12, 18). Endovascular therapy with a mean primary patency rate of 76%, at 15 months, a peri-inervent ional complication rate close to 0%, an initial technical success rate of 96% and a mean mortality rate of 4% seems to be effective as well (20; Fig. 1). Despite visceral PTA being a safe and effective alternative to open surgery, it still seems to offer inferior patency and durability rates (15). However, due to the absence of comparative trials of open revascularization versus endovascular therapy and due to different evaluation criteria with a tendency of referring multimorbid patients to endovascular therapy, it is undoubtedly problematic to easily compare those numbers.

It has to be ruled out that in case of median arcuate ligament syndrome, it should be treated in symptomatic cases by surgery (21). It is discussed that it arises from celiac plexus compression and consequently is not an indication for PTA or stent placement (12, 18, 19).

Unfortunately, there is no specific diagnostic test for CMI. A high index of suspicion should be maintained in patients with post-prandial pain and weight loss. If imaging presents in these patients focal stenoses, the very promising and safe technique of PTA and stent placement should be performed immediately as the initial treatment for patients with CMI.

References

1. Councilman WT (1884) Three cases of occlusion of the superior mesenteric artery. Boston Med Surg J 130:410–411
2. Goodman GH (1918) Angina abdominis. Am J Med Sci 155:524–528
3. Dunphy JF (1936) Abdominal pain of vascular origin. Am J Med Sci 192:109–112
4. van Wanroij JL, van Petersen AS, Huisman AB et al (2004) Endovascular treatment of chronic splanchnic syndrome. Eur J Vasc Endovasc Surg 28:193–200
5. Taylor LM Jr, Moneta GL (1991) Intestinal ischemia. Ann Vasc Surg 5:403–406
6. Cognet F, Ben Salem D, Dranssart M et al (2002) Chronic mesenteric ischemia: imaging and percutaneous treatment. Radiographics 22:863–879
7. Abu Rahma AF, Stone PA, Bates MC et al (2003) Angioplasty/stenting of the superior mesenteric artery and celiac trunk: early and late outcomes. J Endovasc Ther 10:1046–1053
8. Brandt LJ, Boley SJ (2000) AGA technical review on intestinal ischemia. American Gastrointestinal Association. Gastroenterology 118:954–968
9. McShane MD, Proctor A, Spencer P et al (1992) Mesenteric angioplasty for chronic intestinal ischaemia. Eur J Vasc Surg 6:333–336
10. Horton KM, Fishman EK (2001) Multi-detector row CT of mesenteric ischemia: can it be done? Radiographics 21:1463–1473
11. Moneta GL, Lee RW, Yeager RA et al (1993) Mesenteric duplex scanning: a blinded prospective study. J Vasc Surg 17:79–84
12. Allen RC, Martin GH, Rees CR et al (1996) Mesenteric angioplasty in the treatment of chronic intestinal ischemia. J Vasc Surg 24:415–421
13. Kasirajan K, O'Hara PJ, Gray BH et al (2001) Chronic mesenteric ischemia: open surgery versus percutaneous angioplasty and stenting. J Vasc Surg 33:63–71
14. Rose SC, Quigley TM, Raker EJ (1995) Revascularization for chronic mesenteric ischemia: comparison of operative arterial bypass grafting and percutaneous transluminal angioplasty. J Vasc Interv Radiol 6:339–349
15. Maspes F, Mazzetti di Pietralata G, Gandini R et al (1998) Percutaneous transluminal angioplasty in the treatment of chronic mesenteric ischemia: results and 3 years of follow-up in 23 patients. Abdom Imaging 23:358–363
16. Sheeran SR, Murphy TP, Khwaja A et al (1999) Stent placement for treatment of mesenteric artery stenoses or occlusions. J Vasc Interv Radiol 10:861–867
17. Hallisey MJ, Deschaine J, Illescas FF et al (1995) Angioplasty for the treatment of visceral ischemia. J Vasc Interv Radiol 6:785–791
18. Matsumoto AH, Tegtmeyer CJ, Fitzcharles EK et al (1995) Percutaneous transluminal angioplasty of visceral arterial stenoses: results and long-term clinical follow-up. J Vasc Interv Radiol 6:165–174
19. Nyman U, Ivancev K, Lindh M et al (1998) Endovascular treatment of chronic mesenteric ischemia: report of five cases. Cardiovasc Intervent Radiol 21:305–313
20. Schaefer PJ, Schaefer FK, Hinrichsen H, Jahnke T, Charalambous N, Heller m, Muller-Huelsbeck S. Stent placement with the monorail techinque for treatment of mesenteric artery stenosis. J Vasc Interv Radiol. 2006 Apr; 17(4); 637–643
21. Reuter SR, Bernstein EF (1973) The anatomic basis for respiratory variation in median arcuate ligament compression of the celiac artery. Surgery. 73:381–385

Ischemic Heart Disease, CT

Gabriel P Krestin, Filippo Cademartiri, Ludovico La Grutta, Alessandro Palumbo, Giuseppe Runza, Patrizia Malagutti, Francesca Pugliese, W Bob Meijboom, Nico R Mollet, Pim J de Feyter
Department of Radiology, Erasmus Medical Center, Rotterdam, The Netherlands
filippocademartiri@hotmail.com

Short Description

Ischemic heart disease (IHD) remains the leading cause of death in the Western world, and early detection of disease allows optimal therapeutic management. Consequently, substantial effort has been invested to develop techniques that can detect coronary artery disease (CAD).

Noninvasive coronary artery imaging challenges any diagnostic modality because the coronary arteries are small and tortuous, and they course in multiple

planes around the heart, while cardiac contraction and respiration cause motion artifacts. Therefore, noninvasive coronary imaging requires high spatial and temporal resolution. In addition, anatomic coverage should be fast to allow scanning within one breath-hold. One of the most recent noninvasive coronary imaging modalities is multislice spiral computed tomography (CT) or multidetector row helical CT. The literature on four-slice CT and 16-slice CT as applied to the imaging of coronary arteries shows a progressive improvement in detecting coronary stenosis (1). The results of 64-slice-generation scanners show further improvement in diagnostic performance (2). CT of the coronary arteries promises to be the diagnostic modality in the clinical field for assessing the coronary lumen and wall. Preliminary experiences also show potential in assessing left ventricular function, volumes, and delayed-enhancement viability (3, 4).

Characteristics

CT Criteria for Eligibility

Coronary CT angiography (CTA) can be performed with reliable results in a selected patient population with sinus rhythm, heart rate below 70 bpm, and the ability to hold their breath for 20 s (16-slice CT technology) or for less than 12 s (64-slice CT technology). Patients with contraindications to intravenous iodinated contrast material should be excluded or treated accordingly. A high-calcium burden impairs the diagnostic accuracy and, in particular, reduces specificity, but sensitivity generally remains preserved.

CT Technology

Coronary CTA requires retrospective electrocardiographic gating of the image reconstruction. This allows a flexible approach to image reconstruction in virtually any phase of the cardiac cycle. Optimization of the reconstruction windows allows the generation of datasets with the least residual motion artifacts.

A high-temporal resolution of the CT scanner has been achieved by combining a fast gantry rotation speed (down to 330 ms for 64-slice CT) that provides a temporal resolution of half the rotation time (i.e., down to 165 ms for 64-slice CT). For angiographic contrast enhancement, a bolus of 80–100 mL contrast material with high-iodine concentration should be administered through an antecubital vein with a flow rate of 4–5 mL/s. The use of a saline bolus chaser administered after the main bolus of contrast material improves the vascular attenuation and allows a reduction in contrast volume.

The heart rate should be reduced below 70 bpm in order to preserve a diagnostic image quality. For this purpose, β-blockers can be administered before the scan (for instance, 100 mg of metoprolol 1 h in advance).

Routine reconstruction should be performed in the end-diastolic and end-systolic phases. Images should be reconstructed with thin slices and 50% overlap between the slices.

The reconstructed contiguous axial slices are stacked in a volume to generate a three-dimensional dataset from which any paraxial, coronal, sagittal, or oblique plane can be created. Other display modalities are useful for performing the evaluation, such as multiplanar reconstruction (MPR) or curved MPR, thin-slab maximum intensity projections (MIPs), and or volume rendering (VR).

Diagnostic Performance of Coronary CT Angiography

Initial results with four-slice CT were promising, and high sensitivity and specificity to detect IHD were reported. However, 20–30% of coronary segments had to be excluded from analysis due to nondiagnostic quality. Substantial improvement was achieved by the introduction of 16-slice scanners with submillimeter collimation as well as faster rotation times. Pooled analysis of available data (11 studies, 681 patients) has demonstrated a sensitivity of 88% with a specificity of 96%, with a concomitant increase in the number of assessable segments (5). For both, four-slice and 16-slice studies, vessel diameter thresholds for assessment were adopted (i.e., vessels of 1.5–2 mm or more).

Recently the diagnostic performance of the latest 64-slice CT scanner, with increased temporal (165 ms) and spatial (0.4 mm^3) resolution, was evaluated (2). Sensitivity and specificity for assessment of significant stenoses were 99 and 95%, respectively, with no exclusion of segments and with no threshold in vessel size for image evaluation (2).

Clinical Applications

Given the current literature and evidence, there are few clinical applications for coronary CTA. What can be said is based on speculation referring to validation series. The most important feature of coronary CTA is the high-negative predictive value, which indicates a reliable capability of ruling out the presence of significant IHD. Accordingly, CT should be used as a first-line imaging technique to exclude the presence or recurrence of IHD in eligible patients (Fig. 1).

The applications that appear to be feasible, based on current validation literature, are evaluation of patients with a low-pretest likelihood of the presence of a significant coronary stenosis (Figs. 2 and 3), evaluation of patients with recurrent angina, follow-up of proximal

coronary stents (Fig. 4), follow-up of patients with previous coronary artery bypass graft (CABG; Fig. 5), and evaluation of coronary artery anomalies.

Coronary CTA can exclude the presence of significant coronary stenosis in patients with low-intermediate pretest probability because of the high-negative predictive value, and it may be properly used after an inconclusive stress test or in patients with atypical chest pain.

The high density of stent struts limits the reliability of in-stent lumens. However, preliminary data indicate that 16- and 64-slice CT scanners can detect in-stent restenosis. The presence of stent occlusion or in-stent restenosis may be assessed in proximal segments.

The assessment of CABG is reported as being reliable with CT. However, the presence of metallic surgical clips around arterial grafts, extensive atherosclerosis, and previous stenting of native coronary arteries are some of the limitations that have been encountered.

Coronary CTA can show coronary anomalies because of its three-dimensional and volumetric capabilities.

The introduction in clinical practice of 64-slice CT, and most probably the next generation of CT scanners with multiple tube-detector units, will allow the triage of acute chest pain. CT is the noninvasive gold standard for diagnosing pulmonary embolism and aortic dissection. The possibility to include the assessment of coronary arteries in a thoracic scan will provide a totally new approach in assessing acute chest pain.

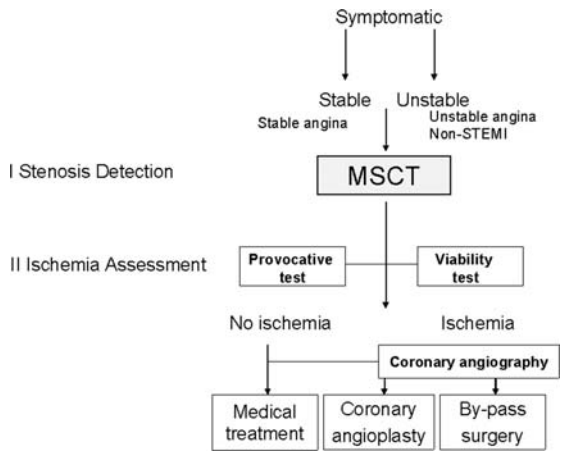

Ischemic Heart Disease, CT. Figure 1 Proposed diagnostic algorithm of suspected coronary ischemia. The first-line imaging modality could be computed tomography, providing two important pieces of information: detection of any atherosclerotic involvement of coronary arteries, and stratification of patients based on the presence of significant stenosis (>50% lumen reduction). The second stage would be evaluation of patients for stress ischemia. Provocative performance is likely to improve when patients are referred after tests that ensure the presence of significant coronary atherosclerosis. In the final stage, morphology and functional information are covered, and a decision for the need for conventional/interventional coronary angiography can be made.

Plaque Imaging with CT

The newer information available since the introduction of coronary CTA is coronary artery wall evaluation. CT can show the presence of plaques and their tissue features (i.e., predominantly calcified, mixed, or predominantly noncalcified). Regarding noncalcified plaque components, it has been suggested that the attenuation measured could indicate the predominant composition as fibrous or lipid.

Other important information that can be derived from CT is the extent of vessel wall remodeling. This information is of great value because the risk of acute coronary syndromes caused by plaque disruption and

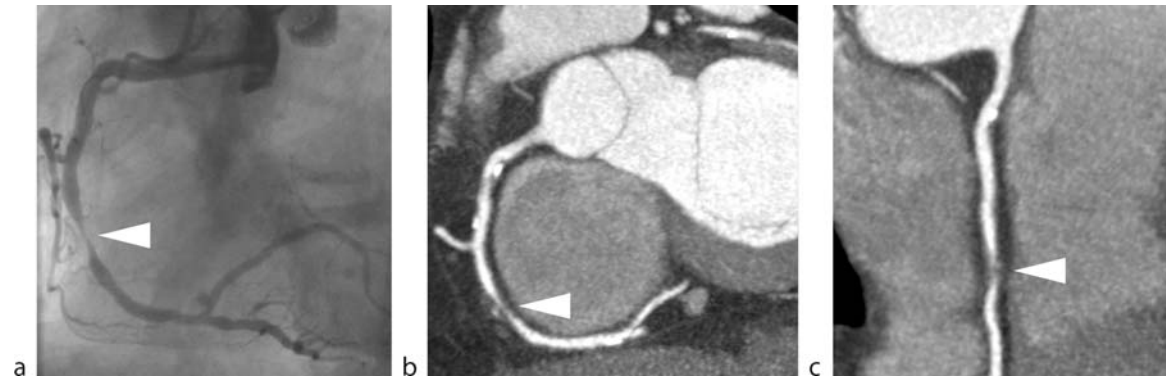

Ischemic Heart Disease, CT. Figure 2 Diagnosis of a patient with stable angina. Conventional coronary angiography displays a significant stenosis (*arrowhead*) in the distal right coronary artery (a). The 64-slice computed tomography maximum intensity projections depict the same lesion (*arrowhead*) in an angiography-like way (b, c).

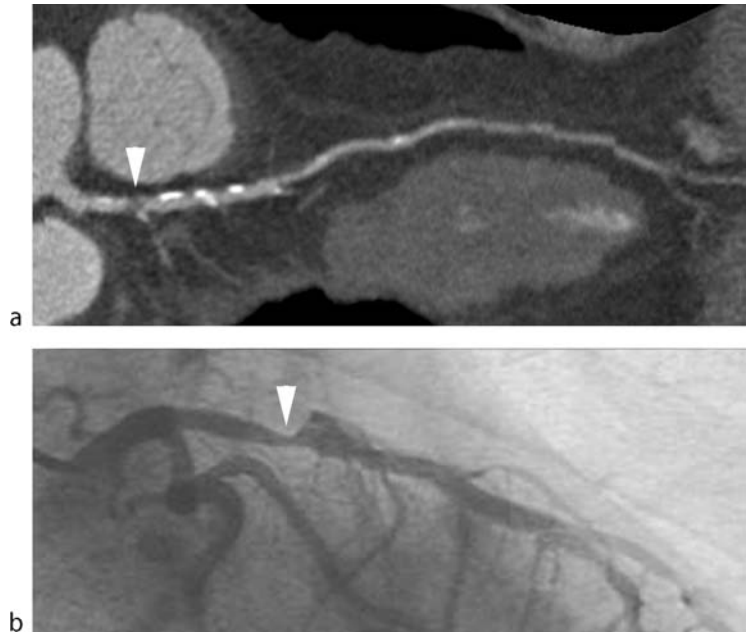

Ischemic Heart Disease, CT. Figure 3 Diagnosis of patient with atypical chest pain. Significant coronary artery stenosis (*arrowhead*) is detected by 64-slice computed tomography (a) and confirmed by conventional coronary angiography (b).

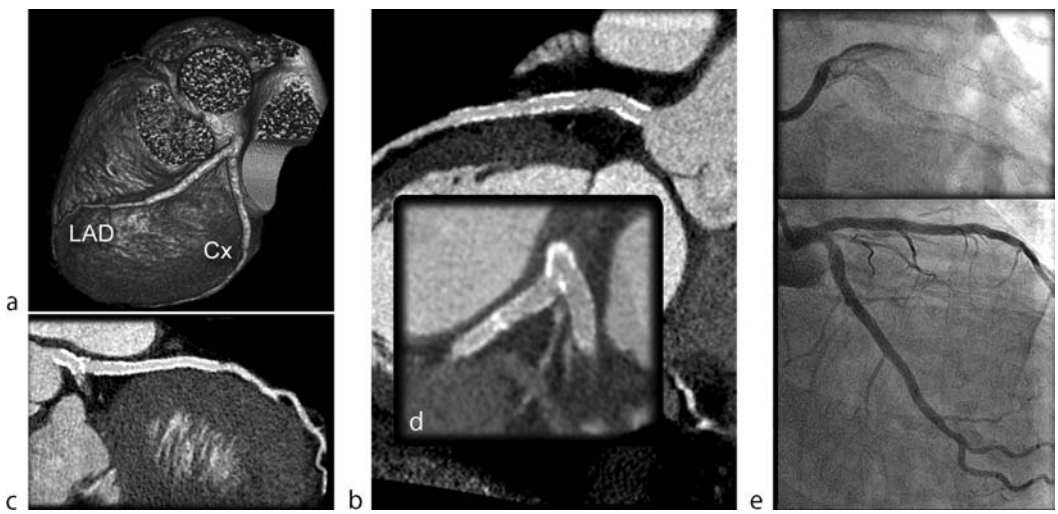

Ischemic Heart Disease, CT. Figure 4 Follow-up of bifurcation stenting of the left main coronary artery using 64-slice computed tomography angiography. The volume-rendered image (a) shows the anatomical configuration of the left coronary artery and the stents. The curved multiplanar reconstructions along the vessels show the lumen in one single plane (b, c). A dedicated plane can be used to display the bifurcation of the stent, which is the main site of restenosis (d). The stent is patent in the proximal region (left main) and in the two main branches (left anterior descending [LAD] and circumflex [Cx]) as confirmed by the conventional coronary angiogram (e).

thrombosis depends on plaque composition (i.e., non-calcified, predominantly lipid plaques with positive remodeling) rather than on stenosis severity. For this reason, reliable noninvasive assessment of plaque constitution could be important in risk stratification of patients with IHD.

Limitations

CT has several limitations in terms of spatial and temporal resolution and contrast-to-noise ratio, which are the reasons for the tight selection of patients for its clinical application. Coronary calcifications limit the

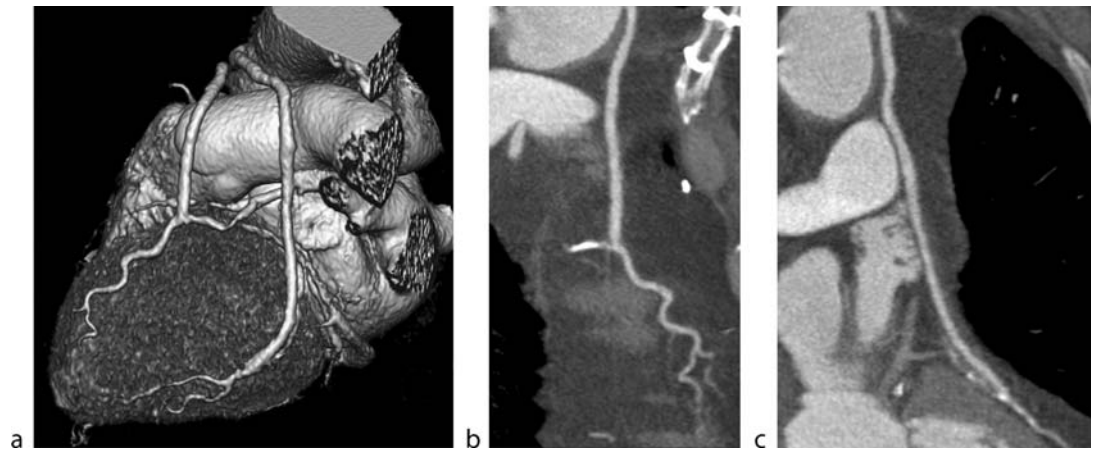

Ischemic Heart Disease, MRI. Figure 5 Follow-up of a coronary artery bypass graft using 64-slice computed tomography angiography. The volume-rendered image displays two venous bypass grafts (a). The first graft runs from the aorta to the first diagonal branch; the second graft runs from the aorta to the second marginal branch. The maximum intensity projections show that both grafts are patent (b, c).

reliability of the assessment of stenosis. Nonsinus heart rhythm, such as atrial fibrillation, prevents diagnostic coronary CTA. Heart rates >70 bpm result in progressively poorer image quality, and a drop out of assessable segments limits the diagnostic accuracy.

Coronary CTA is also a technique that requires highly specific and long training. For this reason it remains a severely operator-dependent modality.

The main concern, though, remains the radiation exposure associated with CT. The effective x-ray doses of 64-slice coronary CTA are reported to be 15.2 mSv and 21.4 m Sv for men and women, respectively, without prospective tube current modulation. This is to allow end-systolic reconstruction for diagnostic purposes. The application of prospective tube current modulation algorithms may reduce the x-ray dose down to 50% of the nominal one, depending on the heart rate.

Conclusion

Coronary CTA is at present the only clinical noninvasive modality for assessing the coronary arteries. The field of application is still restricted by technical limitations and the lack of large clinical trials. This information will become available soon as new generation scanners progressively extend the spectrum of indications.

References

1. Mollet NR, Cademartiri F, Krestin GP et al (2005) Improved diagnostic accuracy with 16-row multi-slice computed tomography coronary angiography. J Am Coll Cardiol 45:128–132
2. Mollet NR, Cademartiri F, van Mieghem CA et al (2005) High-resolution spiral computed tomography coronary angiography in patients referred for diagnostic conventional coronary angiography. Circulation 112:2318–2323
3. Salm LP, Schuijf JD, de Roos A et al (2005) Global and regional left ventricular function assessment with 16-detector row CT: Comparison with echocardiography and cardiovascular magnetic resonance. Eur J Echocardiogr 2006 Aug; 7(4): 308–314
4. Mahnken AH, Koos R, Katoh M et al (2005) Assessment of myocardial viability in reperfused acute myocardial infarction using 16-slice computed tomography in comparison to magnetic resonance imaging. J Am Coll Cardiol 45:2042–2047
5. Schuijf JD, Bax JJ, Shaw LJ et al (2005) Meta-analysis of comparative diagnostic performance of magnetic resonance imaging and multislice computed tomography for noninvasive coronary angiography. Am Heart J 2006 Feb; 151(2): 404–411

Ischemic Heart Disease, MRI

Jörg Barkhausen
Department of Diagnostic and Interventional Radiology and Neuroradiology, University Hospital Essen, Essen, Germany
joerg.barkhausen@uni-essen.de

Short Description

Magnetic resonance imaging (MRI) has emerged as a non-invasive cardiac imaging technique and plays an increasingly important role in the assessment of coronary artery disease (CAD). Its superb spatial and temporal

resolution combined with excellent soft tissue contrast currently allows accurate assessment of cardiac morphology, global cardiac function, regional wall motion and the extent of myocardial infarction. Regional myocardial perfusion can be assessed by first-pass techniques using ultrafast T1-weighted sequences. MR coronary angiography has become feasible and high-resolution imaging with or without contrast-enhancement may allow for characterization of atherosclerotic plaque. Some of the techniques are currently used in clinical routine whereas others must be considered a field of active research (Fig. 1).

There are two common clinical scenarios in which MRI is frequently applied in patients with CAD:

1. To detect CAD and myocardial ischemia
2. To define the extent of myocardial infarction and to distinguish different causes of wall motion abnormalities including scar, myocardial stunning and myocardial hibernation

This review discusses the diagnostic accuracy and the impact of different MRI techniques on management of CAD patients.

Detection of Coronary Artery Disease and Myocardial Ischemia

Several non-invasive tests including stress ECG, stress echocardiography, nuclear techniques, cardiac computed tomography are used in clinical routine for the detection of CAD. However, due to limited sensitivity and specificity of all non-invasive techniques, the final diagnosis as well as the exclusion of CAD is established by catheter angiography in the majority of patients. MRI offers different morphologic and functional techniques including wall motion analysis at stress, first-pass stress perfusion, MR coronary angiography and coronary vessel wall imaging for the detection of CAD.

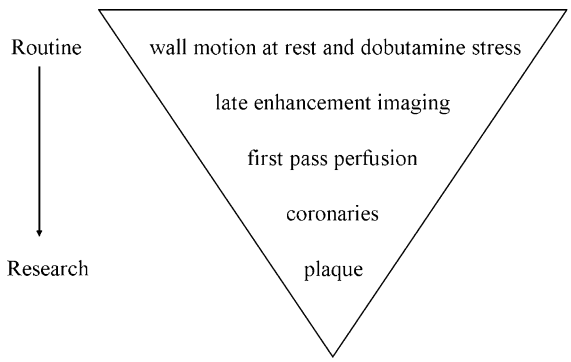

Ischemic Heart Disease, MRI. Figure 1 Status of different MR techniques for the assessment of ischemic heart disease.

Wall Motion Analysis at Stress

CAD may result in global or regional wall motion abnormalities of the left ventricle and lead to heart failure. The MR analysis of the global left ventricular function at rest, expressed as left ventricular ejection fraction, has impact on patient management and predicts patients' prognosis. Regional wall motion abnormalities are classified as hypo-, a- or dyskinesia of the left ventricular myocardium, but the different pathophysiological causes of wall motion abnormalities (scar, stunning, hibernation) cannot be differentiated by analysis of rest function.

The assessment of regional wall motion at pharmacological stress provides additional information to the rest examination. Low-dose dobutamine stress MRI can be used to assess myocardial viability. Dysfunctional myocardium that improves at low-dose dobutamine can be characterized as ischemic myocardium (hibernation), with a high probability of recovery of function after revascularization.

High-dose dobutamine stress MRI can identify myocardial ischemia non-invasively. The positive inotrope and chronotrope effects of dobutamine increase the myocardial oxygen demand and new or worsened wall motion abnormalities at stress are sensitive signs of hemodynamically significant CAD. High-dose dobutamine MRI can be performed with a standard dobutamine/atropine stress protocol, which was introduced for stress echocardiography. However, compared to stress echocardiography, detection of wall motion abnormalities by stress MRI provides a significantly higher accuracy for the diagnosis of significant CAD.

Stress Perfusion

Contrast enhanced first-pass myocardial perfusion imaging uses fast T1-weighted sequences during injection of a contrast bolus. The T1-shortening effect of the contrast agent results in a successive increase of the signal intensity in the right ventricle, the left ventricle and the myocardium. To be well suited for first pass imaging MR pulse sequences have to fulfil several, to some degree contradictory requirements. Most sequences provided for the assessment of myocardial first pass perfusion make use of a saturation-recovery pre-pulse to achieve heavily T1-weighted images followed by a fast data read out by means of gradient echo, echo planar imaging or steady-state free precession techniques. However, sequence optimization must be considered an area of active research and no general recommendations can be given.

Contrast dose varies between 0.025 and 0.15 mmol/kg of extra-cellular Gd-chelates in different studies. As different sequences are more or less sensitive to susceptibility artefacts, the optimum total amount of contrast depends

on the applied MR sequence and on the employed post-processing methods. Myocardial first-pass perfusion studies can be analyzed in different ways including qualitative approaches, semi-quantitative methods and finally a fully quantitative analysis. Visual assessment is operator-dependent whereas semi-quantitative and quantitative methods are time consuming, and approved post-processing tools are not available for clinical applications.

Since the early 1990s, several groups have evaluated the diagnostic potential of first-pass perfusion MRI for the non-invasive detection of CAD against coronary angiography and nuclear techniques in a number of smaller studies. Although coronary angiography must be considered as an imperfect standard of reference, because a morphologic and a functional approach for the detection of significant stenoses are compared, the sensitivity and specificity of perfusion MRI ranged from 65 to 92% and from 76 to 100%, respectively.

However, large clinical trials defining the impact of first pass perfusion MR imaging onto patient management are still lacking, and a consensus on optimal imaging protocols and post-processing techniques has not been achieved so far. Therefore, MR first pass perfusion imaging must still be considered an area of active research, and the technique is not ready for clinical use.

MR Coronary Angiography

Invasive coronary artery angiography still serves as the gold standard for the diagnosis of CAD. However, limitations inherent to catheter coronary angiography include a major complication rate of approximately 0.3–1.1% considerable radiation exposure as well as excessive cost to the health care systems. These drawbacks have promoted alternative imaging strategies. With the development of ultrafast imaging sequences, magnetic resonance angiography of the coronary arteries (MRCA) has recently become possible.

Magnetic resonance angiography has replaced diagnostic catheter angiography for most vascular territories in clinical routine, but magnetic resonance coronary angiography is still an area of active research. The major challenges for MRCA include spatial resolution and coverage, compensation of cardiac and respiratory motion and signal-to-noise issues. Initial studies using two-dimensional (2D) time-of-flight MR angiography techniques suffered from poor through-plane resolution, but these shortcomings were compensated by the introduction of nearly isotropic fast three-dimensional (3D) techniques. Advantageous features of 3D imaging techniques are the acquisition of thinner slices, superior signal-to-noise ratio (SNR) and the total coverage of tortuous coronary arteries.

In order to prevent vessel blurring, compensation of cardiac motion using ECG triggering is mandatory. All data for image reconstruction are collected in an acquisition window of 80–150 msec in mid to late diastole where displacement of the coronaries is minimized. To suppress the effects of respiration MRCA scan can either be performed in a single breath-hold or using respiratory gating. For breath-hold MRCA the scan time must be adapted to the patients' breath-hold capabilities, limiting the number of slices and the spatial resolution. For free-breathing MRCA using the navigator approach can be performed with high spatial resolution, however, image quality may be reduced by navigator failure depending on the patients breathing pattern.

MRCA using standard 3D-gradient echo sequences leads to rather poor contrast between blood and myocardium. To overcome this limitation T2 preparation has been introduced to suppress myocardial signal. Recently, steady-state free precession sequences have become clinically available, improving contrast between blood and myocardial tissue. Another approach for improving the quality of 3D-MRCA is to use T1-shortening contrast agents. Extra-cellular contrast agents are of limited value because they only permit data acquisition directly after intravenous application during the first arterial pass of the agent. Recently, blood pool MR contrast agents have been introduced for MRCA, which are characterized by higher T1-relaxivities and an intravascular distribution. These new intravascular MR contrast agents have recently been shown to improve breath-hold and navigator MRCA.

Until now, only two larger studies have compared free-breathing MRCA with X-ray angiography and reported high sensitivities and specificities for the detection of relevant CAD. Nevertheless, approximately one third of all examinations were not assessable due to impaired image quality. It can be concluded that MRCA is still challenging and the technique is not ready for clinical use in CAD patients.

Plaque Imaging

All luminographic techniques including conventional, computed tomography and magnetic resonance angiography, frequently underestimate the true burden of atherosclerosis because early stage atherosclerotic plaques, which do not compromise the arterial lumen cannot be detected. However, these non-stenotic plaques are of great clinical interest, because about one third of all myocardial infarctions occur due to plaque rupture in a vascular segment without stenoses.

Furthermore, it is well established that the risk of an acute event mediated by plaque rupture is predicted by

the composition of the plaque rather than the degree of luminal narrowing. Plaques with a large necrotic lipid core and a thin fibrous cap are associated with a high risk of rupture.

Due to its ability to distinguish different plaque components like lipids, the fibrous tissue, calcium and thrombi, high-resolution multi-contrast MRI is considered the most promising technique for imaging of the vessel wall. Recently, compounds that accumulate in atherosclerotic plaques or that bind to plaque components have shown promising results in animal studies.

Assessment of Myocardial Infarction and Myocardial Viability

The concept of myocardial 'late enhancement' (LE) or 'delayed enhancement' in contrast-enhanced cardiac MRI is currently being established for the assessment of myocardial viability. Animal studies have demonstrated that myocardial areas accumulating extra-cellular gadolinium-based contrast agents in the equilibrium phase after intravenous administration reliably reflect irreversible myocardial damage after myocardial infarction.

For the detection of late enhancement inversion-recovery gradient echo sequences should be performed 10 to 20 min after injection of 0.1–0.2 mmol/kg Gd-based contrast. The inversion time (TI) has to be adjusted manually between 180 and about 300 msec to null the signal of normal myocardium. These sequences optimize the image contrast and allow a reliable differentiation between infarcted tissue and normal myocardium.

Cardiac MR combining contrast-enhanced imaging (ceMRI) and cine sequences has shown potential characterizing myocardial tissue in patients with ischemic heart disease. Regional myocardial wall motion abnormalities can be caused by irreversible (scar tissue) or reversible myocardial damage, the latter of which can be differentiated in myocardial hibernation and myocardial stunning. MRI allows the discrimination of myocardial infarction (dysfunction with hyper-enhancement), myocardial stunning (dysfunction, normal perfusion, no hyper-enhancement), myocardial hibernation (dysfunction, hypo-perfusion, no hyper-enhancement) and normal myocardium (normal function without hyper-enhancement (Fig. 2).

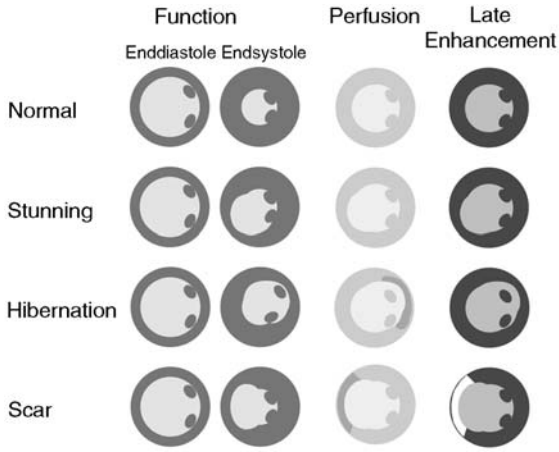

Ischemic Heart Disease, MRI. Figure 2 MR characterization of normal and dysfunctional myocardium.

Acute Myocardial Infarction

Acute myocardial infarctions (MI) are characterized by a loss of the cell membrane integrity. Therefore, standard extra-cellular contrast agent can enter the space formerly occupied by the cells resulting in an increased fractional distribution volume. However, a dark zone in the centre of the enhancing area can frequently be detected in acute MI. Although, the great epicardial coronary arteries are patent after acute percutanenous coronary interventions (PCI) or thrombolysis, there might be areas without early contrast uptake, because the small vessels and capillaries are occluded. This no-reflow phenomenon for MR has been described more than 10 years ago and can now be visualized *in vivo* using MRI.

Within the first week after acute MI wall motion abnormalities can either be caused by infarcted or stunned myocardium. Stunning is defined as dysfunctional but viable myocardium due to a temporary severe ischemia. The differentiation between stunned and infarcted segments in patients with recent myocardial infarction is clinically important and can easily be made by MRI because irreversible damaged myocardium shows late enhancement whereas stunned myocardium does not (Fig. 2). Based on this criterion, contrast-enhanced MR reliably distinguishes stunning from infarction and allows predicting the functional improvement of stunned myocardium.

The true extent of irreversible myocardial injury defined by MRI using the late enhancement approach is a strong predictor of patients' outcome. Furthermore, no-reflow areas detected within the area of late enhancement are an additional independent risk factor and are associated with an increased number of cardiac events and poor prognosis.

Acute myocardial infarction can reliably be distinguished from chronic scar tissue using T2-weighted images. While acute MI appears bright due to myocardial oedema, chronic MI is isointense to myocardium on

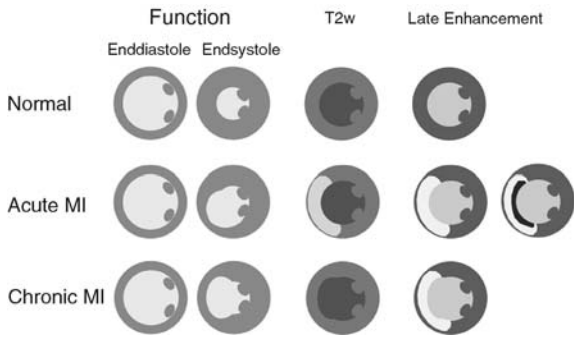

Ischemic Heart Disease, Nuclear Medicine. Figure 3 MR appearance of acute and chronic myocardial infarction.

T2-weighted images (Fig. 3). Additionally, chronic myocardial infarctions frequently show wall thinning due to scar formation, whereas in acute MI the end-diastolic wall thickness is not different from normal myocardium. Another criterion to distinguish acute and chronic myocardial infarctions is the no reflow phenomenon, which can only be detected within the first 4 to 6 weeks after an acute myocardial infarction.

Chronic Myocardial Infarction

Chronic myocardial infarctions show a homogenously increased signal intensity compared to normal myocardium 5 to 30 min after contrast injection (Fig. 3). Whereas the contrast agent is rapidly washed out from normal myocardium, the contrast agent accumulates in the increased interstitial space of non-viable myocardium. Additionally, the reduced perfusion of scar tissue results in a delayed wash out of the contrast agent. Chronic myocardial infarction shows homogenous enhancement after contrast application (Fig. 3).

In patients with a history of myocardial infarction, myocardial dysfunction can be caused by scar tissue or myocardial hibernation. Hibernation is defined as dysfunctional but viable myocardium due to chronic ischemia. The differentiation between hibernating and infarcted segments in patients with a history of myocardial infarction is clinically important and can easily be made by MRI because irreversible damaged myocardium shows late enhancement whereas hibernating myocardium does not.

This differentiation is clinically important because patients with hibernation benefit from re-vascularization whereas patients with scar tissue do not. The delayed enhancement technique has recently been introduced into clinical routine for the assessment of myocardial viability. Contrast-enhanced MRI can reliably discriminate between reversible (hibernation) and irreversible ischemic injury and predicts functional recovery after re-vascularization with high sensitivity and specificity.

Comparing MRI with positron emission tomography (PET) as the reference standard for the detection and quantification of myocardial scar tissue, several studies demonstrated a higher sensitivity of MRI for the detection of small scars, reflecting the higher spatial resolution of the LE images. Furthermore, MRI is superior defining the transmural extent of infarcted myocardium which is a strong predictor of functional recovery after revascularization. Analyzing regional contractility before and after re-vascularization, function improved in about 3/4 of segments without hyper-enhancement, whereas almost none of the segments with hyper-enhancement of more than 75% of the left ventricular wall showed a recovery of function.

However, although LE is very sensitive in detecting and localizing myocardial scarring, it is, on the other hand, not specific for ischemic damage. Pathologically controlled studies have shown that extra-cellular contrast agents accumulate not only in infarction scars, but generally in tissues with increased water content. Thus, the presence of LE has been described in myocardial areas of fibrosis, inflammation and edema where the extra-cellular volume is enlarged. Different entities of myocardial diseases or disorders are accompanied by fibrosis and acute or chronic inflammation and might, therefore, be diagnosed based on the pattern and localization of LE in contrast-enhanced MRI. Whereas myocardial infarctions always involve the sub-endocardial layer of the myocardium and the area of late enhancement is related to the territories of the coronary arteries, non-ischemic entities frequently show a more patchy and sub-epicardial distribution.

Ischemic Heart Disease, Nuclear Medicine

M. P. M. Stokkel
Department of Nuclear Medicine, LUMC, Leiden, The Netherlands
m.p.m.stokkel@lumc.nl

Synonyms

Myocardial perfusion scintigraphy

Definition

Many pathological conditions with respect to the coronary blood flow have been described. Hypoxia is the condition in which the oxygen supply is diminished despite an adequate perfusion of the myocardium. Anoxia

is regarded as the absence of oxygen supply, whereas in ►ischemia the oxygen deprivation is accompanied by inadequate removal of metabolites due to a reduced perfusion. During the ischemic condition an imbalance occurs between oxygen supply and demand, which may manifest as anginal discomfort, deviation of the ST segment on electrocardiography, or impairment of the regional or global left ventricular function. In the presence of coronary obstruction, an increase in myocardial oxygen requirement leads to a transitory imbalance or the so-called demand ischemia. This condition may be caused by exercise, tachycardia, or emotion and is responsible for most episodes of chronic stable angina. On the other hand, imbalance caused by a reduction of the oxygen supply related to increased vascular tone or the presence of thrombi is termed supply ischemia. This form of ischemia is responsible for episodes of unstable angina and myocardial infarction.

Nuclear medicine dedicated to imaging procedures of the heart using radiopharmaceuticals—so-called nuclear cardiology—has been an active clinical specialty for at least three decades. Major advances have occurred over the past years in both radiopharmaceutical development and instrumentation. Nuclear cardiology gives insight into many functional aspects of the heart and thus into risk stratification and prognosis (1). The clinical applications of nuclear cardiology include ►*myocardial perfusion scintigraphy*, measurement of the left ventricular ejection fraction, assessment of myocardial viability, assessment of myocardial fatty acid metabolism, and assessment of receptor integrity.

Pathology/Histopathology

A strong correlation between ischemic heart disease and prognostic factors, such as smoking, hypertension, diabetes, and hypercholesterolemia has been established. Other contributory factors may be lack of exercise and physiological characteristics. These factors lead to initiation and progression of a process of reduction in the lumen of the coronary artery. This process is characterized by the formation of an atheroma affecting the intima, fibrin, and platelet deposition on the intima, hemorrhage under the intima, thrombosis, or a combination of these factors. The anterior descending coronary artery is especially vulnerable to atheroma, and sudden occlusion of this vessel is particularly dangerous. In myocardial infarction, there is usually an occlusion due either to a platelet thrombus or to rupture of an atheromatous plaque, which may result in subendocardial or transmural infarction. During an acute infarction an inflammatory reaction occurs, and if the epicardial surface is affected, it may lead to overlying pericarditis.

Clinical Presentation

►*Angina pectoris* is the name for a clinical syndrome due to myocardial ischemia. The symptoms are commonly provoked by exertion, particularly out of doors, or by anxiety. It is usually experienced as a sense of oppression or tightness in the middle of the chest, and the patient commonly places his or her hand on the sternum. Angina pectoris is likely to be worse on a cold day or when walking against a wind or uphill and it commonly occurs after meals. In all of these circumstances, a greater coronary blood flow is demanded to fulfill the increased oxygen requirement. The pain is commonly accompanied by discomfort in the arms (most often the left), wrists, and hands. Angina may more rarely be epigastric or interscapular or may radiate to the neck and jaw. There may be accompanying breathlessness or even syncope.

Imaging

The acquisition and display of nuclear medicine images depends on detecting photons emitted during the decay process of a radionuclide. These radionuclides are intravenously administered to a patient and are either labeled to specific tracers or are unlabeled. The photons are detected with a scintillation (gamma) camera interfaced with a computer. The photomultiplier tubes translate the scintillations that occur in a large sodium iodide crystal into voltage pulses, which are finally measured as an electrical signal. The computer is a principal component of all nuclear imaging systems as it uses software containing reconstruction algorithms and functionality for quantifying static and dynamic images.

Over the past years, single photon emission computed tomography (SPECT) has been used more commonly in cardiovascular imaging. A series of planar images is acquired over a 180–360° arc around the patient's thorax, which gives the option of three-dimensional imaging of the heart. The transaxial images are reconstructed into short-axis and horizontal and vertical long-axis orientations. The overall result is an improvement in anatomical resolution and contrast in relation to planar imaging, but it requires more stringent quality control measures of the whole imaging device. Finally, by using the electrocardiogram (ECG) signal as a trigger for image acquisition, the so-called ►*gated-SPECT* method, perfusion imaging is combined with functional imaging to reveal data with respect to perfusion, global ejection fraction, and regional wall motion and thickening. As a result, it provides the clinician better information with respect to risk stratification and prognosis.

Nuclear Medicine

Radiopharmaceuticals for Myocardial Perfusion Imaging

The regional distribution of myocardial perfusion can be visualized with radiopharmaceuticals that accumulate proportional to the regional blood flow. In 1874, Thallous chloride-201 (Tl-201) became available, which has the advantage of viability assessment in addition to perfusion evaluation. Over the past decade, however, Technetium-99m (^{99m}Tc)-labeled compounds became available. These latter radiopharmaceuticals have better imaging characteristics and novel biological properties. Although worldwide ^{99m}Tc-labeled compounds are most commonly used, combinations with both radiopharmaceuticals are still in use (2).

Thallium-201

Thallium-201 is a cyclotron-produced radiopharmaceutical that emits mercury X-rays at 69–83 keV and photons with an energy of 135, 165, and 167 keV. Its physical half-life is 74 h, but its biological half-life is 58 h. Because of the relative long half-life and the rather high whole body doses, only a small amount of radioactivity can be administered. The first-pass extraction fraction is approximately 85%, whereas the overall uptake is about 4% of the injected dose. The initial accumulation is proportional to the blood flow, and once it has entered the cell it continuously exchanges across the cell membrane. This process involves the Na^+, K^+-ATP-ase pump. Consequently, with one single injection, this radiopharmaceutical may provide images related not only to the initial blood flow but also to a redistribution process. The latter images reflect the distribution of the potassium pool and hence myocardial viability. A disadvantage of this compound is that because of this redistribution process, acquisition should start very shortly after administration, whereas the acquisition time is limited.

Technetium-99m-Labeled Compounds

Over the past years, a number of ^{99m}Tc-labeled compounds have been introduced in clinical practice. The most commonly used agent is ^{99m}Tc-sestamibi, a lipophilic monovalent cation, which later on came to be used for tumor scintigraphy. The production of these compounds is on site. The advantage of ^{99m}Tc over Tl-201 is the optimal energy of photons emitted, 140 keV, which can be easily detected by sodium iodide crystals in the gamma camera. Consequently, better image quality can be achieved using these compounds. The half-life of ^{99m}Tc is approximately 6 h, whereas the radiation exposure for patients is less than obtained with Tl-201. Because of the favorable dosimetry, up to 1,000 MBq of these agents can be administered per day.

The initial myocardial uptake is similar to Tl-201 and is proportional to the regional blood flow. In contrast to Tl-201, however, there is rapid accumulation in the liver as well as excretion into the biliary tract. Consequently, extracardiac activity may be observed, which may interfere especially with interpretation of the inferior wall. Uptake in the myocardium is by passive diffusion followed by binding to intracellular membranes. The myocardial distribution remains stable over time and can be imaged for several hours after administration. There is no significant redistribution. The most commonly used ^{99m}Tc-labeled compounds are ^{99m}Tc-sestamibi and ^{99m}Tc-tetrofosmin (3).

Stress-Rest Imaging Protocols

To assess myocardial perfusion, different study protocols have become available. The aim of these imaging protocols is to differentiate, on one hand, normal from abnormal perfusion studies. On the other hand, the aim is to differentiate persistent perfusion abnormalities from reversible ischemia and, in the case of the use of Tl-201, to assess the presence of viable tissue. In this respect, different protocols have become available over the past years (3).

Stress Protocols

To assess myocardial perfusion, different stress protocols are available. The choice of protocol depends on the condition, comorbidity, medication, abnormalities on ECG, and so on. In most nuclear cardiology centers, a stress test is followed by a rest study, but it has been stated that in the case of a normal stress study, the performance of a rest study is questionable.

Physical exercise: Several treadmill protocols exist. Endpoints for physical exercise are severe symptoms as dyspnea and angina, hypotension, exhaustion, and ST-segment depression on electrocardiography. During peak exercise, the radiopharmaceutical is administered intravenously in an antecubital line, after which time the patient is encouraged to exercise for another 1 or 2 min.

Pharmacological vasodilatation: If disabilities or contraindications to physical exercise exist, pharmacological alternatives are available. The most commonly used are adenosine infusion and dobutamine stress. Adenosine is a vasodilator with minimal side effects. The only contraindications are chronic obstructive pulmonary disease and AV block. Maximum dilatation is achieved after 4–4.5 min, at which time the radiopharmaceutical is administered, and the infusion continues for 1.5–2 min. Side effects include transient headache, abdominal

discomfort, and nausea. The advantage of adenosine over other techniques is its rapid clearance and, consequently, the instantaneous reversibility of symptoms.

Dobutamine stress increases myocardial oxygen demand by increasing contractility, heart rate, and blood pressure. The increase in flow is comparable to that of physical exercise but less than that with adenosine. The infusion protocol takes about 15 min, with administration of the radiopharmaceutical in the 12th min. The most commonly reported side effects include ventricular ectopy, headache, dyspnea, paresthesia, and flushing; however, their reversibility is less rapid than in adenosine protocols.

One-day stress–rest study: Several study protocols can be used during a one-day stop-and-shop imaging strategy:

1. Tl-201 (100 MBq) injected at peak exercise, delayed imaging after 2–4 h to assess redistribution, followed by reinjection of Tl-201 (75 MBq) to assess the perfusion at rest.
2. ^{99m}Tc-labeled compounds (250–500 MBq) injected at rest, followed by a stress study 2 h later using 750–1,000 MBq of a ^{99m}Tc-labeled compound.
3. Dual isotope imaging, which is based on the injection of Tl-201 at rest and a ^{99m}Tc-labeled compound during stress.

Two-day stress-rest study: This is the most commonly used strategy. The major advantage over a one-day stress-rest study protocol is the fact that the amount of activity is comparable under both circumstances (500–1,000 MBq), revealing better image quality and the option of optimal gating during stress as well as rest. Although Tl-201 can be used in this protocol, the use of ^{99m}Tc-labeled compounds is advised because they give a better option of gating during both studies and, again, better image quality.

Interpretation of Images

Myocardial perfusion studies are reconstructed and presented in short-axis and horizontal and vertical long-axis projections. The initial interpretation is visual, in which the heart is subdivided into segments (e.g., 9, 17, or 20 segments). For each segment, the perfusion is scored as normal (0), slightly to moderately diminished uptake (1), moderately to severely diminished uptake (2), or no uptake (3). It is important to assess the size of the left ventricle and the distribution pattern of the radiopharmaceutical, either homogeneous or irregular. An irregular pattern may indicate microangiopathy caused by diabetes or cardiomyopathy. The visual analysis is done for the stress as well as for the rest study, and the results are combined with a semiautomatic analysis method developed by Germano and Berman (4). This software package gives the option to measure the left ventricular ejection fraction, the regional wall motion, and wall thickening. Furthermore, a polar map, or bull's eye display is used to compare the stress–rest images semiautomatically. The purpose of this map is to generate one single image that encompasses the relative distribution of the radiopharmaceutical. Relative uptake on short-axis images is compressed to a color-coded concentric ring with the apical slice in the center and the basal slices on the periphery of the map. The combination of all data finally results in the following interpretations:

1. Normal intensity, homogeneous distribution, normal function of the myocardium (Fig. 1)
2. Defect in one or more segments, abnormal function in these segments, which may be indicative for infarction (Fig. 2)
3. Reversible defect, which is a defect present on initial stress images and no longer present on the resting or delayed images. This pattern indicates ischemia (Fig. 2). Functional abnormalities may be seen, which commonly correspond to the severity of the perfusion abnormalities.

It must be realized that artifacts may occur, leading to possible misinterpretation of the reconstructed images. Motion artifacts may show up as reversible defects, which can be assessed on the raw data images. A typical motion artifact is the so-called upward creep of the heart, which is caused while the patient recovers from stress and the heart consequently moves into the horizontal position. Other common artifacts are caused by attenuation. Acquisition is normally performed with the patient in the prone position, because in this position the overall attenuation by the camera table at one side is comparable with the attenuation of photons passing through the chest at the other side. When acquisition is done in the supine position, it may cause artifacts in the inferior wall. Attenuation by large and/or dense breast tissue will result in abnormalities in the anteroseptal region.

Diagnosis

Myocardial perfusion scintigraphy is an extremely sensitive and reliable method for the assessment of perfusion abnormalities and prognostic stratification (5, 6). Indications for perfusion scintigraphy are visualization of ischemia (site, extent, and severity), stratification of risk for cardiac death (low, intermediate, or high), identification of the culprit artery, determination of viability of dysfunctioning myocardium, and, in certain cases, recommendation for the type of therapy as medical, coronary artery bypass graft (CABG), or transplantation. In most of the studies published over the past year, myocardial perfusion

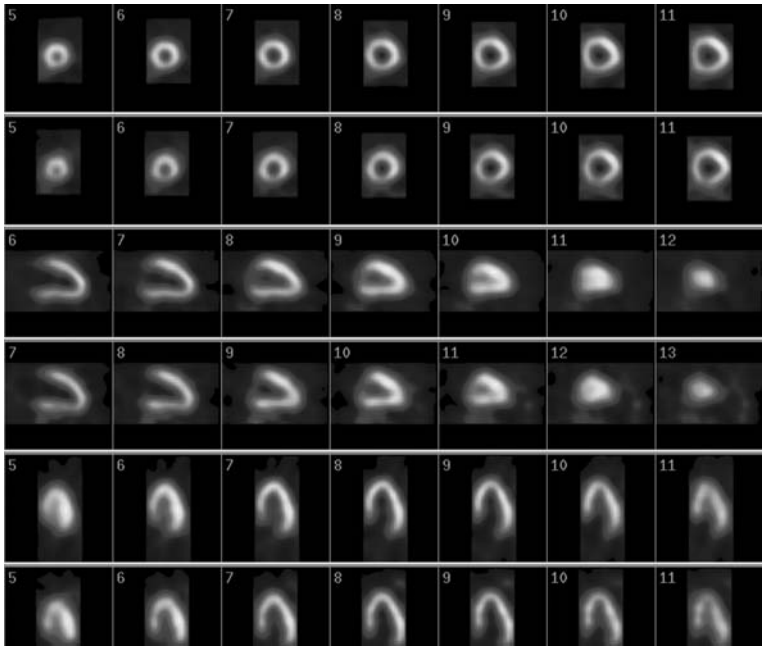

Ischemic Heart Disease, Nuclear Medicine. Figure 1 Standard short-axis and horizontal and vertical long-axis reconstructions of a stress–rest myocardial perfusion study with ^{99m}Tc-tetrofosmin. The first, third, and fifth rows demonstrate stress images, and the second, fourth, and sixth rows demonstrate rest images. A normal distribution pattern is seen without perfusion defects. This patient, who presented with atypical chest pain was categorized into the very-low-probability risk group for cardiac events.

scintigraphy has revealed a sensitivity and specificity of 80–100% and 80–90%, respectively, for detecting ischemia or infarction, whereas the negative predictive value is up to 99%. It has been concluded from these studies that gated-SPECT myocardial perfusion scintigraphy has significant incremental prognostic value regarding individual parameters such as age and gender, risk factors such as hypercholesterolemia and hypertension, and ECG changes. Following perfusion scintigraphy, patients can be stratified into the following risk groups for a major cardiac event:

1. Low risk (<1%)
   a. Normal or near normal perfusion
   b. Normal left ventricular ejection fraction with normal or near normal perfusion
2. Intermediate risk (<1% for cardiac death, but 1% for nonfatal myocardial infarction)
   a. Small perfusion defect (15% of left ventricle volume) with normal left ventricular ejection fraction and absence of nonperfusion markers of left ventricular decompensation with exercise
3. High risk (>3% for cardiac death)
   a. Severe left ventricular dysfunction at rest
   b. Severe left ventricular dysfunction with exercise
   c. Large stress-induced perfusion defect
   d. Moderate stress-induced perfusion defect with abnormal Tl-201 lung uptake
   e. Multiple moderate stress-induced perfusion defects
   f. Large fixed perfusion defect with left ventricular dilatation.

Low-risk patients can be followed medically, whereas high-risk patients are ideal candidates for revascularization. An intermediate-risk patient can be followed medically except for special circumstances such as intolerability of symptoms or other reasons.

In patients who do undergo interventions, follow-up is indicated based on the technique used, the presence of symptoms, the relative risk for subsequent problems, and, finally, the time that has passed since the intervention. For example, the time to assess for restenosis after percutaneous transluminal coronary angioplasty is approximately 3–6 months. The majority of restenoses occur by this time interval regardless of recurrent symptoms. In the published studies, nuclear perfusion imaging demonstrated a superior sensitivity of 87% and a specificity of 78% compared with 46 and 77%, respectively, for the treadmill test. Assessment of perfusion after CABG by gated-SPECT studies definitely provides better insight into the site and extent of ischemia compared with treadmill tests. To understand abnormalities seen on the scans, however, knowledge of pre-CABG anatomy, vessels that were bypassed, and operative reports should be

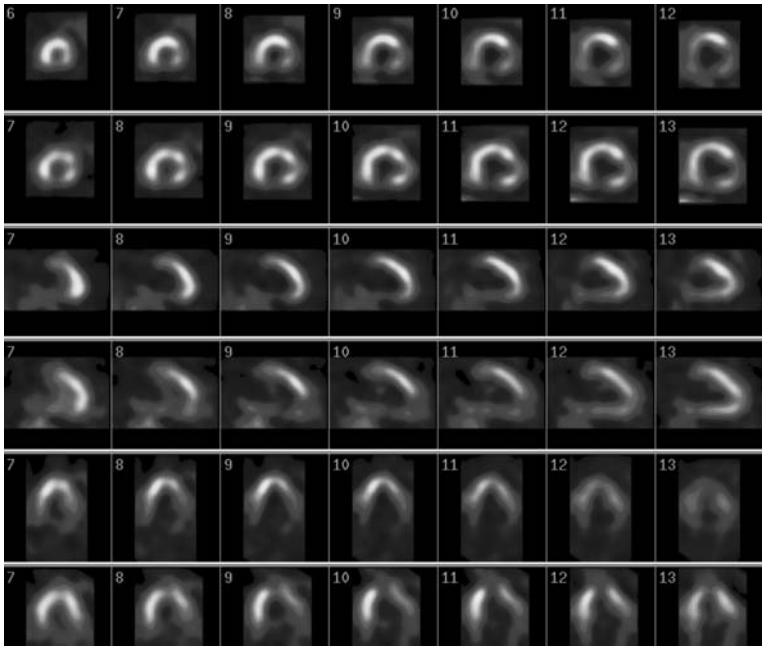

Ischemic Heart Disease, Nuclear Medicine. Figure 2 Myocardial perfusion scintigraphy with ^{99m}Tc-tetrofosmin in a patient with typical angina 1 year after myocardial infarction. The short axis and vertical long axis demonstrate persistent perfusion defects in the inferior and lateral wall in an enlarged left ventricle, consistent with myocardial infarction. Reversibility is seen in the septal and inferolateral wall, categorizing this patient into the high-risk group.

available, as these post-CABG scans may demonstrate a combination of nonrevascularized but diseased vessels, entrapped vessels, new disease, disease beyond anastomotic sites, or pathology of the grafts themselves.

Hibernation and Stunning

Hibernation refers to a condition of chronic sustained abnormal contraction due to chronic underperfusion in patients with coronary artery disease. In these patients, revascularization may cause recovery of function, even more than a year after intervention. In addition to this chronic underperfusion phenomenon, stunning is defined as repeated ischemic attacks, which may also result in chronic dysfunction with flow remaining normal or mildly reduced. The term "jeopardized myocardium" includes the entire spectrum ranging from stunning to hibernation. It is beyond the scope of this essay to describe in detail the principles and applications of jeopardized viable myocardium assessment. In summary, under such conditions glucose metabolism remains preserved in viable tissue. Regional glucose metabolism can be assessed with fluorodeoxyglucose (FDG), a radiolabeled glucose analog, and SPECT imaging. Dysfunctional segments with both preserved perfusion and glucose metabolism are thought to represent stunned myocardium, whereas segments with preserved glucose metabolism but reduced perfusion are considered hibernating myocardium. In contrast, segments with reduced perfusion and concordantly reduced FDG uptake are considered scar tissue. In this respect, myocardial perfusion studies performed at rest are a prerequisite for an optimal viability assessment and, consequently, for the prediction of functional recovery and long-term prognosis.

Bibliography

1. Faber TL, Cooke CD, Folks RC et al (1999) Left ventricular function and perfusion from gated SPECT perfusion images: an integrated method. J Nucl Med 40:650–659
2. Berman B, Germano G, Lewin H et al (1998) Comparison of post-stress ejection fraction and relative left ventricular volumes by automatic analysis of gated myocardial perfusion single photon emission computed tomography acquired in supine and prone positions. J Nucl Cardiol 5:40–47
3. Shridhara B, Sochor H, Rigo P et al (1994) Myocardial single-photon emission computed tomographic imaging with technetium 99m tetrofosmin: stress-rest imaging with same-day and separate-day rest imaging. J Nucl Cardiol 1:138–143
4. Germano G, Berman DS (2005) Quantitative single-photon emission computed tomography imaging. Curr Cardiol Rep 7:136–142
5. Shaw LJ, Iskandrian AE, Hachamatovitch R et al (2001) Evidence-based risk assessment0 in noninvasive imaging. J Nucl Med 42:1424–1436
6. Shaw L, Hachamovitch R, Heller GV et al (2000) Noninvasive strategies for the estimation of cardiac risk in stable chest pain patients. The Economics of Noninvasive Diagnosis (END) Study Group. Am J Cardiol 86:1–7

Ischemic Heart Disease, Ultrasound

Bernard P. Paelinck
University Hospital Antwerp, Antwerp, Belgium
bernard.paelinck@ua.ac.be

Synonyms

Coronary artery disease; Doppler echocardiography

Definitions

Ischemic heart disease results from stenosis and/or occlusion of one or more coronary arteries. When ►myocardial perfusion is reduced, ischemia develops with resulting impairment of myocardial function. Reversible myocardial dysfunction due to transient and chronic ischemia is defined as stunned and hibernating myocardium, respectively (1). Irreversible myocardial dysfunction or myocardial infarction occurs when prolonged ischemia results in myocyte death (2).

Pathology/Histopathology

In ►myocardial stunning, myocardial function is temporarily impaired, which may result from reperfusion injury with generation of free radicals and calcium overload. With maintenance of normal perfusion, myocardial function returns to normal. In hibernating myocardium, a mixture of normal, atrophied, and hypertrophied myocytes is found. Prolonged hypoperfusion leads to reversible downregulation of myocardial function and to variable structural changes, ultimately including loss of myocytes.

Myocardial infarction is characterized by myocardial muscle necrosis. Acute or evolving myocardial infarction is characterized by infiltration of polymorphonuclear leukocytes (after 6 h) in addition to cell death. Acute myocardial necrosis can be recognized by the release of myocardial proteins in the blood (e.g., myoglobin, troponins T and I, creatine kinase) and by the loss of electrically functioning cardiac tissue (Q waves on electrocardiograms). Healed myocardial infarction is manifested as scar tissue without cellular infiltration and requires about 6 weeks or more to develop after the acute event (2).

Clinical Presentation

Ischemic heart disease remains one of the leading causes of morbidity and mortality. Angina pectoris is a typical symptom of ischemia. Dyspnea can occur as a result of extensive ischemic reversible myocardial dysfunction and is referred as "angina equivalent." Acute myocardial infarction is usually accompanied by typical chest pain, lasting for at least 20 min, but may also present without symptoms.

Ultrasound Imaging

Ischemia

Ischemia results in a sequence of events referred to as "the ischemic cascade": initially diastolic dysfunction, at a later stage systolic dysfunction, eventually followed by electrocardiographic changes, and finally by angina pectoris.

The initial diastolic abnormality is prolonged and delayed myocardial relaxation. This is apparent from decreased early left ventricular filling (E) and a decreased early atrial (A) to mitral filling ratio (or E/A) assessed by ►Doppler echocardiography. With worsening diastolic function, the left ventricular compliance is decreased and left ventricular filling becomes dependent on increased left atrial pressure, causing an increased E/A ratio. As the underlying impaired relaxation is masked and because the left ventricular filling pattern resembles the normal filling pattern, it is called pseudonormalization. Combining E peak velocity, which is dependent on both left atrial pressure and myocardial relaxation, with tissue Doppler-assessed early diastolic mitral annulus velocity (Ea), which is mainly dependent on myocardial relaxation, allows differentiation ("unmasking") of a normal from a pseudonormal signal. With ongoing decrease in compliance, the mitral filling pattern becomes restrictive (Fig. 1).

With prolonged ischemia, regional myocardial thickening and motion are decreased (less than 30% = hypokinesia, or absent = akinesia) or systolic outward motion occurs (dyskinesia). Regional wall motion of the left ventricle is assessed in 17 segments (American Heart Association) and analyzed in different views (apical and parasternal ultrasound windows). Each segment is assigned a wall motion score: normal: 1, hypokinesia: 2, akinesia: 3, and dyskinesia: 4. A wall motion score index is calculated as the sum of segmental scores divided by the number of segments. The segmental wall motion abnormalities in ischemia correspond to coronary perfusion territories. Left anterior descending artery disease results in abnormalities of the anterior, anteroseptal, and apical segments, while right coronary artery disease results in abnormalities of the inferior and basal posteroseptal

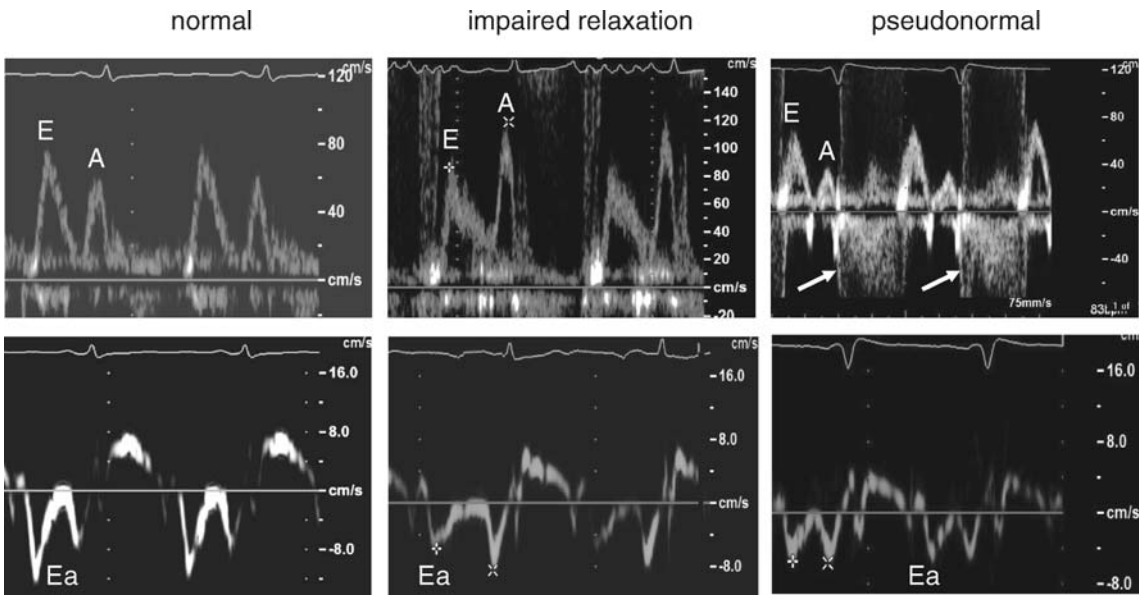

Ischemic Heart Disease, Ultrasound. Figure 1 Doppler echocardiography of mitral filling pattern (upper panel) together with tissue Doppler-assessed mitral annular velocities (lower panel) showing representative traces of normal, impaired relaxation and pseudonormal mitral filling pattern. Note decreased Ea in impaired relaxation and pseudonormal mitral filling pattern. Arrows indicate reverse flow due to mitral regurgitation. E; early left ventricular filling, A; atrial or late ventricular filling, Ea; early diastolic mitral annulus velocity.

segments. Circumflex artery disease affects motion of the lateral and posterior segments. These patterns of segmental dysfunction may vary depending on the coronary dominance pattern and the site of ►coronary artery disease.

Patients with ►coronary artery disease frequently have normal left ventricular function at rest. Diagnosis of coronary artery disease using stress echocardiography is based on the induction of a decreased myocardial oxygen supply/demand ratio resulting in new or worsening segmental systolic wall motion abnormalities. Depending on patient characteristics (capability of exercise) and echolab logistics, physical exercise (treadmill or bicycle) or pharmacological (inotropic stress: dobutamine; vasodilator stress: adenosine, dipyridamole) stress testing can be performed. Exercise echocardiography has a mean sensitivity and specificity of 84 and 82%, respectively, while dobutamine echocardiography has a mean sensitivity and specificity of 80 and 84%, respectively, to detect coronary artery disease (3). The accuracy of stress echocardiography is highly dependent on endocardial border definition. In the case of a suboptimal acoustic window, improved endocardial border delineation can be obtained by using ►Second harmonic imaging. and (optionally) administration of intravenous contrast agents to assess myocardial perfusion.

Besides diagnosis and assessment of the location and extent of myocardial ischemia, stress echocardiography is used for the preoperative risk evaluation in major noncardiac surgery and for the assessment of myocardial viability. Identification of dysfunctional but viable myocardium (as opposed to necrotic myocardium) has important prognostic value and is predictive of the recovery of function after revascularization. Indicators of myocardial viability include contractile reserve to inotropic stimulation (augmentation of regional myocardial function) and preserved myocardial thickness (>6 mm).

Myocardial Infarction

In the emergency department, echocardiography is essential in the bedside evaluation of a patient with chest pain (but a nondiagnostic electrocardiogram). In the acute phase of myocardial infarction, the affected myocardium is dysfunctional (akinetic, hypokinetic, or dyskinetic) but wall thickness is still preserved. Two-dimensional echocardiography has, in addition, prognostic implications and the amount of myocardial dysfunction allows estimation of the amount of myocardium at risk. If wall motion during chest pain is normal, the likelihood of acute myocardial infarction remains low. Echocardiography is also useful in detecting other causes of chest pain such as: pericarditis, pulmonary embolism, and aortic dissection.

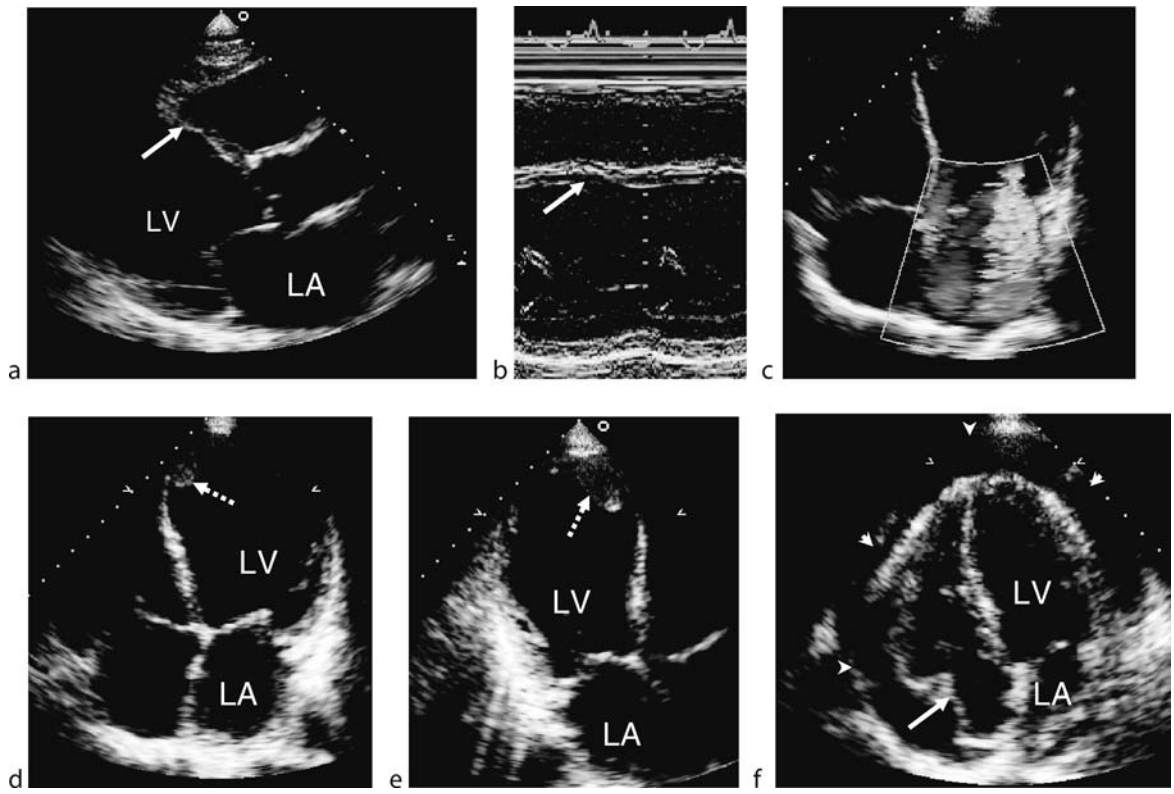

Ischemic Necrosis. Figure 2 (a) Parasternal long-axis view and (b) ►M-mode echocardiogram. showing dilatation of the left ventricle and thin-walled infarcted anteroseptal wall (arrow). Note absence of thickening in infarcted myocardial wall. (c) Two-dimensional echocardiogram of ischemic mitral regurgitation, (d) apical four-chamber, and (e) three-chamber view showing mid and apicoseptal thin-walled aneurysm with intracavitary thrombus (dashed arrow). (f) Large pericardial effusion (arrowheads) with partial collapse of the right atrial wall (arrow). LA; left atrium, LV; left ventricle.

Besides assessment of left ventricular dysfunction, two-dimensional echocardiography with Doppler is the primary imaging technique for the initial evaluation of postmyocardial infarction complications: right ventricular involvement, free wall rupture, ventricular septal rupture, papillary muscle rupture causing acute flail mitral leaflet, pericardial effusion and tamponade, intraventricular thrombus, and false and true ventricular aneurysm (Fig. 2). Transesophageal imaging is often necessary to visualize mechanical complications such as muscular rupture.

After several weeks, myocardial infarction results in thinning and increased intensity of the involved segments. A nontransmural myocardial infarction may result in hypokinesia rather than akinesia. Expansion of the infarction zone, global left ventricular dilatation and distortion, together with segmental compensatory hypertrophy, is referred to as postinfarction remodeling. Due to left ventricular dilatation and/or ischemia, mitral regurgitation is often present in ischemic cardiomyopathy. Doppler interrogation of the mitral filling pattern helps guide therapy, including diuretics. Depressed left ventricular ejection fraction, mitral regurgitation, and restrictive mitral filling pattern are associated with a poor prognosis and cardiac death.

References

1. Underwood SR, Bax JJ, vom Dahl J et al (2004) Imaging techniques for the assessment of myocardial hibernation. Report of a Study Group of the European Society of Cardiology. Eur Heart J 25:815–836
2. Myocardial infarction redefined – A consus document of The Joint European Society of Cardiology/American College of Cardiology Committee for the redefinition of myocardial infarction. (2000) J Am Coll Cardiol 36:959–69
3. Schuijf JD, Shaw LJ, Wijns W et al (2005) Cardiac imaging in coronary artery disease: differing modalities. Heart 91:1110–1117
4. Ommen SR, Nishimura RA (2003) A clinical approach to the assessment of left ventricular diastolic function by Doppler echocardiography: update 2003. Heart 89(Suppl III):iii18–iii23

Ischemic Necrosis

►Infarction, Renal

Ischemic Nephropathy

Renal insufficiency secondary to RAS; it can be stabilized, improved, or cured after revascularization.
▶Stenosis, Artery, Renal

Islet Cells Transplantation

In pancreatic islet transplantation, pancreatic cells are taken from a donor and transferred into the recipient. In this procedure, islet is removed from pancreas of a deceased donor by means of specialized enzymes. A typical transplant requires about 1 million islets, equal to two donor organs. Because the islets are extremely fragile, transplantation occurs immediately after they are removed. The surgeon uses ultrasound to guide placement of a catheter through the upper abdomen and into the liver; the islets are then injected through the catheter into the liver. Then cells attach to new blood vessels and begin releasing insulin. Nowadays the procedure is still experimental and more research is needed to answer questions about how long the islets will survive and how often the transplantation procedure will be successful.
▶Transplantation, Pancreas

Islet Cells Tumors, Pancreatic

Laura Crocetti, Carlo Bartolozzi, Carla Cappelli
Department of Diagnostic and Interventional Radiology University of Pisa, Pisa, Italy
l.crocetti@med.unipi.it

Synonyms

Neuroendocrine tumors of the pancreas

Definitions

Neuroendocrine tumors of the pancreas, or islet cell tumors, are rare pancreatic tumors. Among clinically functioning islet cell tumors of the pancreas, insulinoma is the most frequent; others, such as glucagonomas, VIPomas (tumors producing vasoactive intestinal peptide, VIP), somatostatinomas, PPomas (tumors producing pancreatic polypeptide), GFRomas (growth factor releasing hormone tumors), and others, are very rare. Some neuroendocrine tumors secrete more than one hormone, whereas approximately 15–20% of islet cell tumors do not secrete any hormones and are called nonsecreting tumors. They may be single or multiple and benign or malignant. Islet cell tumors may appear multiple, especially in case of multiple endocrine neoplasia (MEN), and are most often found in the pancreas. An extrapancreatic location is reported with a frequency of 10% for gastrinomas; extrapancreatic insulinomas are very rare. ▶Pancreatic carcinoid tumors, producing serotonin, are exceedingly rare. Patients with von Hippel–Lindau's disease are more prone to the development of tumors such as pheochromocytoma and neuroendocrine pancreatic tumors (1, 2).

Pathology/Histopathology

The most common islet cell tumor is insulinoma. About 70% are solitary adenomas, 10% are multiple adenomas, and 10% are carcinomas, whereas the remainder are a mixed group of diffuse hyperplasia of the islet and adenomas occurring in ectopic pancreatic tissue. Adenomas are usually encapsulated and histologically composed of cords of well-differentiated beta cells with typical granules. Malignant tumors show anaplasia; local invasion and spread to the local lymph nodes occur. Other islet cell tumors are similar in histology and differ in content of granules, which may be identified by means of immunohistochemistry (1, 2).

Clinical Presentation

Insulinomas are most common between the fifth and seventh decades of life. The typical clinical feature is hypoglycemia due to uncontrolled insulin secretion. Symptoms related to recurrent hypoglycemia are headache, slurred speech, psychological alterations, visual disturbances, confusion, and, eventually, coma and death. The body tries to compensate for the hypoglycemia by secreting catecholamines, which can result in tremulousness, diaphoresis, palpitations, cardiac arrhythmias, and irritability. Because symptoms due to hyperinsulinism develop early, insulinomas are usually <15 mm in size and solitary at the time of diagnosis; however, multiple tumors are found in 10% of cases, especially in patients with Wermer syndrome or MEN type I (1, 2).

Gastrinomas are the second most common hormone-secreting tumor of the pancreas. They occur more frequently in men than in women. In 30–50%, gastrinomas are associated with other disorders as a part of the

MEN I syndrome. Approximately 90% of all gastrinomas are found in the "gastrinoma triangle," an area limited by the junction of the cystic and common bile duct, the junction of the body and neck of the pancreas, and the second and third portions of the duodenum. Gastrinomas can also be found outside the pancreas, which has never been described for insulinomas. Approximately 60% of all gastrinomas are malignant. Gastric and/or duodenal ulcers develop in the majority of patients due to uncontrolled secretion of gastrin, which is called the Zollinger–Ellison syndrome. Patients with gastrinoma commonly complain about midgastric pain; and diarrhea and weight loss are present in at least 40% of patients. In approximately one-third of the patients, esophagitis is found (1, 2).

The glucagonoma syndrome is a combination of diabetes mellitus and necrolytic migratory erythema. Glucagonomas are single and slow-growing tumors, with metastatic spreading in more than 75% of cases at the time of the diagnosis, most commonly to the liver and the bones. Glucagonomas have been reported in patients suffering from MEN I. A fasting plasma level of glucagon of more than 1,000 ng/L establishes the diagnosis. An erythematous, raised, sometimes psoriatic, and ultimately crusted skin rash has been described in association with glucagonoma. The face, abdomen, perineum, and distal extremities are often the affected portions of the body. After resolution, the regions of acute eruption usually remain indurate and hyperpigmented. Others symptoms, such as glossitis, stomatitis, angular cheilitis, dystrophic nails, and hair thinning, have also been described. The diabetes is mostly mild or even asymptomatic and may manifest only as an abnormality on an oral glucose tolerance test. Weight loss, hypoaminoacidemia, anemia, and thromboembolic disease can also occur in association with this syndrome. Due to the unspecific and often very mild symptoms, these tumors usually are large at the time of diagnosis (1, 2).

Verner and Morrison described a syndrome of watery diarrhea, hypokalemia, hypochlorhydria, and renal failure in association with non-beta-cell tumors of the pancreatic islets. The clinical features are caused by the high levels of VIP secreted by the tumors. The typical manifestations of VIPoma include secretory diarrhea, profound weakness, hypokalemia, and hypochlorhydria. High plasma VIP levels in combination with a stool volume of least 1 L/day are indicative for a VIPoma. The majority of VIPomas are located in the pancreas. In contrast to insulinomas and gastrinomas, they grow to a considerable size before becoming clinically apparent. Although slow-growing, VIPomas usually are malignant and accompanied by metastases in approximately 60% of cases (1, 2).

Somatostatinomas are extremely rare endocrine tumors. The classic triad of somatostatinoma syndrome includes diabetes mellitus, steatorrhea, and cholelithiasis. These symptoms derive from the inhibitory actions of somatostatin, including inhibition of insulin release, pancreatic enzyme and bicarbonate secretion, and gallbladder motility. Like glucagonomas and VIPomas, somatostatinomas are usually single, large, and malignant (1, 2).

No specific syndrome has been associated with pancreatic polypeptide (PP)-secreting tumors. Possible clinical symptoms of PPomas include rash-like efflorescences, weight loss, jaundice, and abdominal pain. The lack of specific symptoms is the reason such tumors are often diagnosed at a stage when they have a mass effect (size >5 cm). The diagnosis can be established by measuring fasting circulation levels of PP (1, 2).

Nonsecreting islet cell tumors are often considerably large at the time of diagnosis compared to hormone-secreting tumors. Because of their mass effect, they cause symptoms such as abdominal pain, jaundice, bowel obstruction, and weight loss. In most cases, nonsecreting islet cell tumors are solitary lesions, being malignant in more than 80% (1, 2).

Imaging

On ultrasound (US), most of the endocrine pancreatic tumors appear as small, round, hypoechoic lesions compared with the pancreatic parenchyma. Larger tumors, which usually do not secrete any hormones and thus do not cause any symptoms at an early stage, may present with a heterogeneous pattern due to necrosis, calcifications, or hemorrhage. Invasion of the peripancreatic structures, hepatic and lymph nodes metastases, and peritoneal carcinosis are more common in nonsecreting malignant tumors. Due to the low specificity of US, other imaging techniques are a necessity in cases of any positive findings in the US examination. However, the use of harmonic imaging and US contrast agents may improve sensitivity. Endoscopic ultrasound (EUS) imaging of small islet cells tumors of the pancreas is more sensitive than transabdominal US. At intraoperative ultrasound (IOUS), the sonographic appearance of islet cell tumors is identical to that of transabdominal US. With high-frequency scanners, the sensitivity of IOUS is very high (3, 4).

Computed tomography (CT) is widely used to identify and localize islet cell tumors. Single or multislice spiral CT scanners represent the standard equipment. The typical scanning protocol consists of several phases (at least three), including a precontrast phase for detecting hypodense lesions, cystic lesions or calcifications; early arterial and pancreatic phases for detecting hypervascular lesions; and a portal-venous phase for detecting hypovascular lesions, being isodense at the precontrast scan or arterial phase

scan. In some cases, a further scan in the delayed phase may demonstrate a late enhancement, particularly in malignant tumors. For examination of the pancreas, slice thickness may vary between 1 and 3 mm. Typically, 120 mL of highly concentrated contrast agent is administered intravenously at an injection rate of 3–5 mL/sec. Additionally, the previous administration of 1,000 mL of water as a "negative" oral contrast as well as the administration of intravenous butyl scopolamine or glucagon may help detect small lesions in the pancreatic head and define their relationship with the duodenum. Islet cell tumors typically appear hyperdense compared with the surrounding tissue at the early arterial and pancreatic phases (Fig. 1). Large, mostly nonsecreting tumors may be centrally hypointense at the arterial and portal-venous phases due to a central necrosis. Sometimes, tumors can be detected even at the precontrast phase because of microcalcifications. Malignant islet cells tumors may require a scan in the delayed phase to demonstrate a late enhancement (Fig. 2). Rarely, an islet cell tumor may present as a cystic lesion. Without a specific clinical syndrome (and/or elevation of a specific hormone), the typical hyperdense appearance may be not sufficient for differentiating an islet cell tumor from other pancreatic lesions. The main advantage of CT is the possibility to stage malignant lesions by identifying local spread and distant metastases (3, 4).

At magnetic resonance (MR), islet cell tumors appear to be hypointense on T1-weighted images and hyperintense on heavily weighted T2-weighted images. Using intravenous gadolinium-DTPA may help differentiate hyperintense islet cell tumors from the normal-enhancing pancreatic tissue. The use of mangafodipir trisodium (MnDPDP) also may help to increase diagnostic sensitivity. Additionally, MR cholangiopancreatography (MRCP) can be used to depict an obstruction of the common bile duct or the main pancreatic duct as an indirect sign for a malignant tumor; however, it does not help differentiate islet cell tumors from other pancreatic neoplasms (3, 4).

Nuclear Medicine

Nuclear medicine is useful for tumor imaging and staging because neuroendocrine tumors express peptide hormone receptors on their membranes, and radiolabeled compounds can bind to such receptors. Over the last decade, a

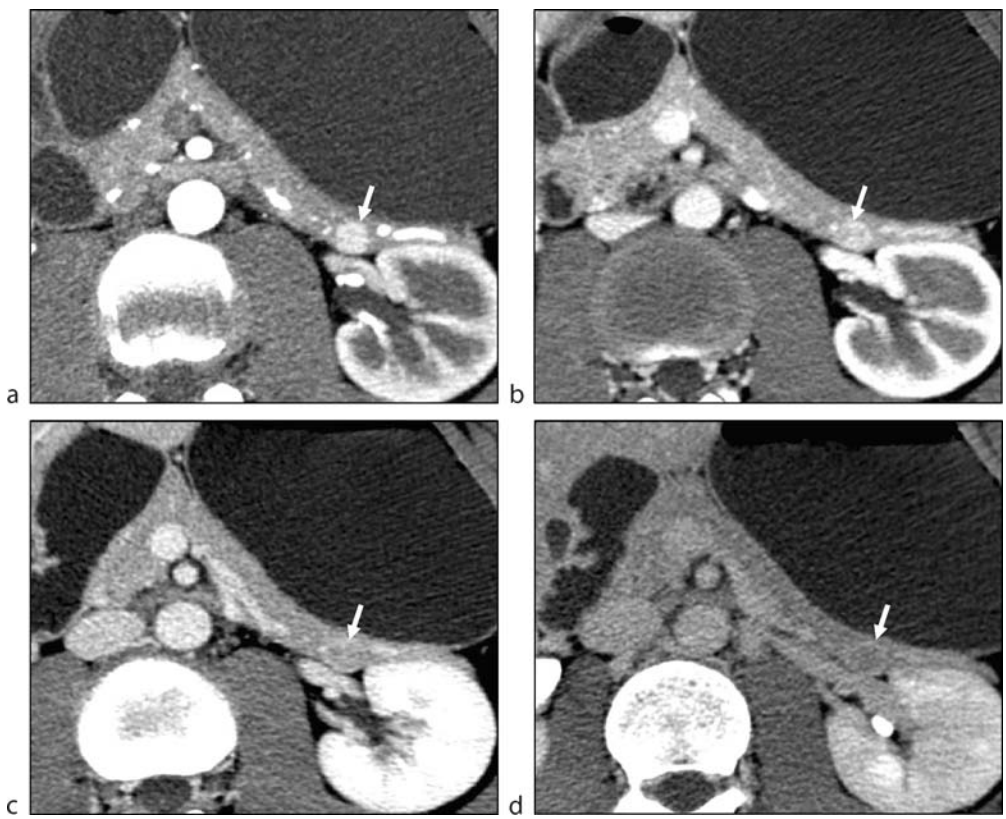

Islet Cells Tumors, Pancreatic. Figure 1 Multidetector computed tomographic study of typical insulinoma of the pancreatic tail. The nodule (*arrows*) appears hyperdense in the early arterial (a) and pancreatic (b) phases, with wash-out and a hypodense appearance in the venous (c) and delayed (d) phases.

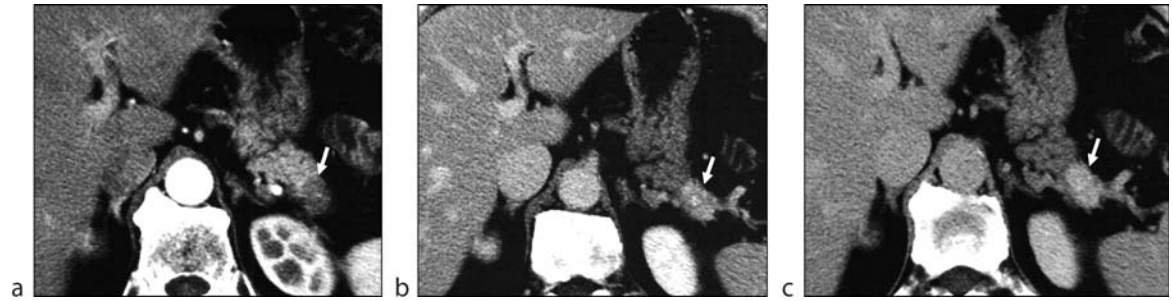

Islet Cells Tumors, Pancreatic. Figure 2 Multidetector computed tomographic study of malignant islet cells tumor of the pancreatic tail. The nodule (*arrows*) appears hypodense in the arterial phase (a) with a late enhancement in the venous (b) and delayed (c) phases.

somatostatin analog labeled with indium-111, ^{111}In-DTPA-D-Phe^{1}-octreotide, has been made available, exhibiting efficient uptake at tissues with high-density receptors for somatostatin. Scintigraphy with ^{111}In-DTPA-D-Phe^{1}-octreotide has been used for evaluating several types of cancer, especially neuroendocrine tumors, as well as medullar thyroid carcinomas, small cell lung cancer, and a certain fraction of breast cancers. In terms of diagnostic accuracy, scintigraphy with ^{111}In-DTPA-D-Phe^{1}-octreotide has shown satisfactory results only in the study of neuroendocrine tumors. Scintigraphic investigation envisages the intravenous administration of 111–148 MBq (3–4 mCi) of ^{111}In-DTPA-D-Phe^{1}-octreotide and "total body" acquisition after 4 and 24 h postinjection. Single photon emission computed tomography (SPECT) should be performed in all patients, preferably at 24 h. In some patients, a 48-h acquisition may be necessary to evaluate unclear accumulation in the abdomen. All images should be obtained with a large-field-of-view gamma camera equipped with a medium-energy parallel-hole collimator (3, 4).

Diagnosis

History taking, clinical examination, and laboratory tests are the basic tools to make up the diagnosis, especially in hormone-producing tumors causing typical symptoms.

Inactive endocrine tumors are generally at an advanced stage of disease at the time of their diagnosis because they become symptomatic only due to their mass effect or, in malignant cases, due to their metastases.

The role of imaging is to localize, demonstrate the extent of, and stage the lesion. Most islet cell tumors are easily identifiable by modern cross-sectional imaging techniques.

Bibliography

1. Pereira PL, Wiskirchen J (2003) Morphological and functional investigations of neuroendocrine tumors of the pancreas. Eur Radiol Sep 3(9):2133–2146
2. Roche A, Baert AL, Therasse E et al (1994) Endocrine tumours of the pancreas. In: Baert AL (ed) Medical Radiology: Radiology of the Pancreas. Springer, Berlin Heidelberg, New York
3. Gouya H, Vignaux O, Augui J et al (2003) CT, endoscopic sonography, and a combined protocol for preoperative evaluation of pancreatic insulinomas. Am J Roentgenol Oct 181(4):987–992
4. Fidler JL, Fletcher JG, Reading CC et al (2003) Preoperative detection of pancreatic insulinomas on multiphasic helical CT. AJR Am J Roentgenol Sep 181(3):775–780

Iso-Osmolality Contrast Media (IOCM)

An iso-osmolality contrast medium is a water-soluble imaging contrast agent that has osmolality (a measure of the number of particles in solution) equal or very close to the osmolality of human blood. See also high osmolality contrast media and low osmolality contrast media.

▶Adverse Reactions, Iodinated Contrast Media, Acute Renal

IVU

▶Intravenous Urography